**Cynthia Bonilha da Silva**

# Estudo longitudinal clínico e de imagem na Ataxia de Friedreich

# *Longitudinal clinical and neuroimaging study in Friedrich's ataxia*

**Campinas**

**2014**

**Universidade Estadual de Campinas**

**Faculdade de Ciências Médicas**

**Cynthia Bonilha da Silva**

# Estudo Longitudinal clínico e de imagem na Ataxia de Friedreich

## *Longitudinal clinical and neuroimaging study in Friedreich's ataxia*

**Tese apresentada à Faculdade de Ciências Médicas da Universidade Estadual de Campinas como parte doa requisitos exigidos para a obtenção do título de Doutora em Ciências Médicas, área de concentração em Neurologia**

***Thesis presented to Faculty of Medical Ciences, University of Campinas, as part of the requirements for obtaining the title PhD in Medical Ciences, area of concentration Neurology***

**Orientador: Marcondes Cavalcante França Junior**

**Este exemplar corresponde à versão final da tese defendida pela aluna Cynthia Bonilha da Silva e orientado pelo Prof. Dr. Marcondes Cavalcante França Junior.**

_____

**Campinas**

**2014**

Si38e

Silva, Cynthia Bonilha da, 1981-
Estudo longitudinal clínico e de imagem na ataxia de Friedreich / Cynthia Bonilha da Silva. – Campinas, SP : [s.n.], 2014.

Orientador: Marcondes Cavalcante França Júnior.
Tese (doutorado) – Universidade Estadual de Campinas, Faculdade de Ciências Médicas.

1. Ataxia. 2. Neuroimagem. 3. Depressão. 4. Fadiga. 5. Transtornos do sono. I. França Júnior, Marcondes Cavalcante. II. Universidade Estadual de Campinas. Faculdade de Ciências Médicas. III. Título.

Informações para Biblioteca Digital

**Título em outro idioma:** Longitudinal clinical and neuroimaging study in Friedreich's ataxia
**Palavras-chave em inglês:**
Ataxia
Neuroimage
Depression
Fatigue
Sleep disorders
**Área de concentração:** Neurologia
**Titulação:** Doutora em Ciências Médicas
**Banca examinadora:**
Marcondes Cavalcante França Júnior [Orientador]
Luiz Eduardo Gomes Garcia Betting
Fernando Kok
Marilisa Mantovani Guerreiro
Fabiano Reis
**Data de defesa:** 24-09-2014
**Programa de Pós-Graduação:** Ciências Médicas

# BANCA EXAMINADORA DA DEFESA DE DOUTORADO

**CYNTHIA BONILHA DA SILVA**

**Orientador (a) PROF(A). DR(A). MARCONDES CAVALCANTE FRANÇA JUNIOR**

**MEMBROS:**

1. **PROF(A). DR(A). MARCONDES CAVALCANTE FRANÇA JUNIOR** 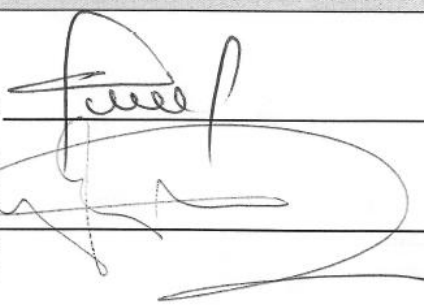
2. **PROF(A). DR(A). LUIZ EDUARDO GOMES GARCIA BETTING** 
3. **PROF(A). DR(A). FERNANDO KOK** 
4. **PROF(A). DR(A). MARILISA MANTOVANI GUERREIRO** 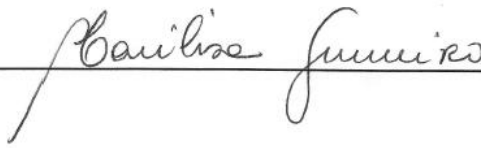
5. **PROF(A). DR(A). FABIANO REIS** 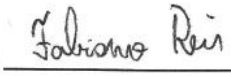

Programa de Pós-Graduação em Ciências Médicas da Faculdade de Ciências Médicas da Universidade Estadual de Campinas

**Data: 24 de setembro de 2014**

**Resumo**

Ataxia de Friedreich é a ataxia autossômiva recessiva mais frequente, causada por uma expansão de tripletos GAA em homozigoze no primeiro *íntron* do gene *FXN*, localizado no cromossomo 9. Trata-se de uma doença neurodegenerativa de início precoce, com curso progressivo. A patologia é caracterizada por perda neuronal nos gânglios das raízes dorsais, seguida por degeneração da coluna dorsal da medula espinhal e dos tractos espinocerebelares, atrofia da medula espinhal e do núcleo denteado de cerebelo. Os estudos clínicos prévios realizados na Ataxia de Friedreich focaram na incapacidade motora e muito pouco é conhecido sobre sintomas não-motores. Da mesma forma, estudos de neuroimagem prévios avaliaram coortes reduzidas e não incluíram avaliação longitudinal. Dessa forma, nosso estudo foi desenhado para caracterizar melhor a história natural da Ataxia de Friedreich. Avaliamos a presença de sintomas neuropsiquiátricos e se há substrato anatômico para tais manifestações. Realizamos, ainda, estudo de neuroimagem multimodal e longitudinal, a fim de identificar possíveis marcadores evolutivos da doença. Os resultados mostraram que fadiga e depressão são freqüentes nos pacientes com Ataxia de Friedreich, enquanto que sintomas relativos ao sono são raros. Evidenciamos que a depressão apresenta correlação com alterações neuroanatômicas, especialmante com a atrofia do giro cingulado anterior. O tempo de relaxação T2 estava significativa e especificamente reduzido nos núcleos denteados dos pacientes. Este parâmetro apresentou progressão ao longo do tempo e de forma paralela à deterioração motora, sugerindo assim que o tempo de relaxação T2 nesta estrutura pode ser um marcador de evolução da doença. O estudo volumétrico evidenciou uma extensa atrofia de substância cinzenta e branca, incluindo regiões profundas do cerebelo, tronco encefálico e também estruturas supratentoriais, como os giros precentrais. Estas alterações se correlacionaram com parâmetros de gravidade da doença.

Na avaliação longitudinal, houve piora da atrofia em regiões dos lobos temporais e frontais (incluindo os giros precentrais), além do lobo posterior do cerebelo. Nos pacientes, evidenciamos também extenso dano microestrutural à substância branca na FRDA. Além dos pedúnculos cerebelares superiores, constatamos alterações em parâmetros de difusão nos tratos piramidais e no corpo caloso. Embora estas alterações tenham se correlacionado com a incapacidade motora, não detectamos progressão ao longo do tempo.

Palavras-chave: ataxia, neuroimagem, depressão, fadiga, transtorno do sono

**Abstract**

Friedreich's ataxia is the most common autosomal recessive ataxia. It is caused by a homozygous triplet GAA expansion in the first intron of the *FXN* gene on chromossome 9. It is an early onset disease, with slowly progressive evolution. Pathology is characterized by neuronal loss in the dorsal root ganglia, followed by degeneration of the dorsal columms of the spinal cord, spinocerebelar tracts and atrophy of dentate nuclei of cerebellum. On clinical grounds, most studies have focused on motor disability and little is known about non-motor symptoms. Also, previous neuroimaging studies evaluated small samples of patients and did not include longitudinal analysis. Therefore, our study was designed to better characterize the course of the disease. In particular, we looked at neuropsychiatric manifestations and their structural substrate. We also performed multimodal MRI scans in a longitudinal setting, in an attempt to find reliable neuroimaging markers. Our results showed that fatigue and major depression are indeed frequent in patients with Friedreich's ataxia, but sleep complaints are rare. In these patients, depression was associated with neuroanatomical abnormalities, especially anterior cingulate cortex atrophy. The dentate nuclei T2 relaxometry was significantly shorter in patients, presented a progressive worsening over time and correlated with clinical parameters. These data suggest that dentate nuclei T2 might be a useful marker in this disease. The volumetric analyses showed widespread gray and white matter atrophy, including deep cerebellar nuclei, brainstem and also supratentorial structures, such as the precentral gyri. Such abnormalities correlated with disease severity. After 2 years of follow-up, we identified progressive volumetric reduction in parts of the temporal and frontal lobes (including the precentral gyri), as well as the posterior cerebellar lobe. We also found widespread microstructural damage to the white matter in Friedreich`s ataxia. Such damage involved not only the superior cerebellar peduncles, but also the pyramidal

tracts and the corpus callosum. Although these abnormalities did correlate with motor disability, we did not find progression over time.

Key-words: ataxia, neuroimage, depression, fatigue, sleep disorders

# SUMÁRIO

# DEDICATÓRIA

**Aos meus pais,**

**Ao meu mentor,**

**Aos meus pacientes,**

**Muito obrigada.**

# AGRADECIMENTOS

Agradeço, primeiramente, meus pais, Airton e Maria Candida, por me mostrar os caminhos que devo seguir, por serem exemplo de vida, por seu apoio às escolhas que fiz na vida, mesmo não concordem totalmente com elas. Obrigada pelo seu amor e carinho.

Agradeço ao meu irmão, Rodrigo, pelo seu apoio e carinho, mesmo de longe.

Agradeço ao meu orientador, Prof. Dr. Marcondes, por ser um grande amigo e mentor, por seus conselhos, ensinamentos, paciência infinita, incentivo e compreensão.

Agradeço aos meus colegas de trabalho e amigos Clarissa, Brunno, Thiago e Felipe, por me ajudarem muito a realizar este trabalho, pela ajuda e paciência, com quem tenho enorme gratidão.

A minha segunda família, a França-Jr! Obrigada meus novos irmãos Milena, Thiago, Rhafael, Helen e Alberto por seu apoio e pelos momentos de risadas

A minha amiga, quase irmã, Paola, por ouvir minhas angústias, dividir minhas alegrias, e seu carinho há tantos anos.

Finalmente, agradeço aos meus pacientes e familiares que participaram deste trabalho.

Muito obrigada.

# LISTA DE ABREVIATURAS

FRDA – Ataxia de Friedreich

FRDA-DP – Pacientes com Ataxia de Friedreich e com depressão

FRDA-NDP – Pacientes com Ataxia de Friedreich e sem depressão

BDI – Beck Depression Inventory – Inventário de Depressão de Beck

CCA – Córtex cingulado anterior

DSM-IV – Manual Diagnóstico e Estatístico de Transtornos Mentais

DTI – Diffusion tensor imaging

ESS – Epworth Sleepiness Scale – Escala de Sonolência de Epworth

FA – Anisotropia fracionada

FARS – Friedreich's Ataxia Rating Scale

FARS III – Exame neurológico da Freidreich's Ataxia Rating Scale

GAA – Tripleto guanina-adenosina-adenosina

ICARS – International Cooperative Ataxia Rating Scale

MFIS – Modified Fatigue Impact Scale – Escala Modificada de Impacto de Fadiga

MFIS-P – Componente físico da Escala Modificada de Impacto de Fadiga

NDC – Núcleo denteado do cerebelo

NDC T2 – Tempo de relaxação do núcleo denteado do cerebelo

RM – Ressonância magnética

ROI – Região de interesse

SB – Substância branca

SC – Substância cinzenta

SCA3 – Ataxia Espinocerebelar tipo 3

SNC – Sistema nervoso central

TBSS – Tract-based spatial statistics

T2 – Tempo de relaxação T2

VBM – Morfometria baseada em voxels

WAIS – Escala de Inteligência Wechsler para adultos

## Introdução

Ataxia de Friedreich (FRDA) é a ataxia autossômica recessiva mais frequente (1) e sua prevalência é estimada entre 1:50000 a 1:29000 (2). A maioria dos pacientes apresenta uma expansão, em homozigose, de tripletos guanina-adenosina-adenosina (GAA) no primeiro intron do gene *FXN* do cromossomo 9q13 (1, 3, 4). Em 2 – 4 % dos casos, os pacientes são heterozigotos e apresentam uma expansão GAA em um alelo e uma mutação de ponto ou deleção no outro (1).

FRDA tem início precoce, geralmente até a segunda década de vida. Observa-se um lento e progressivo prejuízo da deambulação, com instabilidade e alargamento de base da marcha, e da coordenação motora. Outros sinais encontrados são: arreflexia, sinais piramidais (sinal de Babinski), dismetria, disartria, disfagia, tremores de extremidades, alteração de força muscular e anormalidade da sensibilidade profunda (propriocepção e sensibilidade vibratória). A presença de pés cavus, escoliose, cardiopatia hipertrófica e diabetes mellitus também são muito frequentes (3, 5).

## Patofisiologia da Ataxia de Friedreich

A expansão de GAA causa um defeito de transcrição e, assim, a redução ou ausência da Frataxina (1), uma proteína da matriz mitocondrial. Embora todas as suas funções não estejam ainda totalmente esclarecidas, a Frataxina participa do metabolismo de ferro na cadeia respiratória mitocondrial e da biossíntese de clusters de sulfato ferroso (1). Esta proteína também parece interagir diretamente com enzimas de complexos da cadeia respiratória, agir na manutenção da aconitase mitocondrial-cluster de sulfato ferroso e prevenir o estresse oxidativo.

Assim, ela protege proteínas e DNA mitocondriais de lesão causada por radicais livres de ferro ($Fe^{2+}$) (5, 6). Haplodeficiência de frataxina resulta em múltiplos déficits enzimáticos, disfunção mitocondrial e dano oxidativo, e determina morte celular (1, 5, 6).

A deficiência de frataxina atinge diversos tecidos, incluindo coração, pâncreas e sistema nervoso periférico e central, contudo os tecidos apresentam vulnerabilidade diferente (1). Os gânglios da raiz dorsal e seus prolongamentos são as estruturas mais acometidas no sistema nervoso. Na FRDA, seus neurônios são menores que o normal e mais escassos (1). Ocorre também degeneração da coluna posterior da medula espinhal e dos tractos espinocerebelares; a medula espinhal apresenta diâmetro reduzido, especialmente na região torácica e cervical (1, 7). Koeppen et al sugerem que a concentração de ferro nos gânglios da raiz dorsal não está aumentado, mas há redistribuição de ferro e zinco; estes metais concentram-se de forma mais intracelular, tanto nos neurônios quanto em células satélites. A quantidade de ferritina neuronal mostrou-se diminuída nos neurônios, mas continuou elevada nas células satélites hiperplásicas e nódulos (8). A quantidade de ferro estava reduzida e com distribuição irregular nos neurônios pequenos, mas mantida e até aumentada nas células satélites hiperplásicas, sugerindo uma "transferência de ferro e zinco" a partir dos neurônios degenerados para células satélites ativadas e que esta alteração do metabolismo de ferro está ligado à patogênese da lesão neste local (8).

Os núcleos profundos do cerebelo e suas vias eferentes, assim como tractos córtico-espinhais, também sofrem degeneração, especialmente o núcleo denteado (NDC) (1, 7). No NDC, há alteração severa da "transferência de ferro" mitocondrial, evidenciada indiretamente por aumento na biossíntese de ferritina (1). Ocorre atrofia no NDC, grandes neurônios desaparecem, sendo encontrados apenas neurônios pequenos e há degeneração grumosa (1). Embora a quantidade total de ferro não esteja aumentada no NDC, análises histopatológicas

evidenciaram que o ferro está redistribuído no tecido, assim comojá descrito nos gânglios da raiz dorsal, sendo relocado como ferritina nos astrócitos e micróglia (9). Ocorre ainda uma redistribuição de zinco e cobre em conjunto com ferro (10).

No coração, observa-se cardiopatia hipertrófica, com aumento da espessura cardíaca, especialmente do ventrículo esquerdo e de septo interventricular. Há variação anormal do tamanho das fibras cardíacas. Contudo, estudos voltados para quantificar ferro demonstram que há poucas fibras com acúmulo de ferritina no interior da mitocondria e os depósitos não são progressivos. No pâncreas, não se observa destruição tecidual e a fisiopatologia do diabetes mellitus na FRDA é em grande parte desconhecida (1).

**Evolução clínica e tratamento**

A evolução da FRDA é lenta e progressiva. Embora não completamente, a gravidade da doença correlaciona-se com o tamanho da expansão de tripletos GAA, sobretudo no menor alelo (11, 12). A progressão dos sintomas motores e perda da independência nas atividades de vida diária também está relacionada à idade de início, idade do diagnóstico e a presença de acometimento sistêmico, especialmente a cardiomiopatia e escoliose (12).

Não existem tratamentos efetivos para FRDA. O tratamento clínico baseia-se na fisioterapia motora e, quando necessária, respiratória, além da identificação e atuação nas comorbidades, primordialmente da cardiopatia hipertrófica, distúrbios da função pulmonar, escoliose e diabetes mellitus.

Moléculas com ação antioxidante, como Coenzima Q10, Vitamina E, e Idebenona, foram utilizadas em ensaios clínicos para tratamento da FRDA, porém sua eficácia ainda é incerta. Em estudo de fase 2 com Idebenona em 48 pacientes pediátricos, Di Prospero et al não observaram melhora significativa da ataxia nos grupos tratados após 6 meses de seguimento. Entretanto, se considerados somente os pacientes não-cadeirantes, houve melhora significativa nos escores e este resultado foi mais expressivo naqueles em uso de dose mais elevada (13). Os resultados do único estudo de fase 3 realizado até o momento com Idebenona em pacientes com FRDA também não demonstraram benefício neurológico ao final do *follow-up* de 6 meses (14). Estes pacientes também foram avaliados do ponto de vista cardiológico e não apresentaram melhora significativa na espessura de ventrículo esquerdo nem de função cardíaca (15). Posteriormente, a mesma coorte de pacientes foi seguida por 12 meses, em um estudo *open-label*, e com Idebenona na dose ajustada entre 1350 a 2250 mg/dia. Utilizando-se os dados do seguimento de 12 meses, não foi observada melhora significativa nos escores de gravidade da ataxia. Contudo, os autores observaram que houve melhora em algumas subescalas. Ao analisar o estudo original com sua extensão, avaliando os pacientes por 18 meses, melhora clínica significativa foi evidenciada, especialmente no grupo de fez uso de Idebenona em sua maior dosagem desde o início. Os autores sugerem que altas doses de Idebenona podem oferecer benefício terapêutico na população pediátrica (16).

O melhor conhecimento da fisiopatologia da FRDA, por sua vez, possibilitou desenvolvimento de novas intervenções terapêuticas (5). Estudos *in vitro* sugeriram que a Eritropoetina é capaz de aumentar a expressão de frataxina em linfócitos de pacientes com FRDA (17, 18). Os estudos clínicos com Eritropoetina recombinante humana apresentam resultados contraditórios. Boesch et al demonstraram certo benefício na escala clínica após 6

meses da medicação em maior dose (19). Outros autores relataram o mesmo efeito na avaliação clínica, utilizando diferente protocolo (20). Demais estudos, entretanto, não demonstraram benefício (21, 22).

Estudos com quelantes de ferro também foram realizados. Boddart et al seguiram 13 pacientes em uso de Deferiprone por 6 meses, os quais foram avaliados através de escala clínica e de ressonância magnética. Foi realizada relaxometria para quantificar ferro em DNC. Os autores evidenciaram um discreto efeito, mas significativo, da relaxometria de pacientes, mostrando que houve uma redução na quantidade de ferro, contudo não houve alteração na escala clínica (23). O segundo estudo avaliou terapia combinada de Deferiprone e Idebenona por 11 meses em um grupo de 20 pacientes. Estes autores também observaram uma redução na relaxometria, porém sem alterações significativas quanto à escala clínica, exceto em alguns subtestes (24).

Os ensaios clínicos em FRDA apresentam dificuldade de serem realizados, uma vez que sua evolução é lenta e não há outros parâmetros de evolução da doença além da avaliação clínica (25). As escalas clínicas desenvolvidas para FRDA, como ICARS e FARS, são efetivas para mensurar a progressão da doença e sua gravidade (26, 27). Entretanto, estas escalas podem apresentar uma medida não-linear ao longo do tempo, além de vieses relacionadas ao paciente e ao examinador. Por fim, para avaliação com maior confiabilidade, é necessário observaros pacientes clinicamente por longos períodos (sugere-se 2 anos de seguimento) e isto dificulta a realização de testes de novos tratamentos (26, 27). Dessa forma, o desenvolvimento de outros marcadores de evolução para FRDA é primordial.

**Sintomas neuropsiquiátricos na Ataxia de Friedreich**

A importância dos sintomas neuropsiquiátricos tem sido reconhecida em várias doenças neurodegenerativas, como Ataxia Espinocerebelar e Doença de Parkinson, incluindo disfunção cognitiva e desordens afetivas. Contudo, na FRDA, há poucos estudos avaliando tais sintomas, especialmente, distúrbios de humor, fadiga e sono.

Alterações de funções cognitivas superiores foram avaliadas primeiramentena década de 1980, utilizando apenas a escala WAIS (*Wechsler Adult Intelligence Scale*). Estas análises iniciais sugeriam que os pacientes apresentam déficit de velocidade de processamento, com demais funções preservadas (28, 29). Posteriormente, Wollmann et al evidenciaram que as alterações podem ser mais extensas, incluindo a redução no tempo de reação motora e mental, alterações de linguagem, dificuldade na aquisição e consolidação de informações verbais e alterações visuo-construtivas quando comparadas aos controles (30). Muito destes estudos, porém, foram realizados numa época anterior ao mapeamento do gene *FXN* e se utilizaram de testes bastante dependentes de funções motoras.

Nos últimos anos, surgiram estudos incluindo apenas pacientes com confirmação genética de FRDA e com avaliação mais extensa e apropriada (31, 32). De modo geral, observou-se alteração em funções de linguagem, velocidade de processamento de pensamento, funções visuoespaciais e pobre nomeação. Em conjunto, estes achados sugerem disfunção executiva e de região parieto-temporal e atribuem isso à interrupção de circuitos cerebelo-cerebrais.

Quanto aos distúrbios de humor, estudos prévios não avaliaram a frequência e a relevância clínica de depressão e fadiga em pacientes com FRDA, ou sua relação com alterações

estruturais no sistema nervoso central. White et al avaliaram apenas 15 pacientes com diagnóstico clínico de FRDA, sem comprovação genética, e não encontrou nenhum paciente com critérios para depressão maior segundo DSM-IV (29). Outros estudos que avaliaram questionários de qualidade de vida sugerem que a saúde mental de pacientes com FRDA pode estar comprometida. Embora estes autores não tenham avaliado diretamente os critérios de depressão, os subitens relacionados ao funcionamento emocional e saúde mental apresentaram menor escore quando comparados ao grupo controle (33, 34, 35).

A presença de fadiga e distúrbio de sono também tem sido valorizados em diversas doenças neurodegenerativas. Na FRDA, existem poucos estudos que avaliaram a fadiga por meio de questionários de qualidade de vida. Estudos já realizados, tanto na população adulta quanto infantil, mostraram que pacientes com FRDA apresentam piores escores no componente físico destes questionários de qualidade de vida, assim como em escalas voltadas a identificar e quantificar fadiga (33, 34, 35). Embora os distúrbios de sono tenham sido pouco avaliados na FRDA, os dados disponíveis sugerem maior frequência de síndrome das pernas inquietas e apnéia obstrutiva do sono (36, 37).

**Estudos de neuroimagem na Ataxia de Friedreich**

A neuroimagem tem sido cada vez mais utilizada como ferramenta para acompanhamento da progressão em diversas enfermidades neurológicas. No desenvolvimento de terapias para esclerose múltipla, por exemplo, anormalidades evidenciadas na ressonância magnética (RM) e a involução das lesões ao longo do tempo de tratamento com interferon foram primordiais para comprovar sua eficácia no controle da doença (38).

Os primeiros estudos de neuroimagem na FRDA enfatizaram alterações importantes na medula cervical, com relativa preservação do encéfalo. Em análises visuais, evidenciou-se a redução volumétrica no diâmetro ântero-posterior da medula espinhal, principalmente na região torácica e cervical, com a presença de hipersinal nas imagens ponderadas em T2 restritas ao funículo dorsal e relativa preservação do volume cerebelar (39, 40). A análise quantitativa do diâmetro da medula cervical foi realizada por Chevis et al (41). Neste estudo, a atrofia de medula cervical foi sugerida como marcador de prognóstico da ataxia. Através de segmentação de imagens volumétricas, a área da medula cervical foi estimada; observou-se redução significativa deste parâmetro em relação aos controles, a qual se correlacionou com a gravidade da doença (41).

A presença de depósitos de ferro na FRDA também foi investigada através de técnicas de neuroimagem. A distribuição anormal do ferro no NDC causa uma não homogeneidade do campo magnético e reduz o tempo ponderado em T2, com pouca ou nenhuma alteração do tempo ponderado em T1, tornando o NDC mais hipointenso nas imagens em T2 (42, 43, 44). Dessa forma, a quantificação da concentração de ferro pode ser estimada através de diferentes técnicas de RM, métodos de *susceptibility-weighted* erelaxometria (45). Diferentes métodos, baseados em relaxometria, têm sido utilizados no mapeamento de ferro, incluindo métodos de *spin-lattice relaxation rate* (R1=1/T1), *spin-spin relaxation rate* (R2=1/T2) ou *gradient echo* (R2*=1/T2*=R2+R2') (45). Vários trabalhos demonstraram que tanto R1, R2, R2* ou R2' (R2'=R2*-R2) correlacionam-se fortemente com conteúdo de ferro no tecido cerebral (45, 46).

O primeiro estudo, com este objetivo, foi realizado por Waldwogel et al (43). Através de estudo de relaxometria, este autor demonstrou uma alteração do acúmulo de ferro em NDC nos pacientes com FRDA quando comparados a controles. A análise de R2* também foi utilizada

como parâmetro de imagem em dois estudos que investigaram o uso de quelante de ferro como opção terapêutica. No primeiro estudo, que utilizou Deferiprone em um pequeno grupo de pacientes, os autores encontraram uma pequena diferença entre controles e pacientes na relaxometria realizada em NDC no início do seguimento (23). No segundo estudo, que utilizou Deferiprone associado à Idebenona, houve a redução do R2* nos NDC no período de tratamento, indicando de que seria possível quelar estes depósitos de ferro no sistema nervoso central (24).

A partir da análise de Morfometria Baseada em Voxel (VBM), observou-se alterações em fossa posterior e supratentoriais. Della Nave et al, avaliando 13 pacientes,evidenciaramsomente pequenas áreas de atrofia na substância branca (SB) profunda em cerebelo (47). Contudo, França et al observaram atrofia na SB em regiões periventriculares (giro do cíngulo posterior, lóbulos paracentrais e giro frontal médio). Além disso, aplicando-se avaliação por meio de ROIs (regiões de interesse), estes autores demonstraram ainda a redução de substância cinzenta (SC) em porção ínfero-posterior de hemisférios cerebelares e tronco cerebral dorsal (48). Estes dados estão em concordância com os resultados encontrados por Della Nave et al, os quais evidenciaram perda de SC em vérmis e hemisférios cerebelares e atrofia de SB cerebelar profunda (47). As alterações descritas do volume cerebelar apresentaram correlação com a gravidade da ataxia (47, 49) e com duração da doença (48).

Akhlanghi et al, por sua vez, avaliaram a presença de atrofia em pedúnculos cerebelares superiores e sua relação com parâmetros clínicos da ataxia. Relataram que a área dos pedúnculos cerebelares foi significativamente menor em relação aos controles e que o volume desta estrutura correlacionou-se negativamente com a gravidade e duração e, positivamente, com a idade de início. Estes autores sugerem que a atrofia do pedúnculo cerebelar superior seja um potencial marcador de evolução da doença (50).

Estudos de DTI também estão sendo realizados para avaliar dano micro-estrutural na SB em pacientes com FRDA. O primeiro estudo de *tract based spatial statistics* (TBSS) foi realizado por Della Nave et al. (49). Os autores observaram a redução de anisotropia fracionada (FA) em pedúnculos cerebelares superiores e inferiores, tractos córtico-espinhais em bulbo, tractos cerebelares à direita e tracto occipito-frontal e fascículo longitudinal inferior direitos, além do aumento da difusividade média em pedúnculos cerebelares superiores, SB cerebelar profunda bilateral e na SB próxima ao sulco central esquerdo (49). Estudos posteriores confirmaram alterações semelhantes no pedúnculo cerebelar superior. Della Nave et al encontraram redução da FA, com incremento da difusividade radial e axial em pedúnculo cerebelar superior, enquanto que Hohenberg et al demosntraram que a difusividade radial do pedúnculo cerebelar inferior e superior correlacionaram-se com a gravidade da ataxia (51, 52).

Estudos de ressonância magnética funcional identificaram alterações mais difusas no encéfalo, não restritas a cerebelo e tronco cerebral, o que vai de encontro com manifestações clínicas não-motoras já observadas na FRDA. Os estudos sugerem que há disfunção do córtex sensório-motor nos pacientes com FRDA, resultado das alterações de medula espinhal e cerebelo, assim como de estruturas subcorticais (53, 54) e de vias córtico-cerebelares (37, 55).

Disfunções cerebrais mais extensas foram demonstradas por Zalesky et al, os quais realizaram o primeiro estudo de conectividade cerebelo-cerebral (56). Estes autores observaram que áreas corticais e subcorticais estão conectadas de forma aberrante ao cerebelo, incluindo área motora suplementar, putâmem e globo pálido. Notaram, ainda, que áreas não-motoras, como córtex cingulado, hipocampo e córtex frontal, também estão implicadas, sugerindo disfunção de vias, aferentes e eferentes, importantes na conexão entre córtex, cerebelo e tronco cerebral (56).

Neste contexto, realizamos um estudo voltado para melhor caracterização dos pacientes com FRDA, tanto clinicamente quanto do ponto de vista de neuroimagem. Embora sintomas não-motores tenham sido cada vez mais reconhecidos e valorizados em doenças neurodegenerativas, há poucos trabalhos na FRDA especificamente sobre depressão, fadiga e sono. A frequência e suas causas não são bem caracterizados, assim como se há substrato anatômico relacionado ao seu desenvolvimento.

A identificação de biomarcadores ou marcadores de imagem na FRDA é urgente para a realização de novos ensaios clínicos. Os últimos estudos de neuroimagem na FRDA investigaram possíveis candidatos, como atrofia de pedúnculo cerebelar superior ou relaxometria do NDC. Estes estudos, contudo, foram realizados com número reduzido de indivíduos e, em muitos, não investigaram se as alterações estruturais encontradas correlacionam-se com parâmetros clínicos e sua validade como marcador de evolução da FRDA. Além disso, não há nenhum estudo de neuroimagem longitudinal na Ataxia de Friedreich.

Dessa forma, estas questões motivaram a realização de estudo para caracterizar as manifestações neuropsiquiátricas da doença, assim como investigar se há algum substrato estrutural para seu surgimento. Estudamos também diversos parâmetros quantitativos de ressonância magnética nos pacientes com FRDA de modo transversal e prospectivo, tendo como foco a identificação de potenciais marcadores de imagem da gravidade e evolução da FRDA e a caracterização de seu comportamento evolutivo.

***Objetivo geral***

Investigar e caracterizar, do ponto de vista clínico e de neuroimagem, a evolução da Ataxia de Friedreich.

***Objetivos Específicos***

1. Determinar a frequência e intensidade de sintomas não-motores, incluindo depressão, fadiga e sono, em pacientes com FRDA.
2. Correlacionar os sintomas depressivos com achados estruturais cerebrais na FRDA.
3. Determinar se há alteração de relaxometria T2 em núcleos denteados de cerebelo em pacientes com FRDA e compará-los a controles saudáveis.
4. Identificar as áreas de atrofia de substância branca e cinzenta no sistema nervoso central nos pacientes com FRDA e quantificá-las através de técnicas de ressonância magnética encefálica.
5. Identificar e quantificar as áreas dealterações microestruturais de substância branca em pacientes com FRDA através de análise de tensor de difusão.
6. Avaliar o comportamento evolutivo das alterações de neuroimagem nos pacientes com FRDA e sua correlação com parâmetros clínicos e de gravidade da FRDA.

## Materiais e métodos

Os materiais e métodos utilizados neste estudo estão desctritos em detalhes em cada um dos artigos que compõem os resultados desta tese. No anexo, é apresentada uma descrição breve dos métodos de imagem utilizados neste estudo.

Este projeto foi realizado após a análise e aprovação do Comitê de Ética em Pesquisa da Faculdade de Ciências Médicas da Universidade Estadual de Campinas (parecer nº 131/2011 – em anexo). Cada participante assinou Termo de Consentimento Livre e Esclarecido antes da realização dos procedimentos experimentais (termo em anexo).

Parkinsonism and Related Disorders 19 (2013) 766–767

Contents lists available at SciVerse ScienceDirect

Parkinsonism and Related Disorders

journal homepage: www.elsevier.com/locate/parkreldis

Letter to the Editor

# Fatigue is frequent and multifactorial in Friedreich's ataxia

*Keywords:*
Friedreich's ataxia
Depression
Fatigue
Sleep disorders

Friedreich's Ataxia (FRDA) is the most common autosomal recessive ataxia and characterized by severe motor impairment. It is caused by a homozygous triplet GAA expansion in the first intron of the *FXN* gene on chromosome 9q13 in 96% of patients. The disease typically has an early onset and is characterized by slowly progressive gait ataxia, dysmetria, dysarthria, deep sensory abnormalities (especially proprioceptive sensation), *pes cavus*, scoliosis, cardiomyopathy and diabetes. Non-motor features have been increasingly recognized in FRDA and other neurodegenerative disorders, but there are few data specifically about fatigue and daytime sleepiness in FRDA.

We have thus evaluated 27 consecutive FRDA patients regularly followed at UNICAMP hospital and 58 healthy age-and-sex matched controls. All patients were homozygous for the GAA expansions at the first intron of the *FXN* gene. Individuals with concomitant neurological disorders or dementia were excluded. This protocol was approved by our institution Research Ethics Committee and a written informed consent was obtained from all participants.

Each subject answered Brazilian Portuguese-validated questionnaires: Epworth Sleepiness Scale (ESS), Pittsburg Sleep Quality Index (PSQI), Modified Fatigue Impact Scale (MFIS), which is divided into physical (MFIS-P), cognitive (MFIS-C) and psychosocial components (MFIS-S) and Beck Inventory Depression (BDI) [1–4]. ESS, PSQI, MFIS and BDI scores were considered abnormal if ≥9, 5, 38 and 11, respectively. Severity of ataxia was quantified with Friedreich's ataxia rating scale (FARS).

We used Mann–Whitney and Fisher exact test to compare mean scores and proportions between groups. Stepwise multiple linear regression was used to investigate possible associations between MFIS scores and clinical parameters.

Basic clinical, genetic and demographic data of patients and controls are shown in Table 1. Mean age at onset and disease duration were 14.4 ± 4.9 and 12.5 ± 8.5 years, respectively. Mean FARS score was 81.3 ± 28.8. Twenty-five patients had typical FRDA, one had FRDA with retained reflexes and one late-onset FA. Diabetes mellitus/glucose intolerance was found in 7 patients. Five patients (19%) had cardiomyopathy shown by echocardiography, but none of them presented congestive heart failure. Four patients were taking antidiabetic drugs: 2 Metformin and 2 on insulinotherapy. Fourteen patients had scoliosis. Twenty-one patients were using Coenzime Q10 (doses ranging from 200 to 900 mg daily) and 3 were using Idebenone (15 mg/kg/day divided into 2 doses), respectively. Four patients were taking antidepressant drugs (Fluoxetine 20mg/d, Fluoxetine 40mg/d, Venlafaxine 37.5 mg/d, Sertraline 100mg/d).

Mean total MFIS scores were similar between patients and controls ($p = 0.134$). However, the proportion of subjects who had MFIS scores ≥38 was higher in the FRDA group (29.6% vs 5.1%, $p = 0.004$). Mean MFIS scores were similar between patients with and without cardiomyopathy (23.1 vs 20.0, $p = 0.59$). MFIS-P scores were also higher in the FRDA group ($p = 0.018$), but not MFIS-C or MFIS-S ($p = 0.62$ and 0.31, respectively). BDI scores were higher among patients ($p = 0.028$). However, sleep-related complaints were not as relevant, as shown by ESS and PSQI scores (Table 1). In the regression analysis, MFIS was associated with FARS ($p = 0.05$), duration of the disease ($p < 0.001$), ESS ($p = 0.002$) and BDI scores ($p = 0.007$) ($r^2 = 0.77$ in the model).

Our results showed that fatigue and especially its physical component is a major manifestation in FRDA and correlated with the severity and duration of the disease. The results are in accordance with previous studies [5]. Fatigue was not a spontaneous complaint of any patient, so that we cannot ascertain the precise moment of its onset. The novel finding in this paper is that fatigue in FRDA seems to be a multifactorial problem, associated not only with severity of ataxia but also depression and daytime sleepiness. Our data indicate that fatigue seemed to be unrelated to cardiomyopathy, but this should be confirmed in larger trials.

Our results thus indicate that fatigue may be a rather frequent and often under recognized feature in FRDA patients. Effective treatment needs to address its multiple causative factors. Further

**Table 1**
Clinical and genetic data of patients with Friedreich's ataxia and controls.

| | FRDA ($n = 27$) | Controls ($n = 58$) | $p$ |
|---|---|---|---|
| Age (mean ± SD, years) | 26.9 ± 9.9 | 29.0 ± 8.1 | 0.104 |
| Gender (M:F) | 11:16 | 23:35 | 0.92 |
| Larger GAA1 (mean ± SD) | 1006 ± 269 | - | - |
| Smaller GAA2 (mean ± SD) | 846 ± 200 | - | - |
| ESS score (mean ± SD) | 3.1 ± 3.0 | 5.5 ± 2.9 | <0.001 |
| PSQI score (mean ± SD) | 4.0 ± 2.6 | 4.5 ± 2.1 | 0.087 |
| MFIS score (mean ± SD) | 22.3 ± 16.4 | 16.0 ± 11.5 | 0.134 |
| MFIS-P score (mean ± SD) | 12.9 ± 10.5 | 7.1 ± 5.7 | 0.018 |
| MFIS-C score (mean ± SD) | 6.9 ± 6.7 | 7.2 ± 5.8 | 0.62 |
| MFIS-S score (mean ± SD) | 2.6 ± 2.5 | 1.9 ± 1.7 | 0.31 |
| BDI score (mean ± SD) | 10.0 ± 9.5 | 4.7 ± 3.8 | 0.028 |

FRDA – patients with Friedreich's ataxia; ESS – Epworth Sleepiness Scale; PSQI – Pittsburgh Sleep Quality Index; MFIS – Modified Fatigue Impact Scale; BDI – Beck Depression Inventory.


http://dx.doi.org/10.1016/j.parkreldis.2013.04.007

studies with larger samples are certainly needed to better characterize fatigue in FRDA patients.

## Conflict of interests

The authors report no conflict of interests regarding this research.

## References

[1] Bertolazi AN, Fagondes SC, Hoff LS, Pedro VD, Menna Barreto SS, Johns MW. Portuguese-language version of Epworth sleepiness scale: validation for use in Brazil. J Bras Pneumol 2009;35:877–83.
[2] Bertolazi AN, Fagondes SC, Hoff LS, Dartora EG, Miozzo IC, de Barba ME, et al. Validation of the Brazilian Portuguese version of the Pittsburg sleep quality index. Sleep Med 2011;12:70–5.
[3] Pavan K, Schmidt K, Marangoni B, Mendes MF, Tilbery CP, Lianza S. Multiple sclerosis: cross-cultural adaptation and validation of modified fatigue impact scale. Arq Neuropsiquiatr 2007;65:669–73.
[4] Gorenstein C, Andrade L. Validation of a Portuguese version of the Beck Depression Inventory and State-Tract Anxiety Inventory in Brazilian subjects. Braz J Med Biol Res 1996;29:453–7.
[5] Epstein E, Farmer JM, Tsou A, Perlman S, Subramony SH, Gomez CM, et al. Health quality of life in Friedreich ataxia. J Neurol Sci 2008;272:123–8.

Cynthia B. da Silva, Camila F. Chevis, Anelyssa D'Abreu
*Departments of Neurology and Neuroimaging Laboratory, Faculty of Medicine, University of Campinas – UNICAMP, Campinas, SP, Brazil*

Iscia Lopes-Cendes
*Department of Medical Genetics, Faculty of Medicine, University of Campinas – UNICAMP, Campinas, SP, Brazil*

Marcondes C. França Jr.*
*Department of Neurology, University of Campinas – UNICAMP, Rua Tessália Vieira de Camargo, 126. Cidade Universitaria "Zeferino Vaz", Campinas, SP 13083-887, Brazil*

* Corresponding author. Tel.: +55 19 3521 9217; fax: +55 19 3521 7933.
*E-mail address:* mcfrancajr@uol.com.br

5 February 2013

Cerebellum
DOI 10.1007/s12311-012-0424-0

ORIGINAL PAPER

# Neuroanatomical Correlates of Depression in Friedreich's Ataxia: a Voxel-Based Morphometry Study

**Cynthia B. da Silva · Clarissa L. Yasuda · Anelyssa D'Abreu · Fernando Cendes · Iscia Lopes-Cendes · Marcondes C. França Jr**



**Abstract** Affective disorders have been increasingly recognized in neurodegenerative diseases and often result in poor quality of life. However, the frequency, clinical relevance, and anatomical substrate of depression in Friedreich's ataxia were not yet evaluated. We assessed 22 patients with Friedreich's ataxia for major depression using Beck Depression Inventory and cerebral 3 T MRI scans. We then employed whole-brain voxel-based morphometry analyses on volumetric T1 datasets to compare tissue loss between patients with and without major depression. Patients (36.3 %) fulfilled criteria for major depression (8/22). Mean Beck Depression Inventory (BDI) score was 9.63±8.95 and the depressive group had significantly higher score compared to non-depressive group (18.5±8.6 vs 4.4±2.9, $p<0.001$). There was no correlation between Beck Depression Inventory score and age of patients, ataxia severity, age at onset, or duration of the disease. The comparison between patient groups found no significant differences of white matter volumes. In contrast, we found reduction of gray matter volumes in the depressive group in medial and orbital region of frontal lobe and anterior cingulate gyri ($p<0.001$). Regression analyses have shown that BDI scores were inversely correlated with gray matter volume at right superior frontal gyrus. Major depression is frequent in Friedreich's ataxia and possibly under recognized. Our results strongly suggest that this may not be a simply reactive phenomenon, but rather associated to structural abnormalities.

**Keywords** Friedreich's ataxia · Depression · MRI · Voxel-based morphometry

C. B. da Silva · C. L. Yasuda · A. D'Abreu · F. Cendes · M. C. França Jr (✉)
Departments of Neurology and Neuroimaging Laboratory, University of Campinas—UNICAMP, Rua Tessália Vieira de Camargo, 126. Cidade Universitaria "Zeferino Vaz", Campinas, SP 13083-887, Brazil
e-mail: mcfrancajr@uol.com.br

I. Lopes-Cendes
Medical Genetics, Faculty of Medicine, University of Campinas—UNICAMP, Campinas, SP, Brazil

## Introduction

Friedreich's ataxia (FRDA) is the most common autosomal recessive ataxia. It is caused by a homozygous triplet GAA expansion in the first intron of the *FXN* gene on chromosome 9q13 in 96 % of patients [1, 2]. The consequence is reduced expression of Frataxin which ultimately leads to mitochondrial dysfunction and neurodegeneration [3]. The disease typically has an early onset and is characterized by slowly progressive gait ataxia, dysmetria, dysarthria, deep sensory abnormalities (especially proprioceptive sensation), *pes cavus*, scoliosis, cardiomyopathy, and diabetes [3]. The dorsal root ganglia and pyramidal tracts are preferentially damaged in FRDA, resulting in volumetric reduction of cerebellar pathways and especially of the spinal cord [4, 5].

The importance of non-motor features has been increasingly recognized in diseases such as spinocerebellar ataxias and Parkinson's disease (PD) in the last few years, including cognitive dysfunction, fatigue and sleep disorders. Affective disorders and especially depression are very frequent complaints, and often result in poor quality of life in these patients [6–8]. There are few studies evaluating the frequency and clinical relevance of depression in patients with FRDA. Furthermore, available data rely upon small series and scales not specifically designed to assess depressive symptoms [9, 10].

In fact, some authors consider that depression in neurodegenerative diseases could be a reactive process to the disabling motor manifestations [11]. However, functional and structural abnormalities that underlie motor dysfunction in these diseases may also contribute to the origin of

Published online: 24 October 2012

depressive symptoms. Indeed, in patients with PD and depression, volumetric MRI studies showed gray matter atrophy in bilateral orbitofrontal, bilateral rectal gyrus and right superior temporal lobe [8]. In SCAs and particularly in FRDA, little is known about the substrate for depressive manifestations.

In this setting, we designed a study to investigate the frequency of depressive symptoms and whether it correlates with clinical status in adult FRDA patients. We also looked for structural abnormalities that might be associated with depression in FRDA. This was accomplished by comparing volumetric MRI datasets between FRDA patients with and without depression through voxel-based morphometry (VBM) analyses.

## Methods

### Subjects' Selection

We selected a group of 22 FRDA patients older than 18 years that were regularly followed at the Neurogenetics outpatient clinic at UNICAMP hospital between 2010 and 2011. All patients underwent genetic testing and were found to be homozygous for the GAA expansions at the first intron of the *FXN* gene [12]. Individuals with concomitant neurological disorders, dementia (according to DSM-IV criteria) or unable to perform MRI scans were not included in the study. This protocol was approved by our institution Research Ethics Committee and a written informed consent was obtained from all participants.

### Clinical Evaluation

Clinical (gender, age at disease onset, duration of disease, clinical subtype) and genetic data (length of expanded repeat in both shorter, GAA1 and longer, GAA2 alleles) were recorded. Severity of ataxia was quantified with Friedreich's ataxia rating scale (FARS) [13].

We defined major depression according to the DSM-IV criteria and assessed the severity of depressive symptoms using Beck Depression Inventory (BDI) [14, 15]. FRDA patients were then divided into two groups: with depression (FRDA-DP) and without depression (FRDA-NDP).

### MRI Acquisition Protocol and Analysis

All FRDA patients and 22 age- and sex-matched healthy and non-depressed controls underwent MRI scans on a 3-T Achieva-Intera PHILIPS equipment. Volumetric (3D) T1-weighted images were acquired in the sagittal plane with slices of 1 mm thickness (flip angle=8°, TR=7.1 ms, TE=3.2 ms, isotropic voxels 1.0×1.0×1.0, FOV 240×240). These images were converted into a NIfTI file and then used for VBM analysis. We used SPM 8 software (Wellcome Department of Imaging Neuroscience, London, England, www.fil.ion.ucl.ac.uk), VBM 8 (http://dbm.neuro.uni-jena.de/vbm8/) and MATLAB 7.7 to perform several fully automated imaging pre-processing steps, including spatial normalization of all images to the same stereotaxic space, segmentation into white and gray matter and cerebrospinal fluid compartments, correction for volume changes induced by spatial normalization (modulation) and smoothing. Spatial normalization was accomplished with the DARTEL algorithm that significantly reduces the imprecision of intersubject registration [16]. Processed images were compared using a voxel-wise statistical analysis [17]. We used two sample *T* test from SPM to search for differences in WM and GM volumes between: (1) FRDA patients vs controls; and (2) FRDA-DP vs FRDA-NDP. The results were corrected for multiple comparisons and significant differences set at $p<0.001$. Only cluster sizes>50 voxels were reported. We also performed regression analyses with SPM to investigate the correlation between GM and WM volumes and BDI scores. In order to display the results and precise their anatomical location we used an additional SPM extension, XJVIEW (http://www.alivelearn.net/xjview/).

### Statistical Analysis

Demographic data of patients are detailed with descriptive statistics. We compared clinical and genetic parameters between FRDA-DP and FRDA-NDP groups using Mann–Whitney test. Level of significance was set at $\alpha=0.05$ for all comparisons. Statistical analyses were performed with SYSTAT software version 9.0.

## Results

### Clinical Results

Mean age of patients was 29.0±9.8 years and there were 8 men and 14 women. The mean age at onset and disease duration were 15.0±5.1 and 14.0±8.7 years, respectively. The mean length of expanded GAA1 and GAA2 alleles were 1,015 (range 437–1,705) and 835 (range 437–1,330), respectively. Twenty patients had typical FRDA, one had FRDA with retained reflexes and one late-onset FA. Diabetes mellitus/glucose intolerance was found in seven patients, all of them with adequate control of glucose levels. Four patients were taking antidiabetic drugs: two metformin 500 mg bid and two on insulinotherapy. Fourteen patients had scoliosis and 5 had cardiomyopathy. Fourteen patients were using Coenzyme Q10 (doses ranging from 200–900 mg daily) and two were using Idebenone (15 mg/kg/day

divided into two doses). Mean FARS score was 86.4±26.6. This score correlated with age of patients ($r$=0.61, $p$=0.002) and with duration of disease ($r$=0.79, $p$<0.001), however there was no correlation with age at onset ($r$=0.17, $p$=0.425).

Eight out 22 FRDA patients fulfilled DSM-IV criteria for major depression (36.3 %). Mean BDI score in the whole FRDA group was 9.63±8.95, and four patients were taking antidepressant drugs (fluoxetine 20 mg/day, fluoxetine 40 mg/day, venlafaxine 37.5 mg/day, sertraline 100 mg/day). FRDA-DP group had significantly higher BDI scores in comparison to FRDA-NDP group (18.5±8.6 vs 4.4±2.9, $p$<0.001). There was no correlation between BDI and age of patients ($p$=0.884), FARS ($p$=0.096), age at onset of disease ($p$=0.466) or duration of the disease ($p$=0.554). In addition, we found no significant difference between FRDA-DP and FRDA-NDP groups regarding age of patients ($p$=0.64), age at onset ($p$=0.77), duration ($p$=0.89) or FARS score ($p$=0.58).

## VBM Results

### *FRDA vs Controls*

The whole-brain VBM analysis comparing all FRDA patients and controls showed GM atrophy specially in right and left cerebellum posterior lobe (peak MNI coordinates $x$=9, $y$=−52, $z$=−60 and $x$=−20, $y$=−63, $z$=−30, respectively), but also in the left temporal middle gyrus ($x$=−50, $y$=−22, $z$=−14), left temporal middle gyrus ($x$=−40, $y$=−64, $z$=13), left postcentral and precentral gyrus ($x$=−46, $y$=−18, $z$=34), and pons ($x$=−16, $y$=−22, $z$=−33) (Table 1, Fig. 1). WM atrophy was particularly severe at the posterior lobes of the cerebellum and brainstem. We also found WM volumetric reduction in periventricular areas, including bilateral frontal lobes, cingulate gyri, limbic lobes, corpus callosum, lentiform nuclei, thalami and temporal lobes (Table 1, Fig. 2). There were no areas of WM and GM increase in patients with FRDA.

### *FRDA-DP vs FRDA-NDP*

When we compared FRDA-DP and FRDA-NDP groups we found no significant differences of WM volumes. In contrast, we found reduction of GM volumes in the FRDA-DP group encompassing bilateral medial frontal and anterior cingulate gyri ($x$=2, $y$=26, $z$=−12), right superior frontal gyrus ($x$=20, $y$=64, $z$=3), left inferior occipital gyrus ($x$=−45, $y$=−81, $z$=−14), right middle frontal gyrus ($x$=30, $y$=36, $z$=43) and right orbital gyrus ($x$=18, $y$=46, $z$=−27)

**Table 1** Areas of gray matter (GM) and white matter (WM) atrophy in patients with Friedreich's ataxia compared with controls

| Cluster | Cluster size (voxels) | $T$ | $x, y, z$ (mm) MNI coordinates | Anatomic location |
|---|---|---|---|---|
| GM | | | | |
| 1 | 5198 | 5.99 | 9, −52, −60 | R cerebellum posterior lobe |
| 2 | 1983 | 4.28 | −20, −63, −30 | L cerebellum posterior lobe |
| 3 | 729 | 4.92 | −50, −22, −14 | L temporal middle lobe |
| 4 | 253 | 3.97 | −40, −64, 13 | L middle temporal gyrus |
| 5 | 238 | 3.70 | −46, −18, 34 | L postcentral and precentral gyrus |
| 6 | 61 | 3.89 | −16, −22, −33 | Pons |
| WM | | | | |
| 1 | 115428 | 16.25 | −2, −45, −26 | R L frontal lobe |
| | | | | Limbic lobe |
| | | | | Cingulate gyrus |
| | | | | R L cerebellum (anterior and posterior lobe) |
| | | | | R L brainsteim |
| | | | | Corpus Callosum |
| | | | | Pons |
| | | | | Lentiform nucleus |
| | | | | Thalamus |
| | | | | R L temporal lobe |
| 2 | 409 | 4.01 | −30, −69, 15 | R temporal lobe and occipital lobe |
| 3 | 311 | 4.56 | −9, 48, 24 | L frontal superior medial lobe |
| 4 | 112 | 3.85 | −6, 56, 10 | L frontal superior medial lobe |
| 5 | 76 | 3.75 | 21, 58, −11 | R superior frontal gyrus |

Results reported on height threshold: $T$=3.30, clusters>50 voxels

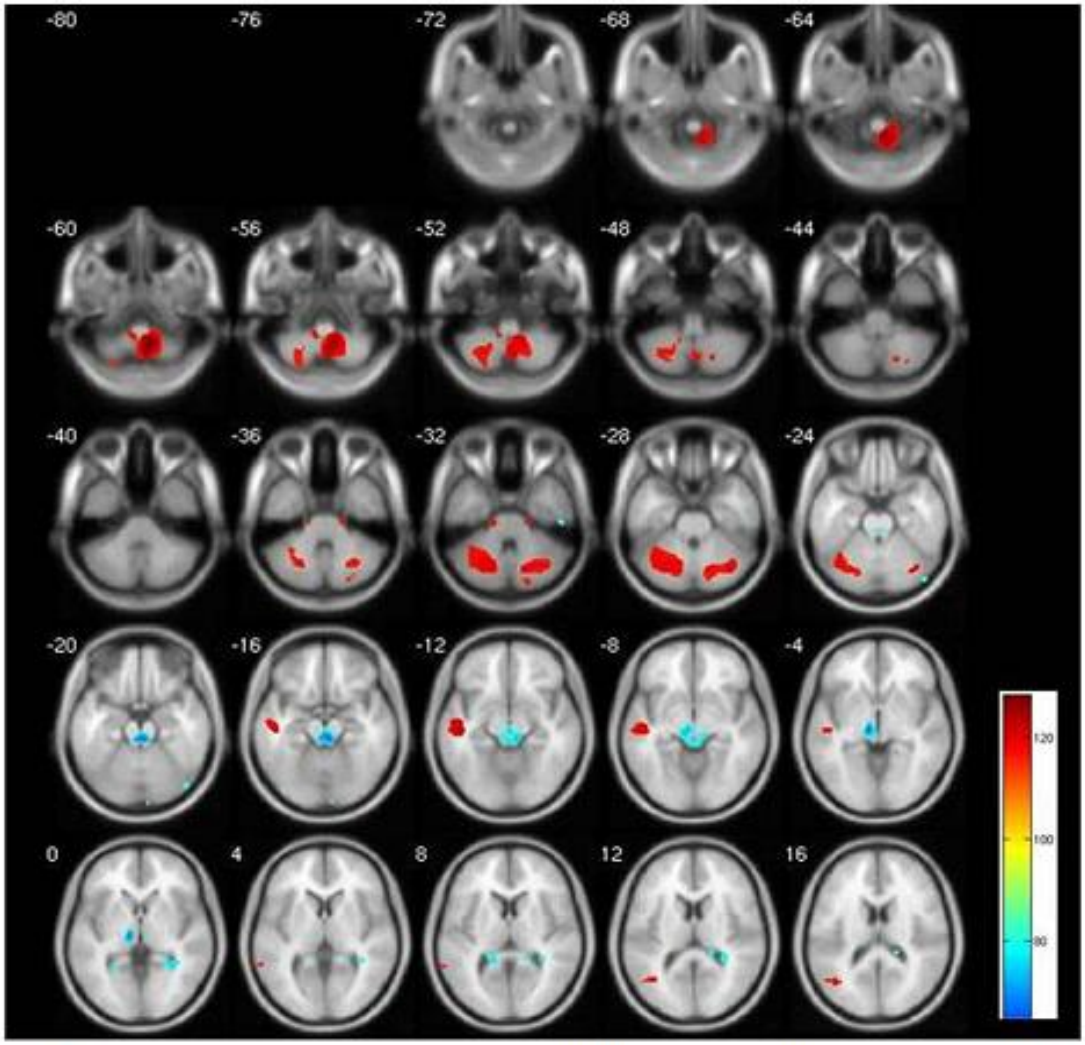


**Fig. 1** Results of voxel-wise analysis showing areas of gray matter volumetric reduction in patients with Friedreich's ataxia after comparison with age- and sex-matched controls. Results are shown on the MNI152 1-mm template. MNI *z*-axis coordinates are shown in millimeter above each image. The *color coded bar* represents the *Z* score

(Table 2, Fig. 3). Regression analyses have shown that BDI scores were inversely correlated with GM volume at right superior frontal gyrus ($x=16.5$, $y=60$, $z=1.5$).

## Discussion

In Friedreich's ataxia, there are few studies that focused in non-motor symptoms and especially depressive complaints. In our study, we found that more than 30 % of patients with FRDA fulfill DSM-IV criteria for major depression. This prevalence is much higher than in the general adult population (3–10 %) and similar to that found in other related neurodegenerative diseases, such as PD (12–37 %) and SCA3 (33.5 %) [11, 18, 19]. This result is in contrast to that reported by White et al. who found that depression was not a common finding in FRDA [20]. In that study, however, authors included a smaller number of patients and FRDA diagnosis was based only on clinical criteria. In addition, they excluded individuals with handgrip strength smaller than 5 kg on dynamometer which might have selected only those FRDA patients with less severe disease. Our data also suggest that depression is probably unrecognized in these patients, since only half of those were in pharmacological treatment. This is possibly due to the overwhelming motor impairment and the lack of awareness of the physicians that treat FRDA patients.

Depression in FRDA was not associated to ataxia severity, age, age at onset, duration of the disease, or FARS. This

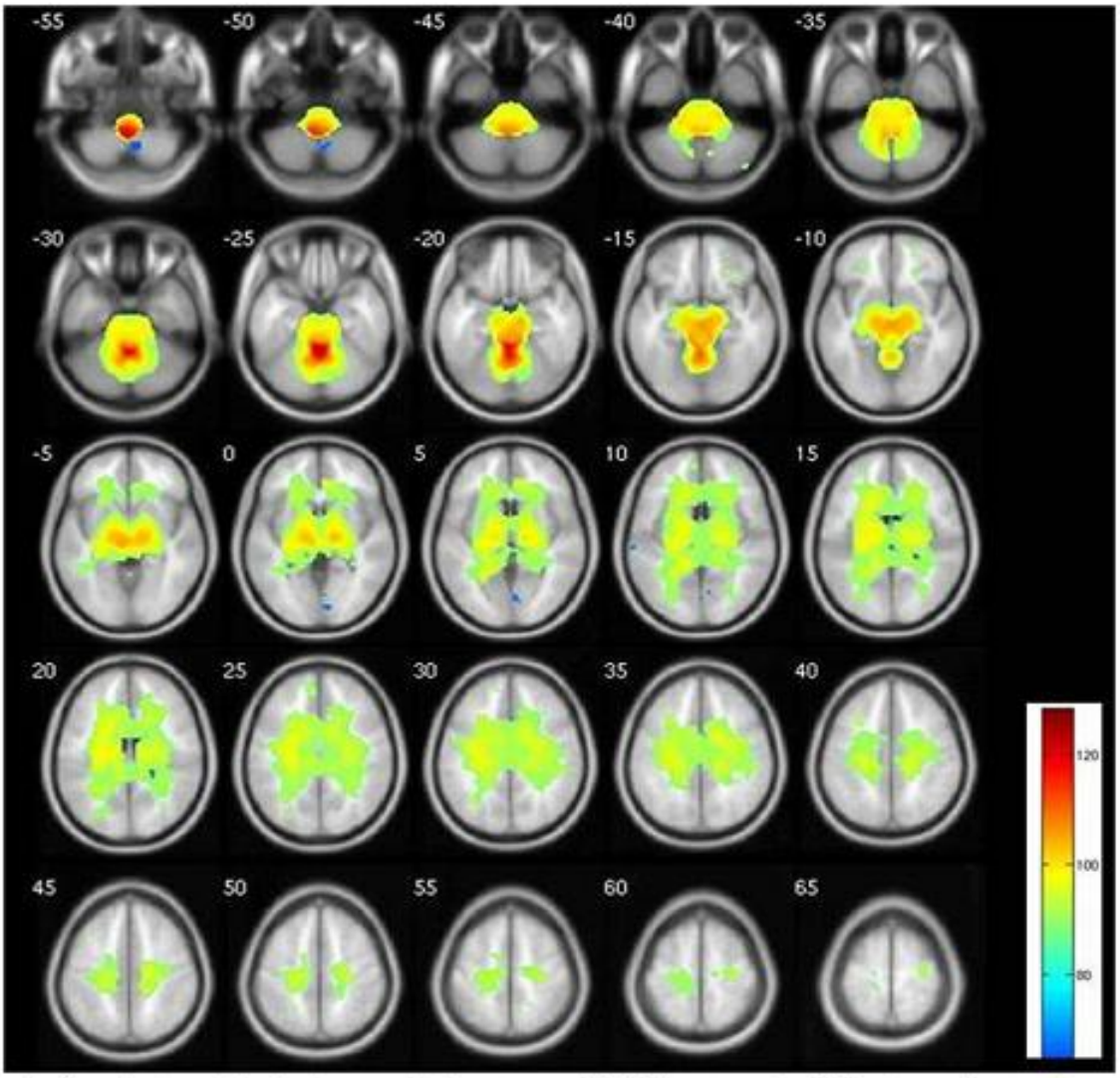


**Fig. 2** Results of voxel-wise analysis showing areas of white matter volumetric reduction in patients with Friedreich's ataxia after comparison with age- and sex-matched controls. Results are shown on the MNI152 1-mm template. MNI *z*-axis coordinates are shown in millimeter above each image. The *color coded bar* represents the *Z* score

is in contrast to previous studies with SCA3 that identified a strong correlation of motor disability and severity of depression [18]. Also, in PD, depressive disorders had been correlated with the degeneration of dopamine

**Table 2** Areas of gray matter atrophy in patients with Friedreich's ataxia and major depression compared with patients with Friedreich's ataxia without major depression

Results reported on height threshold: $T=3.55$, clusters>50 voxels

| Cluster | Cluster size | *T* | *x*, *y*, *z* {mm} MNI coordinates | Anatomic location |
|---|---|---|---|---|
| 1 | 1046 | 6.07 | 20, 64, 3 | R superior frontal gyrus |
| 2 | 749 | 4.47 | 2, 26, −12 | R L medial frontal gyrus anterior cingulate |
| 3 | 257 | 4.97 | −45, −81, −14 | L inferior occipital gyrus |
| 4 | 215 | 4.68 | 28, 48, 37 | R superior frontal gyrus |
| 5 | 138 | 4.92 | 30, 36, 43 | R middle frontal gyrus |
| 6 | 116 | 4.69 | 46, 18, 52 | R middle frontal gyrus |
| 7 | 86 | 4.29 | 18, 46, −27 | R orbital gyrus |

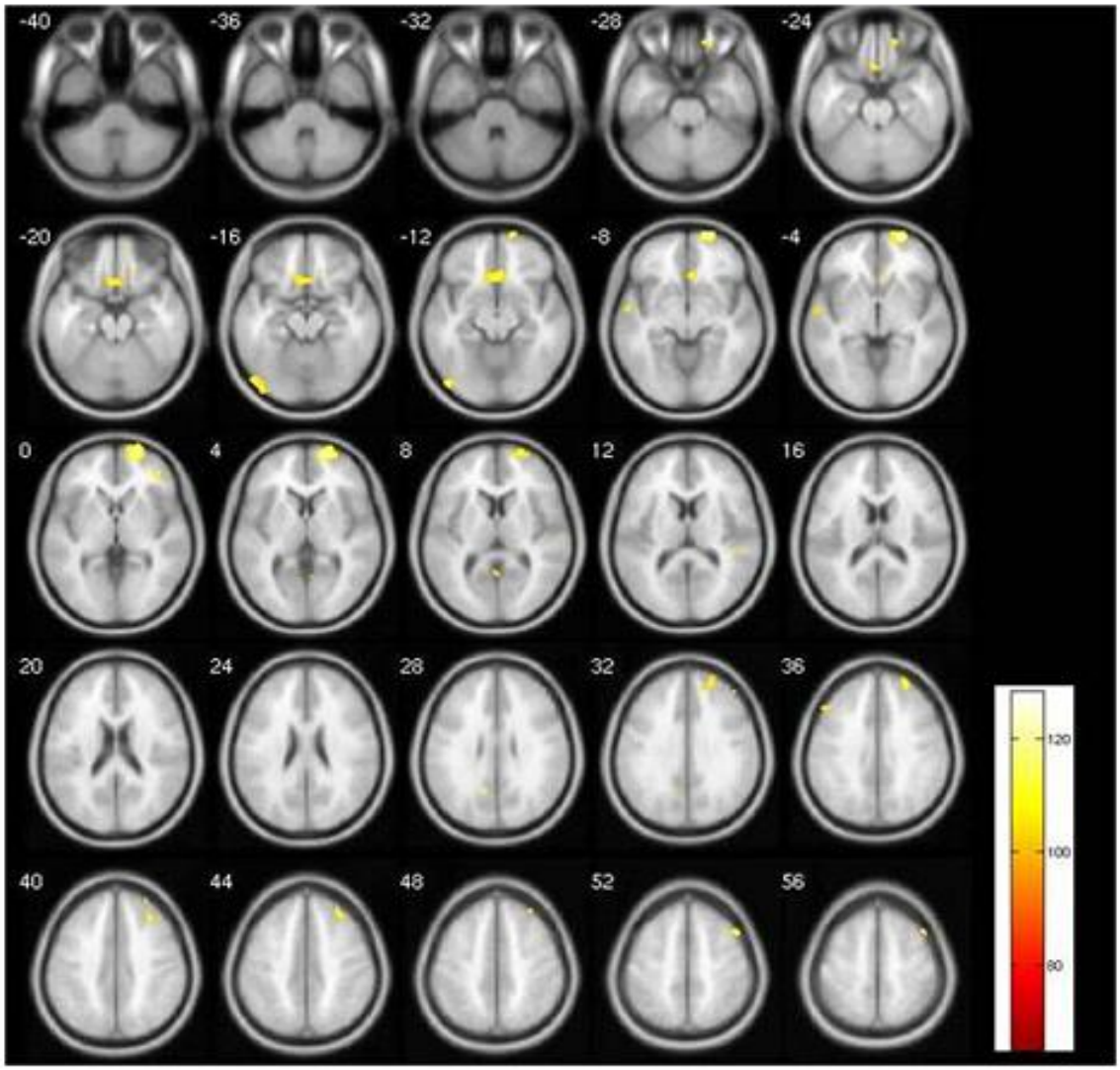


**Fig. 3** Results of voxel-wise analysis showing areas of gray matter volumetric reduction in depressed patients with Friedreich's ataxia after comparison with non-depressed patients with Friedreich's ataxia. Results are shown on the MNI152 1-mm template. MNI *z*-axis coordinates are shown in millimeter above each image. The *color coded bar* represents the *Z* score

neurons and lack in integrity of dopamine mesolimbic pathways [11].

Our MRI-based analyses support the concept of a structural basis for depression in FRDA patients. The whole FRDA group presented significant GM atrophy, especially involving the cerebellum and brainstem, when compared to controls. These results are in accordance with previous reports [21, 22]. The analysis of WM showed volume loss in more extensive areas, including not only the cerebellum and brainstem, but also periventricular areas. Similar findings of damaged WM in supratentorial regions have been reported in VBM and DTI-based studies [22, 23]. Comparing FRDA-DP and FRDA-NDP groups, we did not find significant differences regarding WM volumes. Interestingly, we found in the FRDA-DP group decreased GM volumes in the frontal lobe: bilateral medial frontal gyrus, bilateral anterior cingulate, right superior frontal gyrus, right middle frontal gyrus and right orbital gyrus. In addition, depression severity correlated with GM atrophy at right superior frontal gyrus.

The results of GM atrophy in FRDA-DP patients are in accordance with areas previously described to be affected in neuroimaging studies of major depression. GM volume reductions were reported in many different areas, such as limbic system, temporal lobe, thalamus, cerebellum, and different areas of frontal lobe [24–34]. Two recent meta-analyses showed that anterior cingulate cortex (ACC) was the area mostly correlated with depression. There was evidence of atrophy in other regions, but these were less

consistent across studies: dorsolateral and dorsomedial prefrontal cortex, amygdala and hippocampal and parahippocampal gyrus and thalamus [25, 26].

The prominent GM frontal lobe abnormalities found in FRDA-DP patients are also in line with current neurobiological models for major depression. These support the concept of major depression as a consequence of dysfunctional cortico-limbic networks (involving frontal, limbic, and thalamic regions) [25, 26]. According to the Mayberg model, depression is a disorder that involves abnormalities in a diffuse network, including dorsal (dorsomedial and dorsolateral prefrontal cortex, dorsal anterior cingulate, posterior cingulate cortex) and ventral (subgenual anterior cingulate and amygdala) components as well as the rostral ACC [26]. The ACC has a significant role in emotion regulation, because of its reciprocal connections with both dorsal and ventral components. It is also associated to the generation of negative mood states and internal somatic changes, due to this connection with the amygdala and anterior insula [25, 26, 35].

We have also found damage to the orbitofrontal region, which has been also implicated in the origin of major depression [36]. Functional MRI studies have shown that orbitofrontal cortex is connected to the ACC and dysfunction in this circuit underlies disturbed emotional processing in depressed patients, especially related to the recognition of face expressions [36]. Another region with volumetric reduction in the FRDA-DP group was the prefrontal lobe, namely the superior and middle frontal gyri. Interestingly, these cortical regions have been associated with cognitive aspects in major depression, especially emotion-related attention and the anticipation of negative emotions [37, 38]. In particular, the right superior frontal gyrus seems to be involved in the goal-directed selection of visual stimuli and emotional regulation processes [38].

## Conclusion

Our results thus indicate that major depression might be a rather frequent and often under recognized feature in FRDA patients. Furthermore, depression seems to be associated to structural abnormalities in the frontal lobes. These could be primarily due to the neurodegenerative process related to Frataxin haploinsufficiency. However, previous pathological and in vivo MRI studies did not find cortical damage as a conspicuous finding in FRDA [4]. Therefore, another possibility is that frontal GM abnormalities in FRDA-DP patients could result from the long-term effects of major depression. This hypothesis is particularly interesting if we consider that most individuals in the FRDA-DP group had depressive symptoms for some years. In this setting, the overall pattern of GM abnormalities found in FRDA-DP patients would represent the combination of Frataxin deficiency and long-term depression (with biochemical dysfunction). Further studies with larger samples (including children and teenagers) and employing other MRI-based techniques are certainly needed to better characterize the neuroanatomical abnormalities associated to major depression in FRDA.

**Acknowledgments** This work was supported by Fundação de Amparo à Pesquisa do Estado de São Paulo (FAPESP).

**Conflict of interests** The authors report no conflict of interests regarding this research.

## References

1. Fogel BL, Perlman S. Clinical features and molecular genetics of autosomal recessive cerebellar ataxias. Lancet Neurol. 2007;6:245–57.
2. Campuzano V, Montermini L, Moltó MD, Pianese L, Cossée M, Cavalcanti F, et al. Friedreich's ataxia: autosomal recessive disease caused by anintronic GAA triplet repeat expansion. Science. 1996;271:1423–7.
3. Pandolfo M. Friedreich ataxia. Arch Neurol. 2008;65:1296–303.
4. Koeppen AH. Friedreich's ataxia: pathology, pathogenesis and molecular genetics. J NeurolSci. 2011;303:1–12.
5. Morral JA, Davis AN, Qian J, Gelman BB, Koeppen AH. Pathology and pathogenesis of sensory neuropathy in Friedreich's ataxia. Acta Neuropathol. 2010;120:97–108.
6. Goulart FO, Godke BA, Borges V, Azevedo-Silva SM, Mendes MF, Cendoroglo MS, et al. Fatigue in a cohort of geriatric patients with and without Parkinson's disease. Braz J Med Biol Res. 2009;42:771–5.
7. Friedman JH, Amick MM. Fatigue and daytime somnolence in Machado–Joseph disease (spinocerebellar ataxia type 3). Mov Disord. 2008;23:1323–4.
8. Feldmann A, Illes Z, Kosztolányi P, Illes E, Mike A, Kover F, et al. Morphometric changes of gray matter in Parkinson's disease with depression: a voxel-based morphometry study. Mov Disord. 2008;23:42–6.
9. Epstein E, Farmer JM, Tsou A, Perlman S, Subramony SH, Gomez CM, et al. Health related quality of life measures in Friedreich ataxia. J Neurol Sci. 2008;272:123–8.
10. Paulsen EK, Friedman LS, Myers LM, Lynch DR. Health-related quality of life in children with Friedreich ataxia. Pediatr Neurol. 2010;42:335–7.
11. Cardoso EF, Maia FM, Fregni F, Myczkowski ML, Melo LM, Sato JR, et al. Depression in Parkinson's disease: converge from voxel-based morphometry and functional magnetic resonance in limbic thalamus. NeuroImage. 2009;47:467–72.
12. Filla A, De Michele G, Cavalcanti F, Pianese L, Monticelli A, Campanella G, et al. The relationship between trinucleotide (GAA) repeat length and clinical features in Friedreich ataxia. Am J Hum Genet. 1996;59:554–60.
13. Subramony SH, May W, Lynch D, Gomez C, Fischbeck K, Hallett M, et al. Measuring Friedreich ataxia: interrater reliability of a neurologic rating scale. Neurology. 2005;64:1261–2.
14. Del-Ben CM, Vilela JA, Crippa JA, Hallak JEC, Labate CM, Zuardi AW. Reliability of the structured interview for DSM-IV—clinical scale translated to Portuguese. Rev Bras Psiquiatr. 2001;23:156–9.

15. Gorenstein C, Andrade L. Validation of a Portuguese version of the Beck Depression Inventory and State-Tract Anxiety Inventory in Brazilian subjects. Braz J Med Biol Res. 1996;29:453–7.
16. Ashburner JA. A fast diffeomorphic image registration algorithm. NeuroImage. 2007;38:95–113.
17. Ashburner J, Friston KJ. Voxel-based morphometry—the methods. NeuroImage. 2000;11:805–21.
18. Cecchin CR, Pires AP, Rieder CR, Monte TL, Silveira I, Carvalho T, et al. Depressive symptoms in Machado–Joseph disease (SCA3) patients and their relatives. Community Genet. 2007;10:19–26.
19. Fleck MP, Berlim MT, Lafer B, Sougey EB, Del Porto JA, Brasil MA, et al. Review of the guidelines of the Brazilian Medical Association for the treatment of depression. Rev Bras Psiquiatr. 2009;31:S7–S17.
20. White M, Leconde R, Botez-Marquard T. Neuropsychologic and neuropsychiatric characteristics of patients with Friedreich's ataxia. Acta Neurol Scand. 2000;102:222–6.
21. Della Nave R, Ginestroni A, Giannelli M, Tessa C, Salvatore E, Salvi F, et al. Brain structural damage in Friedreich's ataxia. J Neurol Neurosurg Psychiatry. 2008;79:82–5.
22. França Jr MC, D'Abreu A, Yassuda CL, Bonadia LC, Santos da Silva M, Nucci A, et al. A combined voxel-based morphometry and H-MRS study in patients with Friedreich's ataxia. J Neurol. 2009;256:1114–20.
23. Della Nave R, Ginestroni A, Tessa C, Salvatore E, Bartolomei I, Salvi F, et al. Brain white matter tracts degeneration in Friedreich ataxia. An in vivo MRI study using tract-based spatial statistics and voxel-based morphometry. NeuroImage. 2008;40:19–25.
24. Kostic VS, Filippi M. Neuroanatomical correlates of depression and apathy in Parkinson's disease: magnetic resonance imaging studies. J Neurol Sci. 2011;310:61–3.
25. Du MY, Wu QZ, Yue Q, Li J, Liao Y, Kuang WH, et al. Voxelwise meta-analysis of gray matter reduction in major depressive disorder. Prog Neuropsychopharmacol Biol Psychiatr. 2012;36:11–6.
26. Bora E, Fornito A, Pantelis C, Yücel M. Gray matter abnormalities in major depressive disorder: a meta-analysis of voxel based morphometry studies. J Affect Disord. 2012;138:9–18.
27. Zou K, Deng W, Li T, Zhang B, Jiang L, Huang C, et al. Changes of brain morphometry in first-episode, drug-naive, non-late-life adult patients with major depression: an optimized voxel-based morphometry study. Biol Psychiatry. 2010;67:186–8.
28. Wagner G, Koch K, Schachtzabel C, Reichenbach JR, Sauer H, Schlösser RG. Enhanced rostral anterior cingulate cortex activation during cognitive control is related to orbitofrontal volume reduction in unipolar depression. J Psychiatry Neurosci. 2008;33:199–208.
29. Vasic N, Walter H, Höse A, Wolf RC. Gray matter reduction associated with psychopathology and cognitive dysfunction in unipolar depression: a voxel-based morphometry study. J Affect Disord. 2008;109:107–16.
30. Lee HY, Tae WS, Yoon HK, Lee BT, Paik JW, Son KR, et al. Demonstration of decreased gray matter concentration in the midbrain encompassing the dorsal raphe nucleus and the limbic subcortical regions in major depressive disorder: an optimized voxel-based morphometry study. J Affect Disord. 2011;133:128–36.
31. Peng J, Liu J, Nie B, Li Y, Shan B, Wang G, et al. Cerebral and cerebellar gray matter reduction in first-episode patients with major depressive disorder: a voxel-based morphometry study. Eur J Radiol. 2011;80:395–9.
32. Campbell S, Marriott M, Nahmias C, MacQueen GM. Lower hippocampal volume in patients suffering from depression: a meta-analysis. Am J Psychiatry. 2004;161:598–607.
33. Hamilton J, Siemer M, Gotlib I. Amygdala volume in major depressive disorder: a meta-analysis of magnetic resonance images studies. Mol Psychiatry. 2008;13:993–1000.
34. Koolschijn P, van Haren N, Lensvelt-Mulders G, Hulshoff Pol HE, Kahn RS. Brain volume abnormalities in major depressive disorder: a meta-analysis of magnetic resonance imaging studies. Hum Brain Mapp. 2009;30:3719–35.
35. Ye T, Peng J, Nie B, Gao J, Liu J, Wang G, et al. Altered functional connectivity of dorsolateral prefrontal cortex in first-episode patients with major depressive disorder. Eur J Radiol. 2012. doi:10.1016/j.ejrad.2011.04.058
36. Carballedo A, Scheuerecker J, Meisenzahl E, Schoepf V, Bokde A, Möller HJ, et al. Functional connectivity of emotional processing in depression. J Affect Disord. 2011;134:272–9.
37. Ochsner KN, Gross JJ. The cognitive control of emotion. Trends Cog Sci. 2005;9:242–9.
38. Leung KK, Lee TMC, Wong LS, Li LSW, Yip PSF, Khong L. Neural correlates of attention biases of people with major depressive disorder: a voxel-based morphormetry study. Psychol Med. 2009;39:1097–106.

European Journal of Neurology 2014 doi:10.1111/ene.12448

# Dentate nuclei T2 relaxometry is a reliable neuroimaging marker in Friedreich's ataxia

C. Bonilha da Silva[a], F. P. G. Bergo[a], A. D'Abreu[a], F. Cendes[a], I. Lopes-Cendes[b] and M. C. França Jr[a]

[a]*Department of Neurology and Neuroimaging Laboratory, Faculty of Medicine, University of Campinas – UNICAMP, Campinas, SP; and* [b]*Department of Medical Genetics, Faculty of Medicine, University of Campinas – UNICAMP, Campinas, SP, Brazil*

**Keywords:**
dentate nuclei,
Friedreich's ataxia,
MRI, T2 relaxometry

Received 18 December 2013
Accepted 17 March 2014

**Background and purpose:** In Friedreich's ataxia (FRDA), frataxin deficiency results in iron redistribution in the dentate nuclei (DNC). Clusters of iron cause inhomogeneities in a magnetic field and result in a reduction in T2 relaxation time (T2).

**Methods:** T2 was prospectively evaluated in DNC, putamen, substantia nigra (SN), cerebellar white matter (CWM) and caudate and the correlation with clinical parameters was investigated. Thirty-five patients (range 9–51 years) and 44 controls (12–49 years) underwent T2 multi-echo sequence in a 3T scanner. Twenty-three patients (12–50 years) and 19 controls (14–49 years) were reassessed after 1 year. T2 was evaluated using specialized software (Aftervoxel) and severity of disease was quantified with the Friedreich Ataxia Rating Scale (FARS).

**Results:** T2 of both DNC was significantly shorter in the FRDA group at baseline (right, $58.6 \pm 8.3$ ms vs. $63.7 \pm 8.1$ ms, $P = 0.013$; left, $56.7 \pm 7.7$ ms vs. $62.6 \pm 6.8$ ms, $P = 0.001$). No significant difference was found between groups regarding the SN, putamen, CWM and caudate T2. DNC T2 values correlated with age, FARS total score and FARS III subscore on both sides. Prospectively, there was a significant reduction of T2 in FRDA patients in right and left DNC ($P = 0.001$ and 0.009) but not in other structures. Amongst controls, none of the regions significantly changed after 1 year. DNC T2 change over time correlated with GAA expansions and clinical deterioration (expressed by a change in FARS scores).

**Conclusions:** DNC T2 values are abnormal in FRDA, progress over time and correlate with ataxia severity. These results strongly suggest that DNC relaxometry can be a useful neuroimaging marker in FRDA.

## Introduction

Friedreich's ataxia (FRDA) is the most common autosomal recessive ataxia. The disease typically has an early onset and is characterized by slowly progressive gait ataxia, dysmetria, dysarthria, deep sensory abnormalities (especially proprioceptive sensation), *pes cavus*, scoliosis, cardiomyopathy and diabetes [1,2]. It is caused by a homozygous triplet GAA expansion in the first intron of the *FXN* gene on chromosome 9q13 in 96% of patients [2,3]. The consequence is reduced expression of frataxin, a protein involved with iron–sulfur cluster biosynthesis and oxidative stress inside mitochondria [1].

Frataxin deficiency in FRDA results in abnormal mitochondrial 'iron-trafficking' in the central nervous system [4]. This is especially severe in the dentate nuclei of the cerebellum (DNC), where this iron dysmetabolism was indirectly evidenced by increased light chain ferritin biosynthesis [4]. Although total iron is not increased in DNC, pathological analyses indicate that it is relocated as ferritin in astrocytes and microglia [5]. Interestingly, such abnormal iron distribution in DNC could cause inhomogeneities in the magnetic field and lead to shortened T2 times, with little effect on T1 time [6–8]. Therefore, quantification of iron concentration can be estimated using different magnetic resonance imaging (MRI) techniques, such as magnetic field correlation analyses, susceptibility-weighted methods and relaxation times

Correspondence: M. C. Franca Junior, MD, PhD, Department of Neurology, University of Campinas – UNICAMP, Rua Tessália Vieira de Camargo, 126 Cidade Universitaria 'Zeferino Vaz', Campinas 13083-887, SP, Brazil (tel.: +55 19 3521 9217; fax: +55 19 3521 7933; e-mail: mcfrancajr@uol.com.br).

[9]. Different relaxation-based methods for iron mapping have been used, including spin–lattice relaxation rate (R1 = 1/T1), spin–spin relaxation rate (R2 = 1/T2) and gradient echo methods (R2* = 1/T2* = R2 + R2′) [9]. Several investigations have shown that R1, R2, R2* or R2′ (R2′ = R2* − R2) correlate strongly with iron content in brain tissue [9,10].

A hypointense T2 signal in DNC is indeed a characteristic MRI finding in FRDA [6,7]. However, it is not yet clear whether this abnormality correlates with clinical parameters and what the progression is over time. In this setting, a longitudinal study was designed to investigate the potential usefulness of T2 relaxometry of DNC as a neuroimaging marker in FRDA.

## Methods

### Subject selection

In the cross-sectional study, a group of 35 FRDA patients who were regularly followed at the neurogenetics clinic at UNICAMP hospital between 2010 and 2013 and 44 age- and gender-matched healthy controls were selected. For the prospective analyses, 23 of the 35 FRDA patients and 19 of the 44 controls were reassessed after 1 year. In fact, two patients repeated MRI scans but had major motion artifacts; three patients refused to repeat the scans; five were lost to follow-up (mostly because they moved to distant cities). Two additional patients were unavailable to repeat the scans at the appropriate 1 year interval. In order to keep the interval between examinations as close as possible to 12 months, it was decided not to include them. Regarding controls, our focus was on those individuals who matched the remaining 23 FRDA patients. However, even in this control subgroup, some subjects were not available to repeat the scans and a few presented motion artifacts that precluded the use of their images.

All patients underwent genetic testing and were found to be homozygous for the GAA expansions at the first intron of the *FXN* gene [11]. Individuals with concomitant neurological disorders or unable to perform MRI scans were not included in the study. None of the patients was taking iron-chelating drugs. Clinical (gender, age at disease onset, duration of disease) and genetic data [length of expanded repeat in both longer, $(GAA)_1$, and shorter, $(GAA)_2$, alleles] were recorded. Severity of ataxia was quantified with Friedreich's Ataxia Rating Scale (FARS) on the same day that MRI scans were obtained [12]. FARS total score was defined as the sum of functional staging for ataxia, activities of daily living and neurological examination. FARS III subscore refers only to the neurological examination. This protocol was approved by our institution Research Ethics Committee and written informed consent was obtained from all participants.

In the cross-sectional study, the mean age of patients and controls was 24.8 (range 9–51) years and 26.9 (range 12–44) years, respectively ($P = 0.36$). In the FRDA group there were 13 males and 22 females, whereas in the control group there were 17 males and 27 females ($P = 0.89$). The mean length of $(GAA)_1$ and $(GAA)_2$ alleles was 1021 (range 437–1705) and 878 (range 437–1330), respectively. The mean duration of disease and age at onset were 11.4 ± 8.9 years and 13.3 ± 5.2 years. Mean FARS total score was 77.3 ± 26.7.

In the longitudinal study, the mean age of patients was 26.1 ± 10.8 (range 12–50) years and mean age of controls was 29.2 ± 9.4 (range 14–49 ) years ($P = 0.22$) at baseline. Ten patients were males and 13 patients were females. Nine controls were males and 10 were females ($P = 0.8$). The mean length of $(GAA)_1$ and $(GAA)_2$ alleles was 1024 (range 437–1705) and 864 (range 437–1330), respectively. Mean duration and onset of the disease were 11.4 ± 8.7 and 14.7 ± 5.1 years. The mean interval between evaluations was 12.8 ± 2.1 (range 11–16) months. Mean FARS total score at baseline and follow-up was 77.4 ± 26 and 84.1 ± 25.1, respectively.

### MRI acquisition and analysis

Patients and controls underwent MRI scans in a 3T scanner (Philips Achieva, Amsterdam, the Netherlands) using a standard eight-channel head coil. A T2 multi-echo sequence acquired in a plane perpendicular to the long axis of the hippocampus (TE = 30–60–90–120–150 ms, TR = 3300 ms, voxels of 0.41 × 0.41 × 3.0 $mm^3$, FOV = 180 × 108, 36 slices, 3 mm thickness) was used. In a 3T field, T2 values for gray and white matter range between 40 and 110 ms [13], and our protocol captures this target range. Furthermore, it has been successfully employed to study similar diseases in our laboratory and has an adequate time of acquisition versus image quality balance [14]. The in-house-developed software Aftervoxel 3D Medical Image Visualization (http://www.liv.ic.unicamp.br/~bergo/aftervoxel) was used to visualize DNC, putamen and substantia nigra (SN) bilaterally [14]. Circular regions of interest (ROIs) were placed at each structure and the T2 relaxation times were automatically calculated. T2 relaxation times, computed by the MR scanner, were averaged by Aftervoxel within each ROI (Fig. 1).

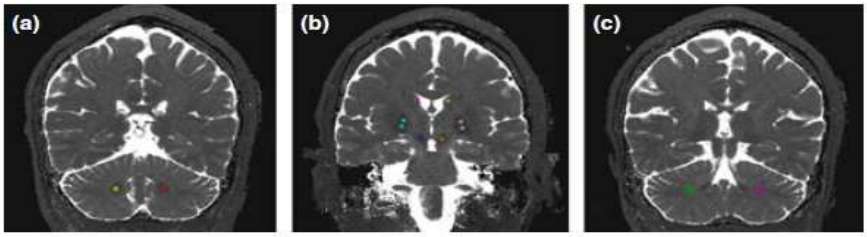


**Figure 1** T2-weighted coronal slices showing the positioning of selected ROIs. (a) Dentate nuclei (yellow and red circles). (b) Substantia nigra (dark blue and orange circles), putamen (light blue and light pink circles) and caudate nuclei (light green and pink circles). (c) Cerebellar white matter (green and pink circles). The ROIs placed in cerebellar white matter are 77.62 $mm^3$, whereas all remaining ROIs are 15.11 $mm^3$.

### Statistical analysis

In the cross-sectional analysis, the Mann–Whitney test was used to compare T2 between patients and controls. The Spearman correlation coefficient was employed to evaluate possible correlations between T2 and disease severity expressed by FARS total score and FARS III subscore. A stepwise backward linear regression was then used to evaluate the association of DNC T2 and $(GAA)_1$, $(GAA)_2$, age, age at onset and duration.

In the longitudinal analysis, a Wilcoxon signed-rank test was used to compare T2 at both time points in each group separately. Percentage change of DNC T2 time, FARS total score and FARS III subscore (neurological examination) for each patient was calculated as described elsewhere [15,16]: [(follow-up of interested value – baseline of interested value)/baseline of interested value]/time (months). The Spearman correlation coefficient was employed to evaluate correlations between percentage changes of DNC T2, FARS total score and FARS III subscore. A stepwise backward linear regression was performed to assess the correlation between DNC T2 change over time and $(GAA)_1$, $(GAA)_2$, age, age at onset and duration. DNC T2 correlated with age both for patients and controls. Therefore, ANCOVA was also employed to compare the percentage change of DNC T2 time in both groups taking into account age as a covariate. All analyses were performed in SYSTAT v.10.2 and the level of significance was set at $P = 0.05$.

## Results

### Cross-sectional study

The T2 relaxation times of the two DNC were significantly different between patients and controls (right side, $P = 0.013$; left side, $P = 0.001$). There was no significant difference between groups regarding SN, putamen, cerebellar white matter and caudate T2 (Table 1). The DNC T2 times correlated with FARS total score and FARS III subscore (right side, $\rho = -0.388$ and $\rho = -0.37$, respectively; left side, $\rho = -0.468$ and $\rho = -0.478$, respectively). In the multiple regression model, age at examination was the only variable significantly associated with DNC T2 both at the right side ($r^2 = 0.51$, $P < 0.001$) and the left side ($r^2 = 0.60$, $P < 0.001$) in the FRDA group (Fig. 2). Amongst controls, DNC T2 also correlated with age (right side, $r^2 = 0.14$, $P = 0.014$, and left side, $r^2 = 0.24$, $P = 0.001$) (Fig. 2).

### Longitudinal study

There was a significant reduction of T2 in FRDA patients in right and left DNC ($P = 0.001$ and $P = 0.009$, respectively). SN, putamen, cerebellar white matter and caudate T2 did not change over time in the patient group. Amongst controls, none of the regions presented change after 1 year. After correction for age, ANCOVA confirmed a significant reduction of DNC T2 in the FRDA group versus controls (right

**Table 1** Transversal results – T2 relaxation time (ms) in patients with FRDA and controls

| | Patients ($n = 35$) | Controls ($n = 44$) | $P$ |
|---|---|---|---|
| R DNC | 58.6 ± 8.3 | 63.7 ± 8.1 | 0.013 |
| L DNC | 56.7 ± 7.7 | 62.6 ± 6.8 | 0.001 |
| R putamen | 52.0 ± 6.3 | 52.7 ± 5.2 | 0.57 |
| L putamen | 52.1 ± 6.1 | 52.7 ± 5.2 | 0.89 |
| R SN | 53.9 ± 6.2 | 52.6 ± 5.7 | 0.29 |
| L SN | 53.7 ± 6.0 | 53.3 ± 5.5 | 0.79 |
| R cerebellar WM | 78.9 ± 3.5 | 79.6 ± 3.7 | 0.33 |
| L cerebellar WM | 80.56 ± 4.9 | 80.0 ± 3.7 | 0.58 |
| R caudate | 77.95 ± 8.0 | 75.6 ± 6.0 | 0.09 |
| L caudate | 73.4 ± 9.1 | 73.1 ± 6.2 | 0.80 |

R, right; L, left; DNC, dentate nuclei of the cerebellum; SN, substantia nigra; WM, white matter.

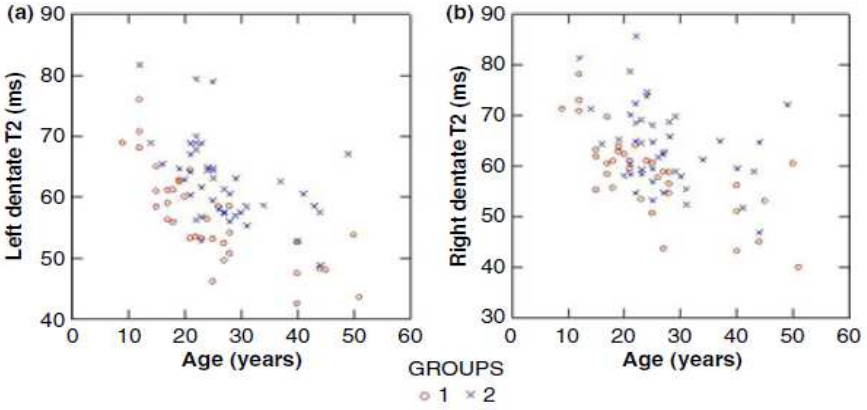


**Figure 2** Scatter plot showing the distribution of DNC T2 times versus age in patients (red) and controls (blue): (a) left side; (b) right side.

**Table 2** Longitudinal results – baseline and follow-up T2 relaxation times (ms) in patients with FRDA and controls

| | Patients ($n$ = 23) | | | Controls ($n$ = 19) | | |
|---|---|---|---|---|---|---|
| | Baseline | Follow-up | $P$ | Baseline | Follow-up | $P$ |
| R DNC | 59.44 ± 9.0 | 54.37 ± 6.7 | 0.001 | 64.00 ± 6.6 | 63.60 ± 5.0 | 0.66 |
| L DNC | 55.93 ± 7.9 | 53.24 ± 6.0 | 0.009 | 62.04 ± 5.0 | 61.58 ± 5.1 | 0.60 |
| R putamen | 52.35 ± 6.5 | 52.04 ± 6.4 | 0.88 | 52.07 ± 4.0 | 52.54 ± 3.9 | 0.84 |
| L putamen | 52.09 ± 6.2 | 52.34 ± 5.7 | 0.90 | 51.9 ± 4.8 | 52.35 ± 4.8 | 0.21 |
| R SN | 52.63 ± 5.9 | 52.77 ± 5.7 | 0.88 | 52.29 ± 3.8 | 53.74 ± 5.6 | 0.14 |
| L SN | 52.88 ± 5.4 | 53.46 ± 6.3 | 0.90 | 51.79 ± 3.9 | 53.29 ± 4.2 | 0.21 |
| R cerebellar WM | 78.73 ± 3.6 | 78.18 ± 2.8 | 0.27 | 79.57 ± 4.6 | 77.43 ± 3.1 | 0.06 |
| L cerebellar WM | 80.27 ± 4.1 | 78.56 ± 4.3 | 0.08 | 79.67 ± 4.8 | 78.28 ± 3.4 | 0.26 |
| R caudate | 78.01 ± 7.5 | 76.22 ± 6.4 | 0.41 | 77.28 ± 7.9 | 76.88 ± 4.9 | 0.93 |
| L caudate | 71.22 ± 6.6 | 71.79 ± 4.8 | 0.40 | 72.85 ± 7.7 | 72.78 ± 5.8 | 0.68 |

R, right; L, left; DNC, dentate nuclei of the cerebellum; SN, substantia nigra; WM, white matter.

side, $P = 0.019$, and left side, $P = 0.026$). The results are presented in Table 2.

In the multiple regression model, percentage change of right DNC T2 correlated with both $(GAA)_1$ and $(GAA)_2$ ($r^2 = 0.316$, $P = 0.025$ and 0.010, respectively). On the left side, the only variable found to be correlated with percentage change of DNC T2 was age at examination ($r^2 = 0.224$, $P = 0.023$). Also, percentage change of right side DNC T2 correlated with percentage change of both FARS total score ($\rho = -0.415$) and FARS III subscore ($\rho = -0.495$) (Fig. 3). On the left, correlation was weaker with these variables ($\rho = -0.35$ and $\rho = -0.22$, respectively).

## Discussion

Biomarkers or neuroimaging markers for FRDA are urgently needed to help in the management of patients and in the design of clinical trials. MRI-based parameters have been investigated recently as possible candidates, e.g. superior cerebellar peduncle volumetry or spinal cord areas [17,18]. Since pathological data identified DNC as a major site of damage in FRDA, some MRI studies focused on this structure [7]. DNC T2 relaxometry was previously shown to be abnormal in subjects with FRDA and considered a surrogate neuroimaging marker for iron deposition in this structure [7,19,20]. However, the correlation of relaxometry with clinical parameters and its progression over time were not investigated. This motivated us to evaluate T2 relaxometry of DNC as a possible neuroimaging marker in FRDA by recruiting a larger sample of subjects in a longitudinal setting.

It was confirmed that T2 relaxation times are abnormal in the DNC but not in the SN or putamen in FRDA [7,19]. In addition, it was found that DNC T2 significantly worsened after 1 year in affected subjects but not in healthy controls. The anatomical substrate for these MRI abnormalities includes neuronal loss, volumetric reduction and especially iron redistribution in the DNC [4,5]. Pathological studies have indeed shown that there is no true accumulation of iron in DNC. In fact, the metal is relocated as ferritin

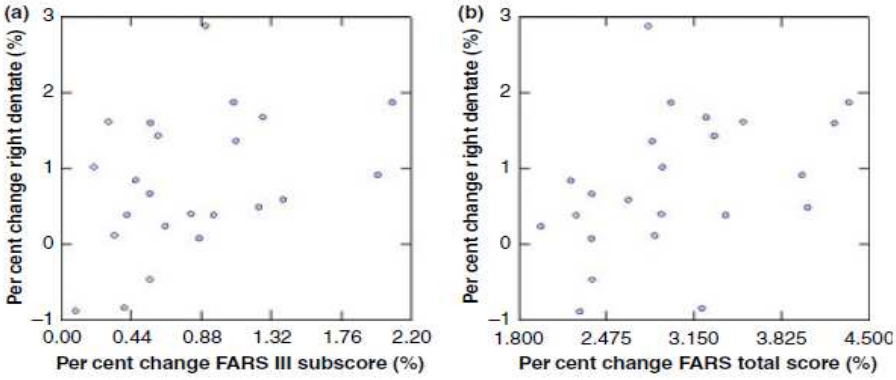


**Figure 3** Scatter plot showing the distribution of percentage change of right DNC T2 times versus (a) percentage change of FARS III subscore and (b) percentage change of FARS total score.

in astrocytes and microglia. As suggested by Koeppen *et al.* it is possible that the local concentration of iron is increased in the DNC (due to marked neuronal loss and atrophy of this structure) and this is the real cause of the shortened T2 found on MRI scans [5]. Another possible explanation for T2 abnormalities would be reduction of water content in DNC. Although there is severe neuronal loss in DNC, it is unclear if there is any modification in water content. Further pathological studies are needed to evaluate this hypothesis [4,8].

Our data also indicate that DNC T2 is strongly related to the age of patients, which is in line with Waldvogel *et al.* [7]. This suggests that iron deposition is dependent on the duration of frataxin deficiency and begins earlier than clinical manifestations. Interestingly, the length of GAA expansions at *FXN* was directly associated with the longitudinal change of DNC T2. Taken together, these data support the idea that GAA expansions accelerate an age-dependent phenomenon of iron deposition in DNC.

On clinical grounds, DNC T2 presented significant correlations with disability. This is especially important because the FARS scale was employed to quantify ataxia severity. This is a disease-specific and validated instrument that has been considered the most reliable one to evaluate FRDA patients [21]. DNC T2 showed an inverse correlation with FARS total score and FARS III subscore. Longitudinal analyses revealed that rates of decline for T2 DNC were associated with clinical deterioration after 1 year. These are novel results that highlight the potential usefulness of DNC T2 relaxometry as a neuroimaging marker for FRDA. Despite this, two open label trials that investigated iron chelators in FRDA have already employed DNC relaxometry [17,18]. In the first one, Boddaert *et al.* treated nine teenage FRDA patients with deferiprone and used T2* relaxometry as an outcome measure [19]. They found small differences between patients and healthy controls regarding DNC T2* relaxometry at baseline. In that cohort, age was surprisingly not associated with DNC relaxometry [19]. These conflicting results are probably due to the small sample recruited. The second study recruited 20 patients receiving deferiprone and idebenone and followed them for 11 months [20]. The authors showed that DNC T2* significantly declined in this period. However, they did not mention whether DNC relaxometry presented any correlation with ataxia severity or age [20]. Note that T2 relaxation times depend on the magnetic field strength of the MR scanner, and measurements obtained with distinct field strengths cannot be compared directly [22,23]. Our focus was also on T2 rather than T2* relaxometry. Although both parameters have robust relationships with brain iron levels, T2 and T2* relaxation times are not exactly the same, which also limits comparison of our results and those of previous studies.

In conclusion, it has been shown that T2 relaxometry shows a change in the DNC of FRDA patients that is consistent with iron accumulation. Furthermore, DNC T2 values are abnormal in FRDA, progress over time and correlate with ataxia severity. These results strongly suggest that DNC relaxometry can be a useful neuroimaging marker in FRDA. Further studies that employ different techniques to estimate iron content in the brain should be performed to validate our data.

## Acknowledgements

Drs MCFJ, AD, FC and IL-C are supported by FAPESP (Fundacão de Amparo à Pesquisa do Estado de São Paulo) and CNPq (Conselho Nacional de Pesquisa-BRAZIL). The funding agencies did not interfere with the design of the study, collection of data or drafting of the paper.

## Disclosure of conflicts of interest

The authors declare no financial or other conflicts of interest.

## References


1. Pandolfo M. Friedreich ataxia. *Arch Neurol* 2008; **65:** 1296–1303.
2. Fogel BL, Perlman S. Clinical features and molecular genetics of autosomal recessive cerebellar ataxias. *Lancet Neurol* 2007; **6:** 245–257.
3. Campuzano V, Montermini L, Moltò MD, *et al*. Friedreich's ataxia: autosomal recessive disease caused by an intronic GAA triplet repeat expansion. *Science* 1996; **271:** 1423–1427.
4. Koeppen AH. Friedreich's ataxia: pathology, pathogenesis and molecular genetics. *J Neurol Sci* 2011; **303:** 1–12.
5. Koeppen AH, Michael SC, Knutson MD, *et al*. The dentate nucleus in Friedreich's ataxia: the role of iron-responsive proteins. *Acta Neuropathol* 2007; **114:** 163–173.
6. Schenck JF. Magnetic resonance imaging of brain iron. *J Neurol Sci* 2003; **207:** 99–102.
7. Waldvogel D, Gelderen P, Hallet M. Increased iron in the dentate nucleus of patients with Friedreich's ataxia. *Ann Neurol* 1999; **46:** 123–125.
8. Martin WR. Quantitative estimation of regional brain iron with magnetic resonance imaging. *Parkinsonism Relat Disord* 2009; **15**(suppl3)**:** S215–S218.
9. Hasan KM, Walimuni IS, Kramer LA, Narayana PA. Human brain mapping using atlas-based T2 relaxometry. *Magn Reson Med* 2011; **67:** 731–739.
10. Hikita T, Abe K, Sakoda S, Tanaka H, Murase K, Fujita N. Determination of transverse relaxation rate for estimating iron deposits in central nervous system. *Neurosci Res* 2005; **51:** 67–71.
11. Filla A, De Michele G, Cavalcanti F, *et al*. The relationship between trinucleotide (GAA) repeat length and clinical features in Friedreich ataxia. *Am J Hum Genet* 1996; **59:** 554–560.
12. Subramony SH, May W, Lynch D, *et al*. Measuring Friedreich ataxia: interrater reliability of a neurologic rating scale. *Neurology* 2005; **64:** 1261–1262.
13. Wansapura JP, Holland SK, Dunn RS, Ball WS. NMR relaxation time in the human brain at 3.0 tesla. *J Magn Reson Imaging* 1999; **9:** 531–538.
14. Guimarães RP, D'Abreu A, Yasuda CL, *et al*. A multimodal evaluation of microstructural white matter damage in spinocerebellar ataxia type 3. *Mov Disord* 2013; **28:** 1125–1132.
15. Reetz K, Costa AS, Mirzazade S, *et al*. Genotype-specific patterns of atrophy progression are more sensitive than clinical decline in SCA1, SCA3 and SCA6. *Brain* 2013; **136:** 905–917.
16. Risacher SL, Shen L, West JD, *et al*. Longitudinal MRI atrophy biomarkers: relationship to conversion in the ADNI cohort. *Neurobiol Aging* 2010; **31:** 1401–1418.
17. Akhlaghi H, Corben L, Georgiou-Karistianis N, *et al*. Superior cerebellar peduncle atrophy in Friedreich's ataxia correlates with disease symptoms. *Cerebellum* 2011; **10:** 81–87.
18. Chevis CF, da Silva CB, D'Abreu A, *et al*. Spinal cord atrophy correlates with disability in Friedreich's ataxia. *Cerebellum* 2013; **12:** 43–47.
19. Boddaert N, Sang KHLQ, Rötig A, *et al*. Selective iron chelation in Friedreich ataxia: biologic and clinical implications. *Blood* 2007; **110:** 401–408.
20. Velasco-Sánchez D, Aracil A, Montero R, *et al*. Combined therapy with idebenone and deferiprone in patients with Friedreich's ataxia. *Cerebellum* 2011; **10:** 1–8.
21. Fahey MC, Corben L, Collins V, Churchyard AJ, Delatycki MB. How is disease progress in Friedreich's ataxia best measured? A study of four rating scales. *J Neurol Neurosurg Psychiatry* 2007; **78:** 411–413.
22. Brooks DJ, Luthert P, Gadian D, *et al*. Does signal-attenuation on high-field T2-weighted MRI of the brain reflect regional cerebral iron deposition? Observations on the relationship between regional cerebral water proton T2 values and iron levels. *J Neurol Neurosurg Psychiatry* 1989; **52:** 108–111.
23. Vymazal J, Brooks RA, Zak O, McRill C, Shen C, Di Chiro G. T1 and T2 of ferritin at different field strengths: effect on MRI. *Magn Reson Med* 1992; **27:** 368–374.

**Longitudinal multimodal neuroimaging study in Friedreich's ataxia**

Cynthia B. da Silva[1], Clarissa L Yassuda[1], Thiago J R Rezende[1], Brunno M Campos[1], Anelyssa D'Abreu[1], Fernando Cendes[1], Iscia Lopes-Cendes[2], Marcondes C. França Jr[1]

Department of Neurology and Neuroimaging Laboratory[1] and Medical Genetics[2], Faculty of Medicine, University of Campinas – UNICAMP, Campinas, SP, BRAZIL

**Word count:** Title – 7 words, Abstract – 347, Total count Manuscript – 4256, Figures –8, Tables –11, References – 38

**Running title:** VBM, DTI and Freesurferanalysis in Friedreich's ataxia

**Keywords:** Friedreich's ataxia, MRI, VBM, DTI, Freesurfer

The authors report no conflict of interests regarding this research.

**Address correspondence to:**

Marcondes C. França Junior, MD, PhD

Department of Neurology, University of Campinas – UNICAMP.

Rua Tessália Vieira de Camargo, 126. Cidade Universitaria "Zeferino Vaz"

Campinas, SP, Brazil- 13083-887

Tel: +55 19 3521 9217, Fax: +55 19 3521 7933

E-mail: mcfrancajr@uol.com.br

Submetido ao periódico *Brain*

**Abstract**

Friedreich's ataxia (FRDA) is the most frequent autosomal recessive ataxia and characterized by slow but relentless progression. Brainstem, cerebellum and superior cerebellar pedunclesare known to be involved in the disease, however,there are few studies looking at supratentorial damage and the natural history of these neuroanatomical abnormalities. Therefore, we designed a multimodal and longitudinal investigation to address these issues in a cohort of 31 patients with FRDA. Subjects were evaluated at baseline, after one year and after 2 years. To assess gray matter (GM), we employed two automated techniques: voxel-based morphometry (VBM) and Cortical thickness measurements using the FreeSurfer toolbox. We also measured the volumes of the dentate nuclei of the cerebellum and superior cerebellar peduncles through a semi-automatic segmentation method. White matter (WM) was evaluated using tract-based spatial statistics (TBSS). We perfomed transversal (comparisons between patients and controls) as well as longitudinal analyses (group-adjusted comparison between two time points). Group comparison between patients and controls revealed macrostructural differences at baseline. There was GM atrophy in the cerebellum (including the dentate nuclei and superior cerebellar peduncles), brainstem, both precentral and inferior frontal gyri, right postcentral gyrus and left middle temporal gyrus; and WM atrophy in cerebellum, brainstem and extensive periventricular areas. TBSS found extensive microstructural damage including superior cerebellar peduncles, corpus callosum and pyramidal tracts. Cerebellar and brainstem abnormalities did correlate with clinical parameters. Longitudinal analyses identified progressive GM atrophy in both inferior temporal gyri, occipital lobes, posterior cerebellar lobes, superior and middle frontal gyrus, left precentral gyrus, right inferior frontal gyrus, insula, inferior parietal lobe and middle and superior temporal gyrus after 2 years. In contrast, there was progressive WM reduction at the

right temporal lobe and hippocampus, left caudate nucleus and left cingulate gyrus. No significant difference in the patient group between baseline and follow-up regarding DTI-based parameterswas found. These data suggest that FRDA patients present more widespread GM and WM damage than previously reported, including not only infratentoral areas, but also supratentorial structures. Furthermore, FRDA patients have progressive structural abnormalities in GM and WM amenable to detection in a 2 year follow-up.

## Introduction

Friedreich's Ataxia (FRDA) is the most common autosomal recessive ataxia with early onset and characterized by slowly progressive gait ataxia, dysmetria, dysarthria, deep sensory abnormalities (especially proprioceptive sensation), *pes cavus*, scoliosis, cardiomyopathy, and diabetes (Pandolfo, 2008). FRDA is caused by a homozygous triplet GAA expansion in the first intron of the *FXN* gene on chromosome 9q13 in 96% of patients (Fogel and Perlman, 2007; Campuzano et al, 1996). As consequence, there is dramatic reduction in the expression of the protein Frataxin that ultimately leads to mitochondrial dysfunction and neurodegeneration (Pandolfo, 2008).

Pathological studies showed that dorsal root ganglia, pyramidal tracts and dentate nuclei (DN) are the major sites of damage in FRDA. (Koeppen, 2011; Morral et al, 2010). These regions are clearly associated to the motor and sensory manifestations typical of the disease. These findings are in accordance with the available neuroimaging studies. Previous Voxel-based morphometry (VBM) studies indeed showed gray matter (GM) and white matter (WM) atrophy in portions of the cerebellum and brainstem (Della Nave el al, 2008; Della Nave el al, 2008;

França et al, 2009). Also, other studies, using different techniques, showed deep WM damage in brainstem, cerebellum and cerebellar peduncles (Della Nave et al, 2008; Rizzo et al, 2011; Pagani et al, 2010; França et al, 2009; Akhlaghi et al, 2011). However, few studies addressed cortical and supratentorial white matter damage in the disease (França et al, 2009). This point certainly deserves further studies because some recent reports identified additional manifestations in subjects with FRDA, such as mood disorders, chorea and cognitive dysfunction, which suggest that neurodegeneration might extend to other regions (Silva et al, 2012; Hanna et al, 1998;Mantovan et al, 2006; Akhlaghi et al, 2014).

Another unsettled issue about FRDA is the natural history of structural damage. Although the disease has a progressive course, few neuroimaging studies addressed structural abnormalities in a prospective setting (Bonilha da Silva et al, 2014; Santner et al, 2014). It is not clear which regions degenerate faster in the disease, and whether the rate of such atrophy is related to the rate of clinical deterioration.

In this setting, we designed a longitudinal study to investigate brain damage in FRDA patients using a multimodal MRI-based evaluation, including volumetric analyses, cortical thickness measurements and diffusion tensor imaging (DTI). Our primary objectives were to identify the extension of brain damage in the disease (including cerebral cortex); to determine whether these structural abnormalities are progressive over the time; and to evaluate whether these abnormalities correlate with disease severity/progression. We hypothesize that some of these MRI metrics might prove useful as neuroimaging markers for FRDA and more sensitive to detect changes than clinical parameters in isolation.

## Materials and Methods

*Subjects' Selection*

We selected a group of FRDA patients that were regularly followed at the Neurogenetics outpatient clinic at UNICAMP hospital between 2009 and 2014. Thirty-one FRDA patients and 40 age-gender matched healthy controls were selected for VBM and Freesurfer cross-sectional analysis. For VBM and Freesurfer longitudinal study, twenty-four FRDA patients and twenty-six controls were reassessed after one year and sixteen FRDA patients and sixteencontrols after two years.

All patients underwent genetic testing and found to be homozygous for the GAA expansions at the first intron of the *FXN* gene (Filla et al, 1996). Individuals with concomitant neurological disorders or unable to perform MRI scans were not included in the study.Clinical (gender, age at disease onset, duration of disease, clinical subtype) and genetic data (length of expanded repeat in both shorter, GAA1 and longer, GAA2 alleles) were recorded. Severity of ataxia was quantified with Friedreich's ataxia rating scale (FARS) (Subramony et al, 2005). FARS total score was defined as the sum of functional staging for ataxia, activities of daily living and neurological examination. FARS III subscore refers only to the neurological examination.

This protocol was approved by Research Ethics Committee of our institution and a written informed consent was obtained from all participants.

For VBM and Freesurfer analysis, in cross-sectional analysis, mean age of patients and controls was 27.3 (range 15-51) and 26.6 years (range 17-49), respectively (p=0.55). In the FRDA group, there were 11males and 20 females, whereas in the control group, there

were16males and 24females. Mean length of $(GAA)_1$ and $(GAA)_2$ alleles were 1013 (range 437-1705) and 853 (range 437-1330), respectively. Mean duration of disease and age at onset were 12.9±9 years and 14.3±5.0 years. Mean FARS total score was 81.5±28.6.

In the VBM-based analysis, with one year follow-up, mean age of patients and controls was 26.4±10.2 and 27.3±4.9 years, respectively (p=0.15) at baseline. In the FRDA group, there were 9 men and 15 women, whereas in the control group, there were 10 men and 16 women. Mean length of $(GAA)_1$ and $(GAA)_2$ alleles were 1062 (range 437-1705) and 876 (range 437-1330), respectively. Mean duration of disease and age at onset were 11.9±8.3 years and 14.5±5.3 years at baseline. Mean FARS total score at baseline and follow-up were 72.4±24.9 and 81.2±24.7, respectively. In two years follow-up, mean age of patients and controls was 27.2±8.9 and 28.1±5.5 years, respectively (p=0.72) at baseline. In the FRDA group, there were 7 men and 9 women, whereas in the control group, there were 6 men and 10 women. Mean length of $(GAA)_1$ and $(GAA)_2$ alleles were 1113 (range 759-1705) and 920 (range 610-1330), respectively. Mean duration of disease and age at onset were 11.8±8.3 years and 15.3±4.2 years at baseline. Mean FARS total score at baseline and follow-up were 74.8±25.7 and 87.9±26.5, respectively.

We also employed a pilot study with DTI analysis, which started after the beginning of VBM and Fressurfer studies. For transversal DTI analysis, twenty-six patients and 29 age-gender matched healthy controls were selected. We also reassessed after twelve patients after one year. In cross-sectional DTI analysis, mean age of patients and controls was 26.8 (range 16-51) and 27.5 years (range 17-49), respectively (p=0.78). In FRDA group, there were 9 males and 17 females, whereas in control group, there were 10 males and 19 females.Mean length of $(GAA)_1$ and $(GAA)_2$ alleles were 1011 (range 437-1705) and 843 (range 437-1330), respectively. Mean duration of disease and age at onset were 12.4±8.6 years and 14±5.3 years. Mean FARS total

score was 78.5±27.1. For longitudinal study, mean age of patients at baseline was 27.5 years (range 15-50). Mean length of $(GAA)_1$ and $(GAA)_2$ alleles were 838 (range 437-1167) and 705 (range 437-880), respectively. Mean duration of disease and age at onset were 11±8.4 years and 16.5±6.7 years. Mean FARS total score at baseline and follow-up were 66±23.7 and 73±21.8, respectively.

*Image acquisition*

All patients and controls underwent MRI scans on a Phillips Achieva-Intera 3 T scanner at UNICAMP hospital. T1 and T2 weighted images were acquired in axial, coronal and sagittal planes with thin cuts. We also obtained two specific sequences that were later employed for volumetric (VBM/ Freesurfer) and DTI analyses, respectively.

1. Volumetric (3D) T1 gradient echo images—acquired in the sagittal plane with 1 mm slice thickness (flip angle=35°, TR=7.1 ms, TE=3.2 ms, matrix=240×240, field of view=24×24 cm).

2. DTI—undertaken a 32 direction non-collinear echoplanar sequence (flip angle=90°, voxel size=1×1×2 $mm^3$, TR=8500 ms, TE=61 ms, matrix=128×128, field of view=256×256 mm, 70 slices with 3 mm thickness, b value=1000).

*VBM protocol and analysis*

Volumetric images were converted into a NIfTI file and then used for VBM analysis. We used the SPM 8 software (Wellcome Department of Imaging Neuroscience, London, England,

www.fil.ion.ucl.ac.uk) and VBM 8 (http://dbm.neuro.uni-jena.de/vbm8/) running on MATLAB 8.0.0 to perform several fully automated imaging pre-processing steps, including spatial normalization of all images to the same stereotaxic space, segmentation into white and gray matter and cerebrospinal fluid compartments, correction for volume changes induced by spatial normalization (modulation) and smoothing. Spatial normalization was accomplished with the DARTEL algorithm that significantly reduces the imprecision of intersubject registration (Ashburner, 2007). Processed images were compared using a voxel-wise statistical analysis (Ashburner and Friston, 2000). We used two sample T-test from SPM to search for differences in WM and GM volumes between FRDA patients vs controls. In cross-sectional study, the results were corrected for multiple comparisons using false discovery rate (FDR) of 5% and significant differences set at $p<0.05$. Only cluster sizes>30 voxels were reported. In order to display the results and precise their anatomical location we used an additional SPM extension, XJVIEW (http://www.alivelearn.net/xjview/). We also performed regression analyses with SPM to investigate the correlation between GM and WM volumes and clinical data (onset, duration, FARS score and FARS III subscore). On longitudinal study, voxel-wise grey and white matter differences were examined using a flexible factorial design assessing time (baseline and follow-up) x groups and significant results were considered at uncorrected $p<0.001$ (Gläscher and Gitelman, 2008; Jason et al, 2014).

*ROI-based volumetry and mean intensity of dentate nuclei and superior cerebellar peduncle*

Regions of interest (ROI) of the dentate nuclei and superior cerebellar peduncles were manually drawn on a normalized template. This template was createdbased on the T1 weighted

images of our control group, aiming to improve the anatomical matching to study demography. Sequentially, the method uses a 3D deformation fields matrix of each subject to apply an inverse normalization operation (SPM8-Deformation fields algorithm), using the variants between native and standardized space to bring the normalized ROIs to each subject specific space. Finally, each deformed ROI was overlaid to the raw images and the quantitative values of mean intensity and volume were estimated individually.

We performed Mann-Whitney test to compare the values from dentate nuclei and superior cerebellar peduncles between patients and controls. We used Spearman correlation coefficient to evaluate possible correlations between DTI values and clinical data. In the longitudinal analysis, a Wilcoxon signed-rank test was used to compare the means at both time points in each group separately. All analysis were performed in SYSTAT v.10.2 and level of significance was set at p=0.05.

*Freesurfer analysis*

Cortical thickness and subcortical volumes were determined using the FreeSurfer software (5.3 version) according to the protocol suggested by Fischl and Dale (Fischl and Dale, 2000). The images were corrected for inhomogeneity from magnetic field, ranged to Talairach and Tournoux atlas (Tailarach and Tournoux, 1988) and skull-stripped. Next, voxels were labeled as WM, GM and cerebral spinal fluid CSF. Then, using triangles meshes, two surfaces are created: the white surface, which is the interface between GM and WM, and the pial surface (Fischl and Dale, 2000). Cortical thickness was calculated as the shortest distance between the pial and white surface at each vertex across the cortical mantle. For all analyses, we used a

Gaussian filter with 10 mm FWHM for smoothing. Furthermore, estimated total intracranial volume (eTIV) (Buckner et al, 2004) and the volume for subcortical regions (Fischl et al, 2002) were calculated. Regional cortical thickness variations between the patient and control groups were assessed using a General Linear Model (GLM) with age, gender and eTIV as regressors. We considered cortical regions defined by parcellation according to the anatomical atlas of Desikan (Desikan et al, 2006). In order to correct for multiple comparisons, Dunn-Sidak multiple comparison test was employed (level of significance alpha=0.001). We then performed GLM to assess the correlation between these cortical thickness and subcortical volumes with clinical parameters (GAA, onset, duration of the disease FARS score and FARS III subscore). In these analyses, we considered those regions with significant cortical atrophy and those subcortical regions with significant volumetric reduction compared to controls. We employed age, eTIV and gender as covariates. P values $< 0.05$ were considered significant. All analyses were performed in SYSTAT v.10.2.

*TBSS*

We obtained maps of fractional anisotropy (FA), mean diffusivity (MD), radial diffusivity (RD, which was created by averaging the eigenvectors L2 and L3), and axial diffusivity (AD) using the FMRIB diffusion toolbox which is part of the FSL software version 4.1.4 (Smith et al, 2004). Comparison of groups was then carried out using TBSS on the FSL software version 4.1.4 (Smith et al, 2006). TBSS involves several pre-processing steps before final analyses. All FA images are first aligned to a standard space using the nonlinear registration. The next step involves the creation of a mean FA template which then enables the

creation of the mean FA skeleton. Thereafter, each patient aligned FA map is then projected over this skeleton; this is an essential step in the processing algorithm because it removes the effect of cross-subject spatial variability. To visualize the statistical maps of MD, AD and RD, these parameters were applied over the mean FA skeleton.

The statistical analysis was done using a two-sample t-test to look for differences between patients and controls in FA, MD, AD and RD parameters. We used a Threshold-Free Cluster Enhancement (TFCE) to correct the statistical maps for multiple comparisons (p-value<0.05). In addition, we used Johns Hopkins white matter DTI based atlas, available in the FSL software, to identify the impaired white matter fiber tracts.

*Tractography*

Based on TBSS results, we opted to study separately the pyramidal tracts andcorpus callosum of each subject usingdeterministic tractography. The tensor calculation of all images was performed using the Explore DTI software (A. Leemans, University Medical Center, Utrecht, The Netherlands) and the subsequent fiber tractography through a unbiased semiautomatic deterministic methodology briefly described below (Lebel et al, 2008). Basically, regions of interest (ROIs) to seed the tract were manually drawn on a normalized template. This template was created with non-diffusion weighted images of 10 Brazilian control subjects (mean age=33 years; age range=22-47 years; 50% women). Sequentially, the method uses the 3D deformation fields matrix of each subject to apply an inverse normalization operation (SPM8-Deformation fields algorithm), using the variants between native and standardized space to bring

the normalized ROIs to that subject specific space. Finally, the adjusted (native space) ROIs were used as strategy to the fiber tracking.

The fiber tracking parameters were set the same for all subjects: minimal FA to start track=0.25; minimal FA to keep tracking=0.25; maximal tract angle=20° minimal fiber length=10 mm. The resultant tracts were visually checked and the average FA, AD and RD were separately calculated for each hemisphere. The diffusion values were estimated by averaging over all voxels in a given tract.

We performed Mann-Whitney test to compare patients and controls the values from pyramidal tract and corpus callosum on automatic tractography. We used Spearman correlation coefficient to evaluate possible correlations between DTI values and clinical data. In the longitudinal analysis, a Wilcoxon signed-rank test was used to compare the means at both time points in each group separately. All analysis were performed in SYSTAT v.10.2 and level of significance was set at p=0.05.

## Results

*VBM transversal results*

The whole-brain VBM analysis comparing all FRDA patients and controls showed GM atrophy in the posterior and anterior lobes of both cerebellar hemispheres, brainstem and occipital lobes, but also bilateral precentral gyri, right postcentral gyrus, bilateral inferior frontal gyri and left middle temporal gyrus (Table 1; Figure 1). WM atrophy was particularly severe at the posterior lobes of the cerebellum, superior cerebellar peduncles and brainstem. We also found WM volumetric reduction in periventricular areas, including bilateral frontal lobes,

cingulate gyri, limbic lobes, corpus callosum, lentiform nuclei, thalami, temporal lobes, occipital lobes, precentral and postcentral gyrus (Table 1; Figure 1).

Regression analyses have shown that duration of disease correlated inversely with GM and WM volumes at both cerebellar hemispheres, frontal regions, including precentral gyri and suplementar motor areas, and limbic structures, such as the cingulate gyri. We also found correlation with an extensive area at occipital, temporal lobes, and deep structures. FARS score and FARS III subscore showed similar results, which had an important negative correlation with both cerebellar structures, brainstem, caudate, putamen and thalami, and also cingulate gyrus, precentral and postcentral gyri and others regions at frontal, temporal and occipital lobes (Table 2-4; Figure 2-4).

*VBM longitudinal study -one year follow-up results*

After one year, we foundprogressive GM atrophy in right inferior temporal gyrus, bilateral middle temporal gyrus, left uncus, left middle frontal gyrus, left inferior frontal gyrus in the patient group (Table 5; Figure 5, 7). There were no areas of significant WM loss in patients with FRDA.

*VBM longitudinal study - two years follow-up results*

The whole-brain VBM analysis showed GM atrophy in bilateral inferior temporal gyrus, bilateral posterior cerebellar lobes, bilateral occipital lobes, bilateral superior and middle frontal gyrus, right insula, left precentral gyrus, right inferior frontal gyrus, right inferior parietal lobe,

right middle and superior temporal gyrus. We found WM atrophy at right temporal lobe and hippocampus, left caudate and left cingulate gyrus, including the anterior region (Table 5; Figure 6-7).

*ROI-based volumetry of dentate nuclei and superior cerebellar peduncle transversal results*

On transversal study, FRDA patients significantly difference in ROI-based volumetry of both DN and SCP compared with controls (DN – right: 0.3949±0.0725 vs 0.5221±0.0578, $p<0.001$; left: 0.3983±0.0601 vs 0.5267±0.0481, $p<0.001$, respectively; SCP – right: 0.0652±0.0118 vs 0.0823±0.013, $p<0.001$; left: 0.0515±0.015 vs 0.0785±0.0115, $p<0.001$, respectively) (Table 6).

In regression analysis, both DN correlated negatively with FARS III subscore (right: r=-0.4813, p=0.01; left: r=-0.4898, p=0.01), FARS score (right: r=-0.5033, p=0.008; left: r=-0.5011, p=0.009). Left DN correlated negatively with duration (r=-0.391, p=0.04). Left SCP correlated negatively with FARS III subscore (r=-0.4047, p=0.04), FARS score (r=-0.4025, p=0.04) and duration (r=-0.4042, p=0.04) and positively with onset (r=0.406, p=0.04).

*ROI-based volumetry of dentate nuclei and superior cerebellar peduncle longitudinal results*

ROI-based volumetry of DN and SCP did not present significantly difference between baseline and follow-up in FRDA patients or controls (Table 7).

*Freesurfer transversal results*

FRDA patients showed significantly thinner cerebral cortex in left calcarine gyrus, at both precentral gyri and left superior temporal gyrus. On volumetric analysis, several subcortical structures presented significant smaller volumes in FRDA patients, which includes brainstem, corpus callosum, bilateral cerebellar cortex, both putamen, thalami and ventral diencephali (Tabela 8).

In multiple regression model, FARS score correlated with volume of brainstem ($r^2$=0.632, p=0.002), left and right cerebellar cortex ($r^2$=0.587, p=0.018 and $r^2$=0.599, p=0.006, respectively), right putamen ($r^2$=0.525, p=0.049), right thalamus ($r^2$=0.699, p=0.001) and left and right ventral diencephali ($r^2$=0.62, p=0.002 and $r^2$=0.699, p=0.001, respectively). FARS III sub-score correlated with brainstem ($r^2$=0.659, p=0.001), left and right cerebellar cortex ($r^2$=0.577, p=0.025 and $r^2$=0.583, p=0.01), left and right ventral diencephali ($r^2$=0.656, p=0.001 and $r^2$=0.714, p=0.000, respectively) and right thalamus ($r^2$=0.717, p=0.001). Brainstem volumes correlated with duration ($r^2$=0.671, p=0.001) and onset ($r^2$=0.664, p=0.002).

*DTI transversal results*

TBSS identified extensive microstructural damage when patients with FRDA were compared with healthy controls. We identified reduced FA mostly in bilateral superior cerebellar peduncles (SCP), corpus callosum and pyramidal tracts. These same areas presented increased MD, AD and RD (Figure 8).

Automatic tractography showed significantly reduced FA values at pyramidal tracts and corpus callosum for either hemisphere individually and on average among FRDA patients. MD values were significantly higher in FRDA patients at corpus callosum for both sides and average, but not at pyramidal tracts. AD values were significantly higher in FRDA patients for the right and left means, but not for the average at pyramidal tract; at corpus callosum, all AD values were significantly higher. RD values were significantly higher in FRDA patients at right hemisphere and average of pyramidal tract and for all means at corpus callosum (Table 9-10).

In regression analysis, some corpus callosum values correlated with clinical parameters. Age correlated inversely with FA average (r=-0.425, p=0.031) and positively with MD average and RD average (r=0.392, p=0.048 and r=0.440, p=0.025, respectively). The same results were found with FARS score (FA average: r=-0.398, p=0.044; MD average: r=0.438, p=0.025; RD average: r=0.468, p=0.016) and duration of disease (FA average: r=-0.457, p=0.019; MD average: r=0.45, p=0.021; RD average: r=0.491, p=0.011), while FARS III subscore correlated with RD average (r=0.403, p=0.041). FA, MD, AD and RD average of controls did not correlate with age (p=0.35, p=0.41, p=0.80 and p=0.26, respectively).

*DTI longitudinal results*

After one-year follow-up, there was no significant difference at FA, MD, AD and RD average at pyramidal tract (p=0.69, p=0.44, p=0.38 and p=0.71, respectively) and corpus callosum (p=0.43, p=0.43, p=0.51 and 0.40, respectively) (Table 11).

## Discussion

There are some neuroimaging studies devoted to investigate patients with FRDA (Della Nave et al, 2008; Pagani et al, 2010; França Jr et al, 2009; Della Nave et al, 2008). Although they have contributed significantly to improve our knowledge about the disease, very few employed a multimodal approach and a longitudinal setting. One of the major goals in FRDA research is to identify reliable biomarkers for long term follow-up. Recent studies highlighted some MRI-based parameters as interesting candidates, such as dentate nuclei T2 relaxometry and spinal cord area quantification (Bonilha da Silva et al, 2014; Chevis et al, 2012). In this scenario, we designed a longitudinal and multimodal MRI study including a large cohort of patients with FRDA. Our objective was to determine the extent of neurodegeneration related to the disease as well as to characterize the natural history of such damage.

Our transversal results identified widespread macrostructural CNS damage in FRDA, including both GM and WM. We found significant GM and WM reduction in the deep cerebellar nuclei (dentate and peridentate regions) and brainstem, which is in accordance with previous studies (Della Nave et al, 2008; Pagani et al, 2010; França Jr et al, 2009; Della Nave et al, 2008). The new finding is that we also observed GM atrophy affecting supratentorial areas, including both precentral gyri. WM atrophy was much more widespread than previously reported (Della Nave et al, 2008; Pagani et al, 2010; França Jr et al, 2009; Della Nave et al, 2008). We found diffuse WM loss in periventricular areas, and especially in the corpus callosum (CC). Several infratentorial WM tracts were also found to be atrophic, such as SCP. Damage to this particular pathway reflects degeneration of the major efferent cerebellar tracts that emerge from DN – dentate-thalamic and dentate-rubral (Akhlaghi et al, 2011; Della Nave et al, 2008).

Microstructural damage revealed by DTI was also prominent. We confirmed that SCP was affected, as presented by Della Nave et al and Hohenberg et al (Della Nave et al, 2011; Hohenberg et al, 2013). Degeneration in cerebello-cerebral tracts, as dentate-rubral and dentate-thalamic-cortical, were also evidenced by Akhlaghi et al and Zalesky et al (Akhlaghi et al, 2014; Zalesky et al, 2014). WM fibers from pyramidal tracts and CC were also damaged. These results are novel observations that highlight involvement of supratentorial structures in the disease. Previous studies probably failed to identify such abnormalities because of smaller sample sizes and more restricted MRI analyses (Della Nave, 2008; Della Nave, 2011; Pagani et al, 2010; Rizo et al, 2011). The involvement of CC might be associated with cognitive dysfunction in FRDA patients, while corticospinal tract compromise might be responsible for the pyramidal signs. These results are in line with pathological report that emphasize reduction of giant Betz cells in the layer V of primary motor cortex (Koeppen and Mazurkiewicz, 2013). Overall DTI revealed increased values for both RD and AD, which are considered markers for oligodendrocyte and axonal dysfunction, respectively. This suggests that not only axons but also myelin of these CNS tracts are involved. Interestingly, a similar pattern of mixed damage – axonal and myelinic has been reported in the peripheral nerves; sural nerve biopsy reveal marked axonal and Schwann cells loss (Koeppen and Mazurkiewicz, 2013).

We did not find an association between GAA repeat lengths and volumetric parameters. In contrast, the extent of atrophy is most regions was associated with duration of the illness. Disease severity, expressed by FARS total score and FARS III subscore, presented a significant correlation with GM and WM loss in the cerebellum and its connections. Striking negative correlations were indentified between DN volumes and these ataxia scores. This supports the concept that DN are a major target of neurodegeneration in the disease (Koeppen, 2011). In

addition, CC microstructural abnormalities also had a correlation with motor handicap in our patients. CC is the larger WM commissure in the brain and found to be important in the execution of complex bimanual motor tasks, possibly due to the transfer of sensory input between hemispheres (Bonzano et al, 2008). In multiple sclerosis, fractional anisotropy of the CC has emerged as a promising candidate biomarker because it is closely related to physical and cognitive disability. Taken together, these data indicate that DTI of the CC might also be a useful marker for FRDA.

Longitudinal analyses showed after 2 years of follow-up that there were progressive GM atrophy in frontal and temporal regions, as well as precentral gyri and cerebellar hemispheres. WM atrophy was also progressive in areas such as the limbic lobe and the left cingulate gyrus. Such evolving volumetric reduction in motor areas, such as precentral gyri, might be related to the clinical deterioration seen in these subjects. We did not identify progressive atrophy in the SCP and DN. This was somewhat unexpected, but possibly due to a floor effect, ie, these structures already have severe atrophy, so that detection of additional reduction is made difficult in the short term follow-up. We hypothesize that a similar reason explains the lack of significant findings in the longitudinal DTI study. Perhaps, one needs a longer interval between examinations to detect significant changes, since the disease course is very slowly progressive. As an alternative, a study that enrolls kids and teenagers with short FRDA duration might prove more successful to identify such progression.

**Conclusion**

In conclusion, we have shown that FRDA patients present more widespread GM and WM damage than previously reported, including not only infratentoral areas, but also

supratentorial structures. These results correlated with clinical parameters. Furthermore, we evidenced that there were progressive structural abnormalities in GM and WM in FRDA patients.

**References**

Akhlaghi H, Corben L, Georgiou-Karistianis N, Bradshaw J, Storey E, Delatycki MB, et al. Superior cerebellar peduncle atrophy in Friedreich's ataxia correlates with disease symptoms. Cerebellum 2011; 10: 81-7.

Akhlaghi H, Yu J, Corben L, Georgiou-Karistianis N, Brandshaw J, Storey E, et al. Cognitive deficits in Friedreich ataxia correlate with micro-structural changes in dentatorubral tract. Cerebbelum 2014; 13: 187-98.

Ashburner JA. A fast diffeomorphic image registration algorithm. Neuroimage 2007; 38: 95-113.

Ashburner J, Friston KJ. Voxel-based morphometry – the methods. Neuroimage 2000; 11: 805-21.

Bonilha da Silva C, Bergo FPG, D'Abreu A, Cendes F, Lopes-Cendes I, França Jr MC. Dentate nuclei T2 relaxometry is a reliable neuroimaging marker in Friedreich's ataxia. Euro J Neurol 2014; doi: 10.1111/ene.12448. [Epub ahead of print]

Bonzano L, Tacchino A, Roccatagliata L, Abbruzzese G, Mancardi GL, Bove M. Callosal contributions to simultaneous bimanual finger movements. J Neurosci 2008; 28: 3227-33.

Buckner RL, Head D, Parker J, Fotenos AF, Marcus D, Morris JC, et al. A unified approach for morphometric and functional data analysis in young, old, and demented adults using automated atlas-based head size normalization: reliability and validation against manual measurement of total intracranial volume. Neuroimage. 2004; 23: 724-38.

Campuzano V, Montermini L, Moltò MD, Pianese L, Cossée M, Cavalcanti F, et al. Friedreich's ataxia: autosomal recessive disease caused by anintronic GAA triplet repeat expansion. Science 1996; 271: 1423-7.

Chevis CF, Silva CB, D'Abreu A, Lopes-Cendes I, Cendes F, Bergo FPG, et al. Spinal cord atrophy correlates with disability in Friedreich's ataxia. Cerebellum 2012; 12: 43-7.

Della Nave R, Ginestroni A, Tessa C, Salvatore E, Bartolomei I, Salvi F, et al. Brain white matter tracts degeneration in Friedreich ataxia. An in vivo MRI study using tract-based spatial statistics and voxel-based morphometry. NeuroImage 2008; 40:19-25.

Della Nave R, Ginestroni A, Tessa C, Salvatore E, Salvi F, Dotti MT, et al. Brain structural damage in Friedreich's ataxia. J Neurol Neurosurg Psychiatry 2008; 79: 82-5.

Della Nave R, Ginestroni A, Diciotti S, Salvatore E, Soricelli A, Mascalchi M. Axial diffusivity in increased in the degenerating superior cerebellar peduncles of Friedreich's ataxia. Neuroradiology 2011; 53: 367-72.

Desikan RS, Segonne F, Fischl B, Quinn BT, Dickerson BC, Blacker D, et al. An automated labeling system for subdividing the human cerebral cortex on MRI scans into gyral based regions of interest. Neuroimage. 2006; 31: 968-80.

Filla A, De Michele G, Cavalcanti F, Pianese L, Monticelli A, Campanella G, et al. The relationship between trinucleotide (GAA) repeat length and clinical features in Friedreich ataxia. Am J Hum Genet 1996; 59: 554–60.

Fischl B, Dale AM. Measuring the thickness of the human cerebral cortex from magnetic resonance images. Proc Natl Acad Sci USA 2000; 97: 11050-5.

Fischl B, Salat DH, Busa E, Albert M, Dieterich M, Haselgrove C, et al. Whole brain segmentation: automated labeling of neuroanatomical structures in the human brain. Neuron 2002; 33: 341-55.

Fischl B, van der Kouwe A, Destrieux C, Halgren E, Séginne F, Salat DH, et al. Automatically parcellating the human cerebral cortex. Cereb Cortex. 2004; 14: 11-22.

Fogel BL, Perlman S. Clinical features and molecular genetics of autosomal recessive cerebellar ataxias. Lancet Neurol 2007; 6: 245-57.

França Jr MC, D'Abreu A, Yassuda CL, Bonadia LC, Silva MS, Nucci A, et al. A combined voxel-based morphometry and $^{1}$H-MRS study in patients with Friedreich's ataxia. J Neurol 2009; 256: 1114-20.

Gläscher J, Gitelman D. Contrast weights in flexible factorial design with multiple groups of subjects. https://www.jiscmail.ac.uk/cgibin/webadmin?A2=ind0803&L=SPM&P=R1

6629, 2008.

Hanna MG, Davis MB, Sweeney MG, Noursadeghui M, Ellis CL, Elliot P, et al. Generalized chorea in two patients harboring the Friedreich's ataxia gene trinucleotide repeat expansion. Mov Disord 1998; 13: 339-40.

Hohenberg CC, Schoke MF, Wigand MC, Nachbauer W, Guttmann CRG, Kubicki M, et al. Radial diffusivity in cerebellar peduncles correlates with clonical severity in Friedreich ataxia. Neurol Sci 2013; 34: 1459-62.

Jason S, Menekka KS, Winston GP, Bartlett P, McEvoy AW, Symms MR, et al. Working memory network platicity after anterior temporal lobe resection: a longitudinal functional magnetic resonance imaging study. Brain 2014; 137: 1439-53.

Koeppen AH. Friedreich's ataxia: pathology, pathogenesis and molecular genetics. J Neurol Sci 2011; 303: 1-12.

Koeppen AH, Mazurkiewicz JE. Friedreich ataxia: neuropathology revised. J Neuropathol Exp Neurol 2013; 72: 78-90.

Lebel C, Walker L, Leemans A,Phillips L, Beaulieu C.Microstructural maturation of the human brain from childhood to adulthood. Neuroimage2008; 40*:*1044–1055.

Mantovan MC, Martinuzzi A, Squarzanti F, Bolla A, Silvestri I, Liessi G, et al. Exploring mental status in Friedreich's ataxia: a combined neuropsychological, behavioral and neuroimaging study. Euro J Neurol 2006; 13: 827-35.

Morral JA, Davis AN, Qian J, Gelman BB, Koeppen AH. Pathology and pathogenesis of sensory neuropathy in Friedreich's ataxia. Acta Neuropathol 2010; 120: 97-108.

Pagani E, Ginestroni A, Della Nave R, Agosta F, Salvi F, De Michele G, et al. Assessment of brain white matter bundle atrophy in patients with Friedreich ataxia. Radiology 2010; 255: 882-7.

Pandolfo M. Friedreich ataxia. Arch Neurol 2008; 65: 1296-303.

Rizzo G, Tonon C, Valentino ML, Manners D, Fortuna F, Gellera G, et al. Brain diffusion-weighted imagind in Friedreich's ataxia. Mov Disord 2011; 26: 705-12.

Santner W, Schoke M, Boesch S, Nachbauer W, Egger K. A longitudinal VBM study monitoring treatment with erythropoietin in patients with Friedreich ataxia. Acta Radiol 2014; 3: 1-6.

Silva CB, Yasuda CL, D'Abreu A, Cendes F, Lopes-Cendes I, França Jr MC. Neuroanatomical correlates of depression in Friedreich's ataxia: a voxel-based morphometry study. Cerebellum 2012; 12: 429-36.

Smith SM, Jenkinson M, Woolrich MW, Beckmann CF, Behrens TE, Johansen-Berg H, et al. Advances in functional and structural MR image analysis and implementation as FSL.Neuroimage 2004; 23: S208-19.

Smith SM, Jenkinson M, Johansen-Berg H, Rueckert D, Nichols TE, Mackay CE, et al. Tract-based spatial statistics: voxelwise analysis of multi-subject diffusion data.Neuroimage 2006; 31: 1487-505.

Subramony SH, May W, Lynch DR, Gomez C, Fischbeck K, Hallett M, et al. Measuring Friedreich ataxia: Interrater reliability of a neurologic rating scale. Neurology 2005; 64: 1261-2.

Talairach J, Tournoux P. Co-planar Stereotaxic Atlas of the Human Brain, Thieme, NY. 1988.

Zalesky A, Akhlaghi H, Corben LA, Bradshaw JA, Delatychi MB, Storey E, et al. Cerebello-cerebral connectivity deficits in Friedreich ataxia. Brain Struct Funct 2014; 219: 969-81.

Table 1. Transversal Study - Areas of Gray (GM) and White matter (WM) atrophy in patients with Friedreich's ataxia compared with controls

| **GM** | | | | |
|---|---|---|---|---|
| **Cluster** | **Cluster size (voxels)** | **T** | **X,Y,Z {mm} MNI coordinates** | **Anatomic location** |
| 1 | 1124 | 5.13 | -9 -48 -60 | L posterior cerebellar lobe |
| 2 | 1077 | 4.96 | 36 -64.5 -27 | R posterior and anterior cerebellar lobes |
| 3 | 655 | 4.24 | 1.5 -87 1.5 | R occipital lobe, calcarine gyrus |
| 4 | 583 | 4.07 | -22.5 -57 31.5 | L anterior cerebellar lobe |
| 5 | 259 | 3.87 | -7.5 -103.5 3 | L occipital lobe, calcarine gyrus |
| 6 | 225 | 4.20 | 61.5 -1.5 21 | R frontal lobe, precentral and postcentral gyri |
| 7 | 210 | 4.36 | -51 -14 24 | L frontal lobe, precentral and inferior frontal gyri |
| 8 | 181 | 3.67 | -39 34.5 7.5 | L frontal lobe, inferior frontal gyrus |
| 9 | 133 | 3.80 | 10.5 -76.5 -13.5 | R occipital lobe, lingual gyrus |
| 10 | 128 | 4.07 | 43.5 30 12 | R frontal lobe, inferior frontal gyrus |
| 11 | 97 | 3.96 | -52.5 -13.5 -13.5 | L temporal lobe, middle temporal gyrus |
| 12 | 61 | 3.96 | 54 -36 22.5 | R parietal lobe, inferior parietal lobule |
| 13 | 57 | 3.86 | 25.5 -40.5 -43.5 | R posterior cerebellar lobe, tonsil |
| 14 | 49 | 5.67 | -19.5 -22.5 -33 | Brainstem, pons |
| 15 | 30 | 3.67 | -24 -27 52.5 | L frontal lobe, precentralgyrus |
| **WM** | | | | |
| **Cluster** | **Cluster size (voxels)** | **T** | **X, Y, Z {mm} MNI coordinates** | **Anatomic location** |
| 1 | 182159 | 16.97 | -1.5 -46.5 -61.5 | R L frontal lobe<br>R L limbiclobe<br>R L temporal lobe<br>R L parietal lobe<br>Cingulate gyrus<br>R L medial frontal gyrus<br>R L precentral gyrus<br>R L occipital lobe<br>Corpus calllosum<br>R L anterior cerebellar lobes<br>R L brainstem, midbrain, pons<br>R L lentiformnuclei<br>R L posterior cerebellar lobes<br>R L thalami<br>R L postcentral gyrus |

Results reported on Height thershold: T = 3.37, clusters> 30 voxels. GM – gray matter; WM – white matter; R – right; L - left

Table 2. Transversal study - Areas of Gray matter (GM) and White matter (WM) atrophy in patients with Friedreich's ataxiacorrelated with duration of the disease

| **GM** | | | | |
|---|---|---|---|---|
| **Cluster** | **Cluster Size (voxels)** | **T** | **X, Y, Z {mm} MNI coordinates** | **Anatomic location** |
| 1 | 20779 | -6.8 | -19.5 -64.5 -31.5 | R L posterior cerebellar lobes, occipital lobes |
| 2 | 4035 | -4.76 | 60 13.5 13.5 | R superior temporal, precentral, inferior frontal gyri |
| 3 | 2808 | -4.26 | -10.5 28.5 30 | L limbic lobe, anterior cingulate gyrus |
| 4 | 2552 | -4.74 | -30 6 -31.5 | L superior temporal gyrus, limbic lobe |
| 5 | 1975 | -5.35 | -12 7.5 16.5 | L caudate, putamen |
| 6 | 1545 | -5.64 | -43.5 40.5 27 | L middle and inferior frontal gyri |
| 7 | 1431 | -3.95 | 6 -60 10.5 | R limbic and occipital lobes, posterior cingulate gyrus |
| 8 | 1113 | -4.01 | 13.5 13.5 13.5 | R caudate |
| 9 | 594 | -4.08 | -57 -63 31.5 | L parietal lobe, supramarginal gyrus |
| 10 | 448 | -3.94 | 10.5 -33 3 | R thalamus |
| 11 | 417 | -4.52 | -64.5 -40.5 21 | L superior temporal gyrus |
| 12 | 390 | -3.62 | -57 7.5 15 | L inferior frontal and precental gyri |
| 13 | 294 | -4.16 | 60 -54 18 | R superior temporal gyrus |
| 14 | 292 | -4.34 | 33 -1.5 63 | R middle frontal gyrus |
| 15 | 289 | -3.26 | -19.5 -25.5 -12 | L limbic lobe, parahippocampal gyrus |
| 16 | 253 | -4.11 | -25.5 -13.5 -3 | L lentiform nucleus |
| 17 | 209 | -3.71 | -16.5 3 49.5 | L limbic lobe, cingulate gyrus |
| 18 | 85 | -3.33 | -66 -30 -1.5 | L middle temporal gyrus |
| 19 | 81 | -3.20 | 49.5 -75 7.5 | R middle occipital gyrus |
| **WM** | | | | |
| **Cluster** | **Cluster Size (voxels)** | **T** | **X, Y, Z {mm} MNI coordinates** | **Anatomic location** |
| 1 | 21980 | -4.80 | -6 -27 -13.5 | R L brainstem, pons, midbrain<br>R L posterior and anterior cerebellar lobes<br>R L thalami<br>R L limbic lobes<br>R L lentiform nuclei |
| 2 | 12914 | -4.38 | 34.5 -58.5 31.5 | R frontal and limbic lobes, cingulate and inferior frontal gyri |
| 3 | 11098 | -4.63 | -28.5 34.5 9 | L frontal and limbic lobes, cingulate gyrus |
| 4 | 840 | -3.54 | -13.5 -81 7.5 | L occipital lobe |
| 5 | 524 | -3.87 | 4.5 -21 18 | R sub-lobar, corpus callosum |
| 6 | 209 | -3.22 | -15 64.5 -1.5 | L medial frontal gyrus |

Results reported on Height thershold: T = 2.78, clusters> 80 voxels. GM – gray matter; WM – white matter; R – right; L - left

Table 3. Transversal study - Areas of Gray matter (GM) and White matter (WM) atrophy in patients with Friedreich's ataxiacorrelated with FARS score

| **GM** | | | | |
|---|---|---|---|---|
| **Cluster** | **Cluster Size (voxels)** | **T** | **X, Y, Z {mm} MNI coordinates** | **Anatomic location** |
| 1 | 83014 | -8.02 | -16.5 -64.5 -31.5 | R L posterior and anterior cerebellar lobes<br>R L frontal lobe<br>R L temporal lobe<br>R L occipital lobe<br>R L anterior cingulate gyri<br>R L caudate, putamen and thalami |
| 2 | 19236 | -5.70 | -37.5 6 -18 | L superior temporal gyrus<br>L inferior and middle frontal gyri<br>L precentral gyrus<br>L caudate |
| 3 | 1167 | -3.94 | 48 -6 -31.5 | R inferior and middle temporal gyri |
| 4 | 1166 | -4.91 | -10.5 -30 76.5 | L precentral gyrus |
| 5 | 973 | -4.99 | 30 4.5 61.5 | R middle frontal gyrus |
| 6 | 894 | -3.95 | -30 -6 60 | R middle frontal gyrus |
| 7 | 722 | -3.39 | 18 -97.5 18 | R occipital lobe<br>R superior and middle occipital gyri |
| 8 | 680 | -3.76 | -60 -25.5 42 | L postcentral and inferior parietal gyri |
| 9 | 562 | -4.00 | 64.5 -15 37.5 | R postcentral and precentral gyri |
| 10 | 350 | -3.26 | 64.5 -36 39 | R parietal lobe, supramarginal gyrus |
| 11 | 249 | -3.62 | -27 -58.5 67.5 | L superior parietal lobe |
| 12 | 187 | -2.62 | -40.5 -7.5 -45 | L inferior temporal gyrus |
| **WM** | | | | |
| **Cluster** | **Cluster Size (voxels)** | **T** | **X, Y, Z {mm} MNI coordinates** | **Anatomic location** |
| 1 | 63430 | -7.85 | -6 -43.5 -28.5 | R L frontal lobes<br>R L anterior cerebellar lobes<br>Brainstem<br>R L posterior cerebellar lobes<br>Midbrain, pons<br>R L limbic lobes<br>R L temporal lobes<br>Cingulate gyrus<br>Corpus callosum<br>Thalami<br>R L parietal lobes<br>R L lentiform nuclei<br>R L occipital lobes |
| 2 | 344 | -3.64 | -15 64.5 -1.5 | L medial frontal gyrus |
| 3 | 205 | -3.63 | -22.5 -54 55.5 | L parietal lobe |
| 4 | 178 | -4.15 | 46.5 28.5 -6 | R inferior frontal gyrus |

Results reported on Height thershold: T = 2.36, clusters > 80 voxels. GM – gray matter; WM – white matter; R – right; L - left

Table 4. Transversal study - Areas of Gray matter (GM) and White matter (WM) atrophy in patients with Friedreich's ataxiacorrelated with FARS III subscore

| **GM** | | | | |
|---|---|---|---|---|
| **Cluster** | **Cluster Size (voxels)** | **T** | **X, Y, Z {mm} MNI coordinates** | **Anatomic location** |
| 1 | 75609 | -7.51 | 34.5 -54 -37.5 | R L anterior cerebellar lobes<br>R L posterior cerebellar lobes<br>R L limbic lobes<br>R L frontal lobes<br>R L temporal lobes<br>R L occipital lobes<br>Anterior and posterior cingulate gyri<br>R L caudate, putamen, thalami<br>R L parietal lobes |
| 2 | 13797 | -5.26 | -37.5 6 -18 | L temporal and frontal lobes<br>L superior and inferior temporal gyrus<br>L caudate |
| 3 | 920 | -3.76 | 46.5 -6 -31.5 | R inferior temporal gyrus |
| 4 | 861 | -3.73 | 58.5 -52.5 16.5 | R superior and middle temporal gyrus |
| 5 | 697 | -4.55 | -36 42 33 | L middle frontal gyrus |
| 6 | 677 | -4.70 | 30 6 61.5 | R middle frontal gyrus |
| 7 | 658 | -3.34 | 19.5 -99 18 | R occipital lobe, cuneus<br>R superior and middle occipital gyrus |
| 8 | 572 | -3.50 | -31.5 -6 61.5 | L middle frontal gyrus |
| 9 | 563 | -3.62 | -58.5 -27 45 | L postcentral gyrus |
| 10 | 388 | -4.08 | 66 -16.5 34.5 | R precentral and postcentral gyrus |
| 11 | 380 | -4.31 | -49.5 7.5 34.5 | L inferior frontal and precentral gyrus |
| 12 | 377 | -3.46 | -67.5 -28.5 -4.5 | L middle temporal gyrus |
| 13 | 368 | -3.40 | 63 -36 39 | R supramarginal gyrus |
| 14 | 274 | -3.20 | -34.5 -27 64.5 | L precentral gyrus |
| 15 | 175 | -3.43 | 43.5 30 6 | R inferior frontal gyrus |
| **WM** | | | | |
| **Cluster** | **Cluster Size (voxels)** | **T** | **X, Y, Z {mm} MNI coordinates** | **Anatomic location** |
| | 75609 | -7.51 | 34.5 -54 -37.5 | R L frontal lobes<br>R L anterior cerebellar lobes<br>Brainsteam, midbrain, pons<br>R L posterior cerebellar lobes<br>Limbic lobes<br>Thalami<br>R L temporal lobes<br>Corpus callosum<br>R L lentiform nuclei<br>R L parietal lobes<br>R L occipital lobes |
| | 383 | -3.85 | -42 34.5 9 | L inferior frontal gyrus |
| | 174 | -3.42 | -15 64.5 -1,5 | L medial frontal gyrus |
| | 134 | -3.43 | -22.5 =54 55.5 | L pariental lobe |
| | 118 | -3.16 | -46.5 -49.5 13.5 | L superior temporal gyrus |

Results reported on Height thershold: T = 2.41, clusters > 80 voxels. GM – gray matter; WM – white matter; R – right; L - left

Table 5. Prospective study - One and two year follow-up - Areas of Gray matter (GM) and White matter (WM) atrophy in patients with Friedreich's ataxia compared with controls

| **GM – One year follow-up** | | | | |
|---|---|---|---|---|
| **Cluster** | **Cluster size (voxels)** | **T** | **X,Y,Z {mm} MNI coordinates** | **Anatomic location** |
| 1 | 241 | 4.08 | 55.5 -4.5 -33 | R inferior temporal gyrus |
| 2 | 126 | 3.63 | -48 6 -33 | L middle temporal gyrus |
| 3 | 78 | 3.96 | -27-3 -45 | L uncus |
| 4 | 74 | 3.57 | 64.5 -25.5 -18 | R middle temporal gyrus |
| 5 | 53 | 3.65 | -43.5 -14 49.5 | L middle frontal gyrus |
| 6 | 46 | 3.47 | -51 7.5 24 | L inferior frontal gyrus |
| **GM – Two years follow-up** | | | | |
| **Cluster** | **Cluster size (voxels)** | **T** | **X,Y,Z {mm} MNI coordinates** | **Anatomic location** |
| 1 | 319 | 4.00 | -57 -6 -24 | L temporal lobe, L inferior temporal gyrus |
| 2 | 325 | 4.06 | 55.5 -4.5 -30 | R inferior temporal and fusiform gyri |
| 3 | 228 | 3.67 | 40.5 -55.5 -42 | R posterior cerebellar lobe, R tonsil |
| 4 | 143 | 3.93 | 54 -64.5 -7.5 | R temporal and occipital lobes, R middle occipital gyrus |
| 5 | 123 | 3.94 | 24 58.5 15 | R superior frontal gyrus |
| 6 | 119 | 3.91 | -39 -63 -51 | L posterior cerebellar lobe |
| 7 | 115 | 4.07 | 43.5 48 -7.5 | R middle frontal and precentral gyri |
| 8 | 85 | 4.03 | -16.5 49.5 36 | L superior frontal gyrus |
| 9 | 70 | 3.68 | -33 -85.5 19.5 | L superior and middle occipital gyri |
| 10 | 74 | 3.66 | 37.5 15 -14 | R sub-lobar and insula |
| 11 | 67 | 3.95 | -30 -4.5 58.5 | L middle frontal and precentral gyri |
| 12 | 46 | 3.55 | 57 9 19.5 | R inferior frontal gyrus |
| 13 | 64 | 3.53 | 60 -33 36 | R inferior parietal lobe, R supramarginal gyrus |
| 14 | 42 | 3.43 | 61.5 -21 -6 | R middle and superior temporal gyri |
| 15 | 41 | 3.73 | -39 45 15 | L middle frontal gyrus |
| 16 | 40 | 3.63 | 61.5 -22.5 -19.5 | R temporal inferior gyrus |
| 17 | 35 | 3.69 | -63 -48 -9 | R middle temporal gyrus |
| **WM – Two years follow-up** | | | | |
| **Cluster** | **Cluster size (voxels)** | **T** | **X, Y, Z {mm} MNI coordinates** | **Anatomic location** |
| 1 | 283 | 3.67 | 36 -22.5 -16.5 | R temporal lobe, R hippocampus |
| 2 | 270 | 3.80 | -18 -9 21 | L sub-lobar, L caudate |
| 3 | 258 | 4.22 | 3 -13.5 34.5 | L limbic lobe, L cingulate gyrus |
| 4 | 171 | 3.70 | -13.5 -15 43.5 | L limbic and frontal lobes, L cingulate gyrus |
| 5 | 106 | 3.63 | -9 16.5 -7.5 | L caudate, L anterior cingulate gyrus |
| 6 | 86 | 3.68 | -16.5 4.5 42 | L limbic lobe, L cingulate gyrus |

One year follow-up: results reported on Height thershold: T = 3.17, clusters > 30 voxels. Two years follow-up: Results reported on Height thershold: T = 3.23, clusters> 30 voxels. GM – gray matter; WM – white matter; R – right; L - left

Table 6. Transversal study – ROI-based volumetry of dentate nuclei (DN) and superior cerebellar peduncles (SCP)

| **DN** | **Controls (ml)** | **Patients (ml)** | **p-value** |
|---|---|---|---|
| **Right hemisphere** | 0.5221 ± 0.0578 | 0.3949 ± 0.0725 | < 0.001 |
| **Left hemisphere** | 0.5267 ± 0.0481 | 0.3983 ± 0.0601 | < 0.001 |
| **SCP** | **Controls (ml)** | **Patients (ml)** | **p-value** |
| **Right hemisphere** | 0.0823 ± 0.0130 | 0.0652 ± 0.0118 | < 0.001 |
| **Left hemisphere** | 0.0785 ± 0.0115 | 0.0515 ± 0.0151 | < 0.001 |

DN – dentate nuclei; SCP – superior cerebellar peduncle

Table 7. Longitudinal study – One and two years follow-up – Means ROI-based volumetry of dentate nuclei (DN) and superior cerebellar peduncles (SCP) in FRDA patients and controls

| **Patients – One year follow-up** | | | |
|---|---|---|---|
| **DN** | **Baseline** | **Follow-up** | **p-value** |
| **Right hemisphere** | 0.3960 ± 0.0609 | 0.3905 ± 0.0617 | 0.58 |
| **Left hemisphere** | 0.3950 ± 0.0499 | 0.3933 ± 0.0560 | 0.80 |
| **SCP** | | | |
| **Right hemisphere** | 0.0684 ± 0.0108 | 0.0699 ± 0.0116 | 0.44 |
| **Left hemisphere** | 0.0531 ± 0.0107 | 0.0525 ± 0.0103 | 0.71 |
| **Controls – One year follow-up** | | | |
| **DN** | **Baseline** | **Follow-up** | **p-value** |
| **Right hemisphere** | 0.5169 ± 0.0498 | 0.5136 ± 0.0488 | 0.56 |
| **Left hemisphere** | 0.5190 ± 0.0419 | 0.5218 ± 0.0391 | 0.77 |
| **SPC** | | | |
| **Right hemisphere** | 0.0813 ± 0.0114 | 0.0818 ± 0.0119 | 0.88 |
| **Left hemisphere** | 0.0752 ± 0.0121 | 0.0762 ± 0.0118 | 0.84 |
| **Patients – Two years follow-up** | | | |
| **DN** | **Baseline** | **Follow-up** | **p-value** |
| **Right hemisphere** | 0.3925 ± 0.0630 | 0.3739 ± 0.0586 | 0.07 |
| **Left hemisphere** | 0.3885 ± 0.0541 | 0.3953 ± 0.0538 | 0.50 |
| **SCP** | | | |
| **Right hemisphere** | 0.0704 ± 0.0115 | 0.0678 ± 0.0117 | 0.50 |
| **Left hemisphere** | 0.0543 ± 0.0117 | 0.0503 ± 0.0092 | 0.13 |
| **Controls – Two years follow-up** | | | |
| **DN** | **Baseline** | **Follow-up** | **p-value** |
| **Right hemisphere** | 0.5316 ± 0.0532 | 0.5303 ± 0.0491 | 0.79 |
| **Left hemisphere** | 0.5349 ± 0.0349 | 0.5402 ± 0.0373 | 0.25 |
| **SCP** | | | |
| **Right hemisphere** | 0.0819 ± 0.0117 | 0.0850 ± 0.0114 | 0.25 |
| **Left hemisphere** | 0.0731 ± 0.0127 | 0.0783 ± 0.0108 | 0.40 |

DN – dentate nuclei; SCP – superior cerebellar peduncle

Table 8. Freesurfer transversal study – Areas of volumetric reduction and cortical thickness in FRDA patients compared with controls

| **Subcortical volumetric analysis** | | |
|---|---|---|
| **Structure** | **Patients ($mm^3$)** | **Controls ($mm^3$)** |
| Brainstem | 16915 ± 2712 | 21172 ± 2261 |
| Middle-posterior corpus callosum | 353 ± 103 | 455 ± 83 |
| Posterior corpus callosum | 751 ± 116 | 972 ± 123 |
| L Cerebellum cortex | 42181 ± 6600 | 46981 ± 6153 |
| L Putamen | 5831 ± 897 | 6581 ± 753 |
| L Thalamus | 6658 ± 1200 | 7922 ± 963 |
| L Ventral diencephalon | 3203 ± 490 | 3904 ± 276 |
| R Cerebellar cortex | 42553 ± 6257 | 47297 ± 5852 |
| R Pallidum | 1488 ± 198 | 1689 ± 214 |
| R Putamen | 5837 ± 898 | 6587 ± 704 |
| R Thalamus | 5838 ± 845 | 7111 ± 677 |
| R Ventral diencephalon | 3374 ± 552 | 4080 ± 368 |
| **Cortex thickness analysis** | | |
| **Structure** | **Patients ($mm^3$)** | **Controls ($mm^3$)** |
| L calcarine | 2.009 ± 0.181 | 2.202 ± 0.148 |
| L precentral | 2.854 ± 0.217 | 3.058 ± 0.148 |
| L superior temporal | 3.192 ± 0.236 | 3.393 ± 0.161 |
| R precentral | 2.868 ± 0.190 | 3.105 ± 0.126 |

R – right; L - left

Table 9. DTI transversal study – Comparisson between FRDA patients and controls in pyramidal tracts for automatic tractography

| **Pyramidal Tracts** | | | |
|---|---|---|---|
| **FA values** | **Mean controls** | **Mean patients** | **p-value** |
| **Right hemisphere** | 0.652565 ± 0.041935 | 0.616221 ± 0.032807 | 0.001 |
| **Left hemisphere** | 0.656652 ± 0.031762 | 0.631543 ± 0.035991 | 0.009 |
| **Average** | 0.605450 ± 0.020818 | 0.583692 ± 0.019092 | 0.000 |
| **MD values** | **Mean controls** | **Mean patients** | **p-value** |
| **Right hemisphere** | 0.000801 ± 0.000038 | 0.000804 ± 0.000035 | 0.728 |
| **Left hemisphere** | 0.000789 ± 0.000036 | 0.000786 ± 0.000033 | 0.683 |
| **Average** | 0.000753 ± 0.000019 | 0.000762 ± 0.000028 | 0.246 |
| **AD values** | **Mean controls** | **Mean patients** | **p-value** |
| **Rigth hemisphere** | 0.001486 ± 0.000058 | 0.001436 ± 0.000059 | 0.003 |
| **Left hemisphere** | 0.001473 ± 0.000067 | 0.001428 ± 0.000062 | 0.013 |
| **Average** | 0.001341 ± 0.000031 | 0.001341 ± 0.000045 | 0.150 |
| **RD values** | **Mean controls** | **Mean patients** | **p-value** |
| **Rigth hemisphere** | 0.000458 ± 0.000051 | 0.000489 ± 0.000046 | 0.018 |
| **Left hemisphere** | 0.000448 ± 0.000038 | 0.000464 ± 0.000038 | 0.114 |
| **Average** | 0.000460 ± 0.000023 | 0.000479 ± 0.000026 | 0.006 |

FA – fractional anisotropy; MD – mean diffusivity; RD – radial diffusivity; AD – axial diffusivity

Table 10. DTI transversal study – Comparisson between FRDA patients and controls in corpus callosum for automatic tractography

| **Corpus Callosum** | | | |
|---|---|---|---|
| **FA values** | **Mean controls** | **Mean patients** | **p-value** |
| **Right hemisphere** | 0.605051 ± 0.019602 | 0.584376 ± 0.024789 | 0.001 |
| **Left hemisphere** | 0.604833 ± 0.019925 | 0.584165 ± 0.025317 | 0.001 |
| **Average** | 0.587390 ± 0.017457 | 0.569977 ± 0.023407 | 0.003 |
| **MD values** | **Mean controls** | **Mean patients** | **p-value** |
| **Right hemisphere** | 0.000881 ± 0.000035 | 0.000907 ± 0.000044 | 0.022 |
| **Left hemisphere** | 0.000881 ± 0.000035 | 0.000905 ± 0.000046 | 0.031 |
| **Average** | 0.000836 ± 0.000033 | 0.000861 ± 0.000055 | 0.045 |
| **AD values** | **Mean controls** | **Mean patients** | **p-value** |
| **Rigth hemisphere** | 0.001547 ± 0.000045 | 0.001560 ± 0.000048 | 0.313 |
| **Left hemisphere** | 0.001547 ± 0.000045 | 0.001557 ± 0.000049 | 0.410 |
| **Average** | 0.001449 ± 0.000042 | 0.001465 ± 0.000060 | 0.275 |
| **RD values** | **Mean controls** | **Mean patients** | **p-value** |
| **Rigth hemisphere** | 0.000548 ± 0.000035 | 0.000580 ± 0.000046 | 0.006 |
| **Left hemisphere** | 0.005480 ± 0.000035 | 0.005798 ± 0.000048 | 0.007 |
| **Average** | 0.000530 ± 0.000031 | 0.000560 ± 0.000054 | 0.015 |

FA – fractional anisotropy; MD – mean diffusivity; RD – radial diffusivity; AD – axial diffusivity

Table 11 – Longitudinal analysis of pyramidal tract and corpus callosum for automatic tractography in FRDA patients

| **Pyramidal Tract** | | | |
|---|---|---|---|
| | **Baseline** | **Follow-up** | **p-value** |
| **FA average** | 0.590362 ± 0.024990 | 0.592953 ± 0.024477 | 0.69 |
| **MD average** | 0.000757 ± 0.000033 | 0.000764 ± 0.000029 | 0.44 |
| **AD average** | 0.001337 ± 0.000055 | 0.001351 ± 0.000052 | 0.38 |
| **RD average** | 0.000467 ± 0.000033 | 0.000479 ± 0.000029 | 0.71 |
| **Corpus Callosum** | | | |
| | **Baseline** | **Follow-up** | **p-value** |
| **FA average** | 0.590403 ± 0.032251 | 0.595037 ± 0.029046 | 0.43 |
| **MD average** | 0.000854 ± 0.000066 | 0.000844 ± 0.000053 | 0.43 |
| **AD average** | 0.001503 ± 0.000071 | 0.001492 ± 0.000054 | 0.51 |
| **RD average** | 0.000530 ± 0.000065 | 0.000519 ± 0.000053 | 0.40 |

FA – fractional anisotropy; MD – mean diffusivity; RD – radial diffusivity; AD – axial diffusivity

Figure 1 - Results of voxel-wise analysis showing areas of gray matter (A) and white matter (B) volumetric reduction in patients with Friedreich's ataxia after comparison with age-and-sex matched controls. Results are shown on the MNI152 1-mm template. MNI z-axis coordinates are shown in mm above each image. The color coded bar represent the Z-score.

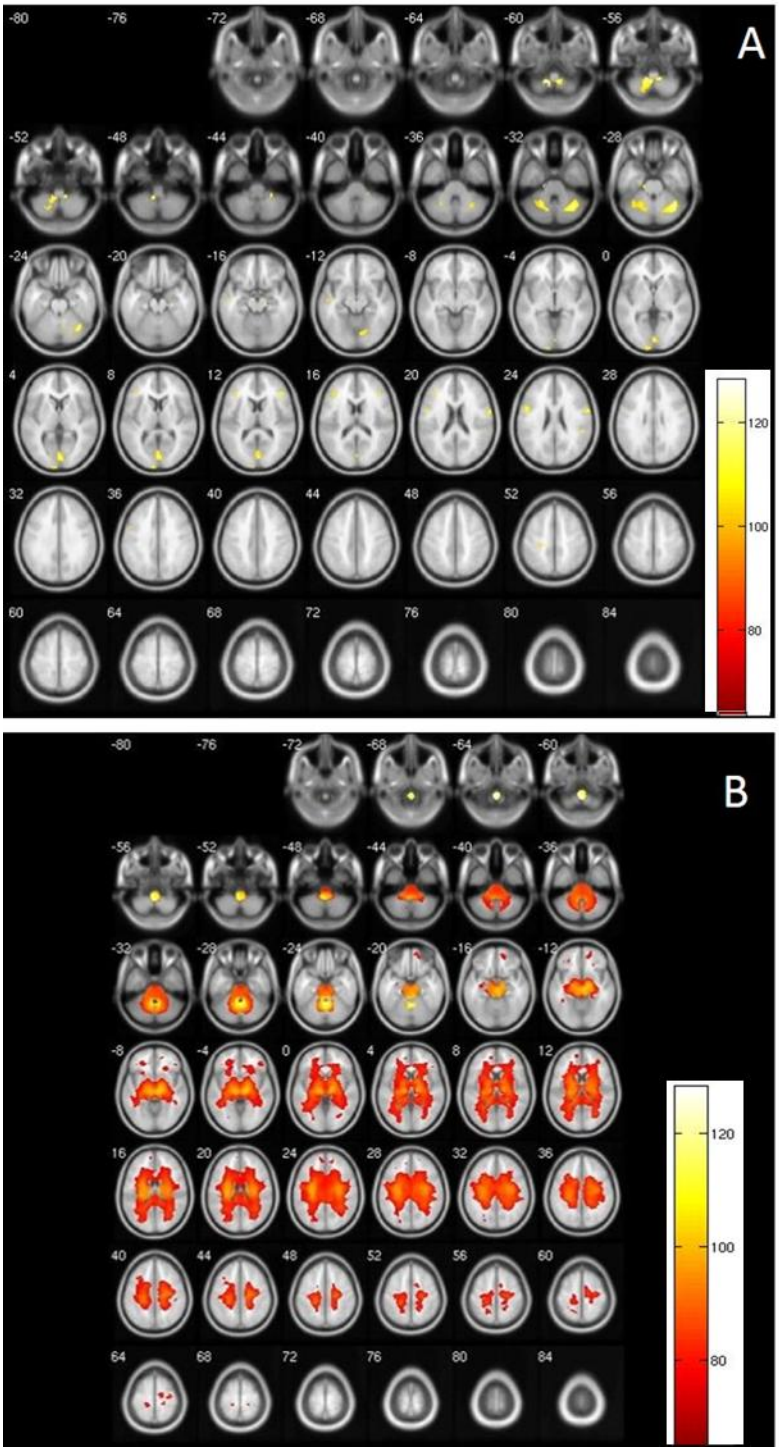

Figure 2 - Results of voxel-wise analysis showing areas of gray matter (A) and white matter (B) volumetric reduction in patients with Friedreich's ataxia after regression with duration of the disease. Results are shown on the MNI152 1-mm template. MNI z-axis coordinates are shown in mm above each image. The color coded bar represent the Z-score.

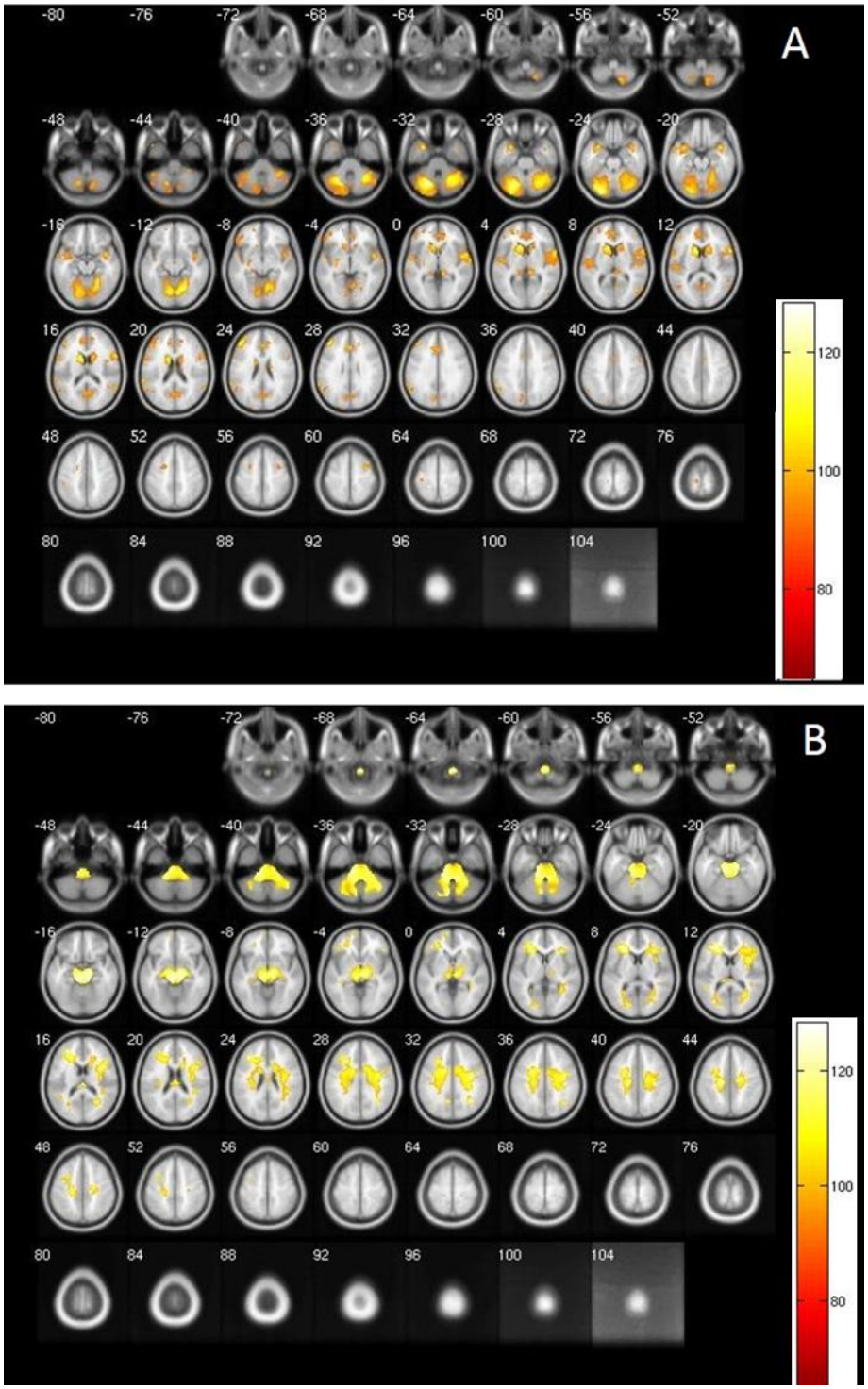

Figure 3 - Results of voxel-wise analysis showing areas of gray matter (A) and white matter (B) volumetric reduction in patients with Friedreich's ataxia after regression with FARS score. Results are shown on the MNI152 1-mm template. MNI z-axis coordinates are shown in mm above each image. The color coded bar represent the Z-score.

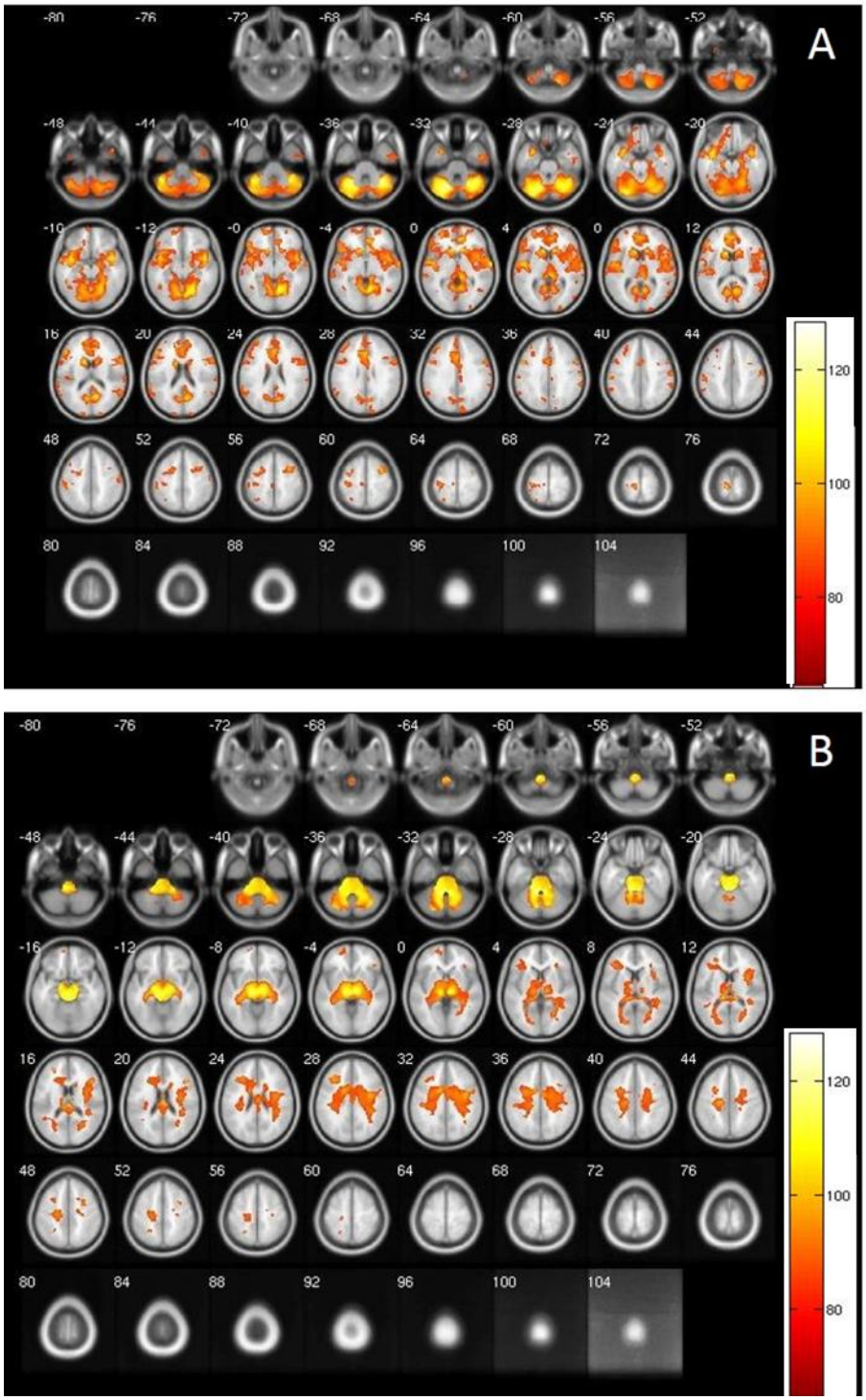

Figure 4 - Results of voxel-wise analysis showing areas of gray matter (A) and white matter (B) volumetric reduction in patients with Friedreich's ataxia after regression with FARS III subscore. Results are shown on the MNI152 1-mm template. MNI z-axis coordinates are shown in mm above each image. The color coded bar represent the Z-score.

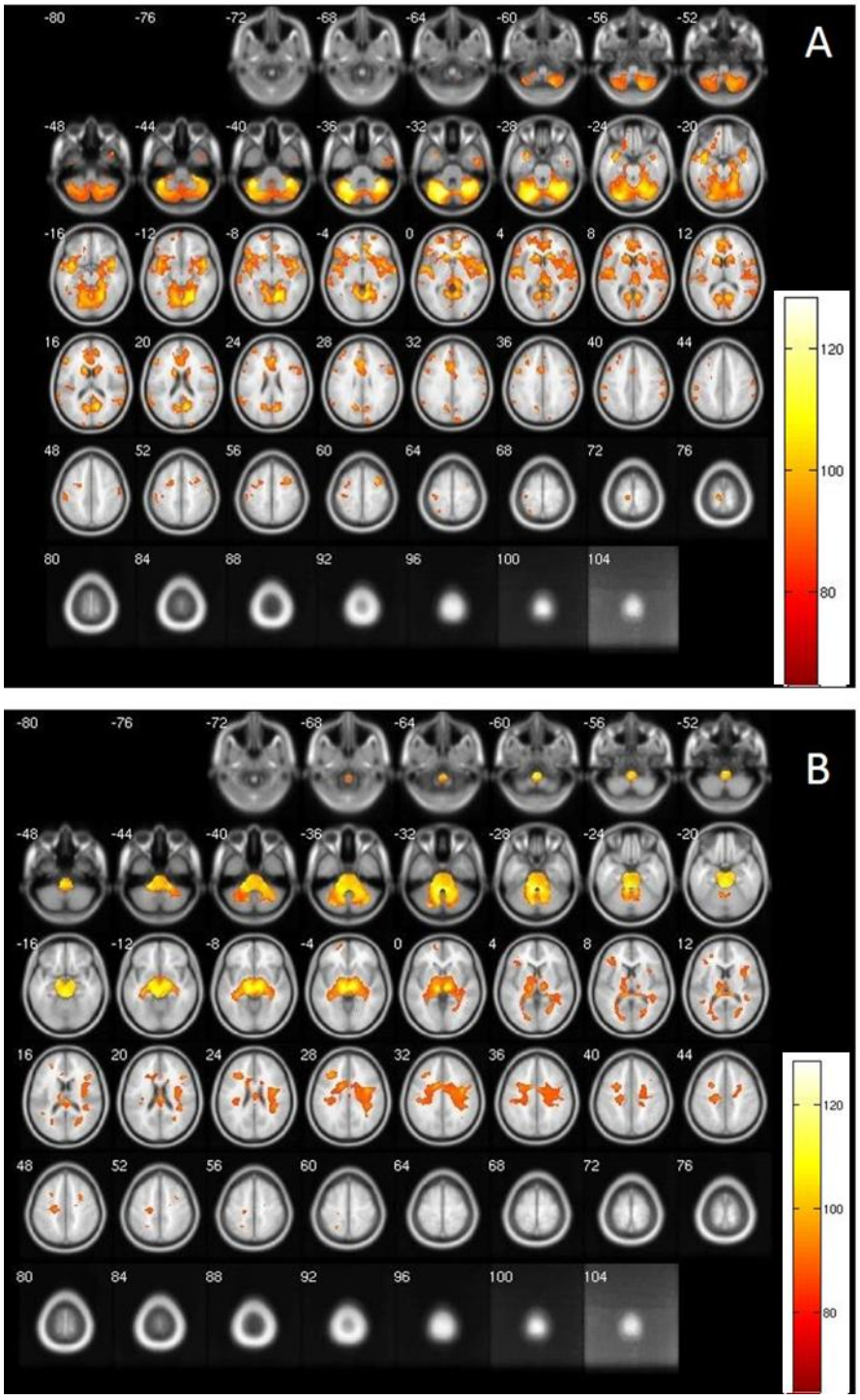

Figure 5 – One year follow-up – Results of voxel-wise analysis showing areas of gray matter volumetric reduction in patients with Friedreich's ataxia after comparison with age-and-sex matched controls. Results are shown on the MNI152 1-mm template. MNI z-axis coordinates are shown in mm above each image. The color coded bar represent the Z-score.

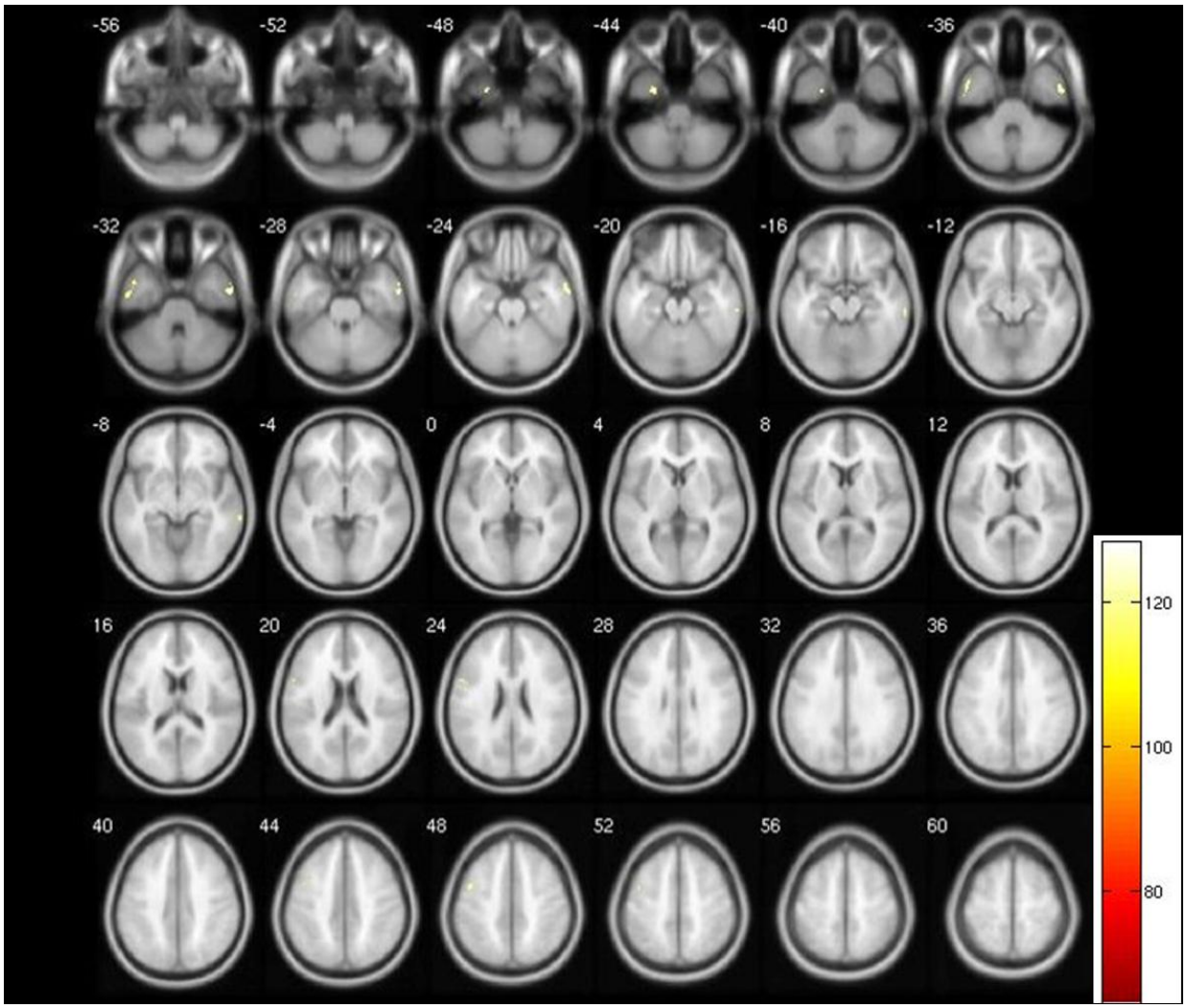

Figure 6 – Two years follow-up – Results of voxel-wise analysis showing areas of gray matter (A) and white matter (B) volumetric reduction in patients with Friedreich's ataxia after comparison with age-and-sex matched controls. Results are shown on the MNI152 1-mm template. MNI z-axis coordinates are shown in mm above each image. The color coded bar represent the Z-score.

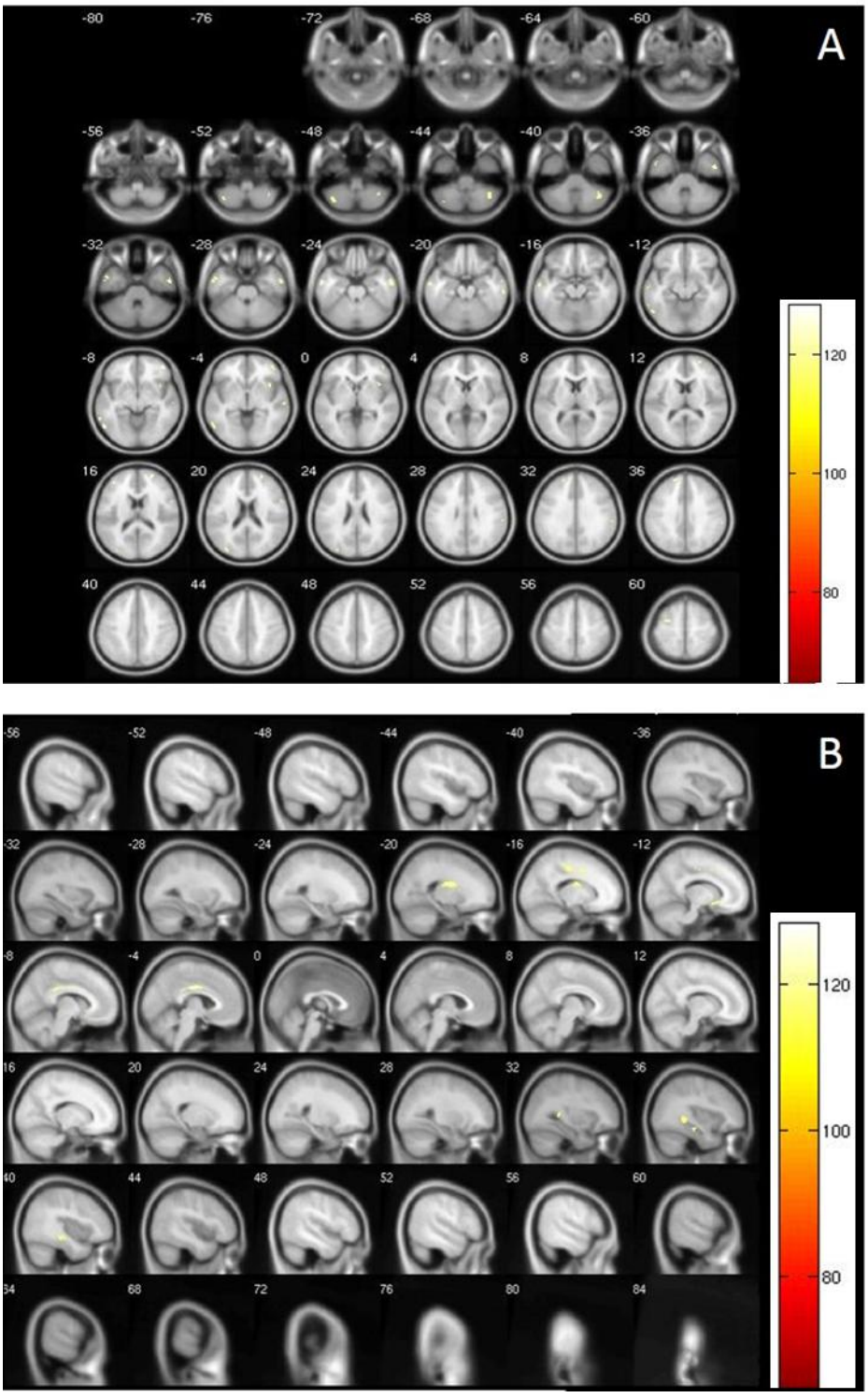

Figure 7 – Longitudinal VBM-based study – Results of voxel-wise analysis showing areas of gray matter volumetric reduction at one year follow-up (A and C) and at two years follow-up (B and D) volumetric reduction at two years follow-up in patients with Friedreich's ataxia after comparison with age-and-sex matched controls. Results are shown on the MNI152 1-mm template. MNI z-axis coordinates are shown in mm above each image. The color coded bar represent the Z-score.

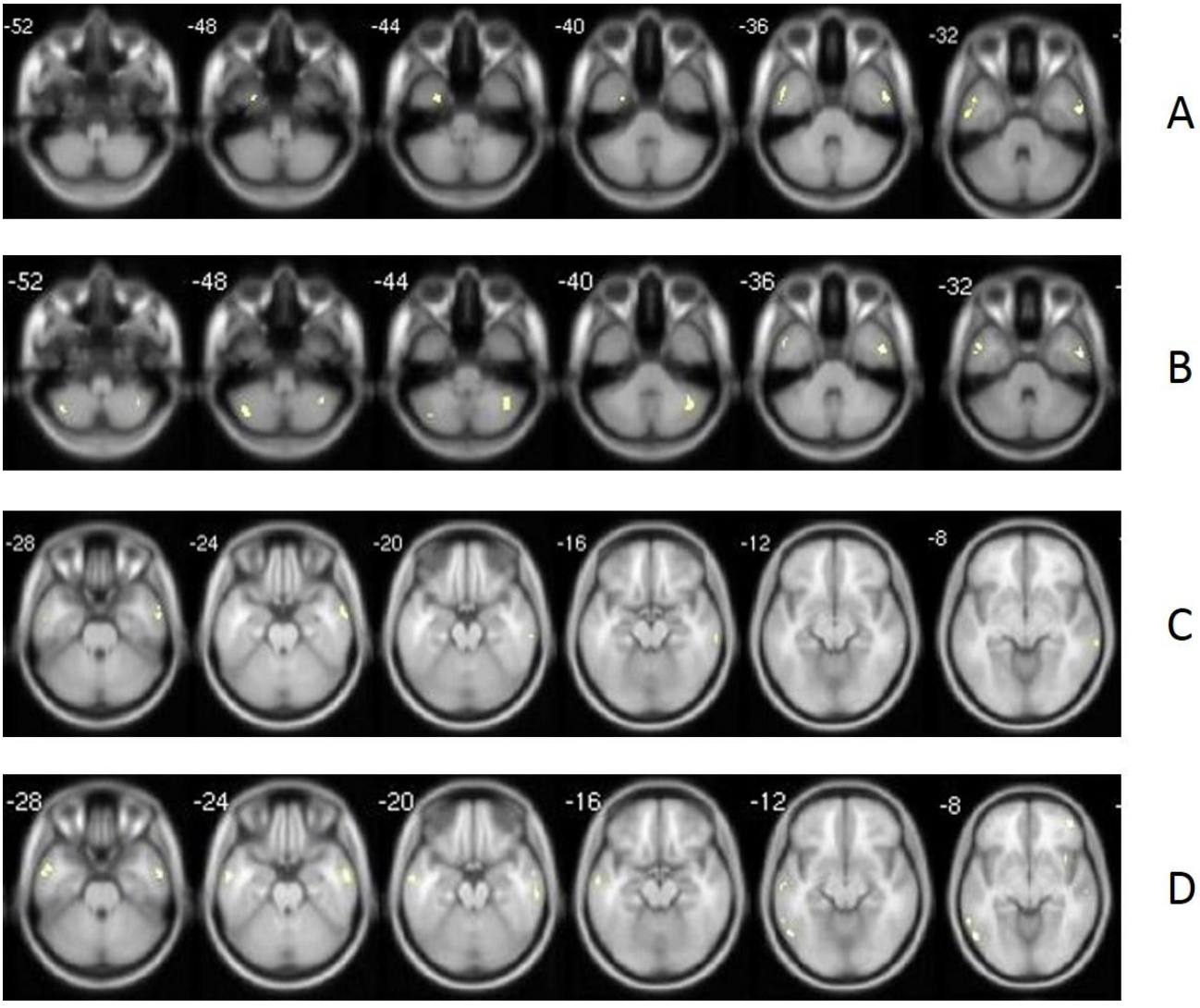

Figure 8 – TBSS results showing areas of reduced FA and increased MD, AD and RD in patients with FRDA after comparison with age-and-sex matched controls. Areas of FA, RD and AD are shown in yellow and MD are in red. Results are shown on the MNI152 template.

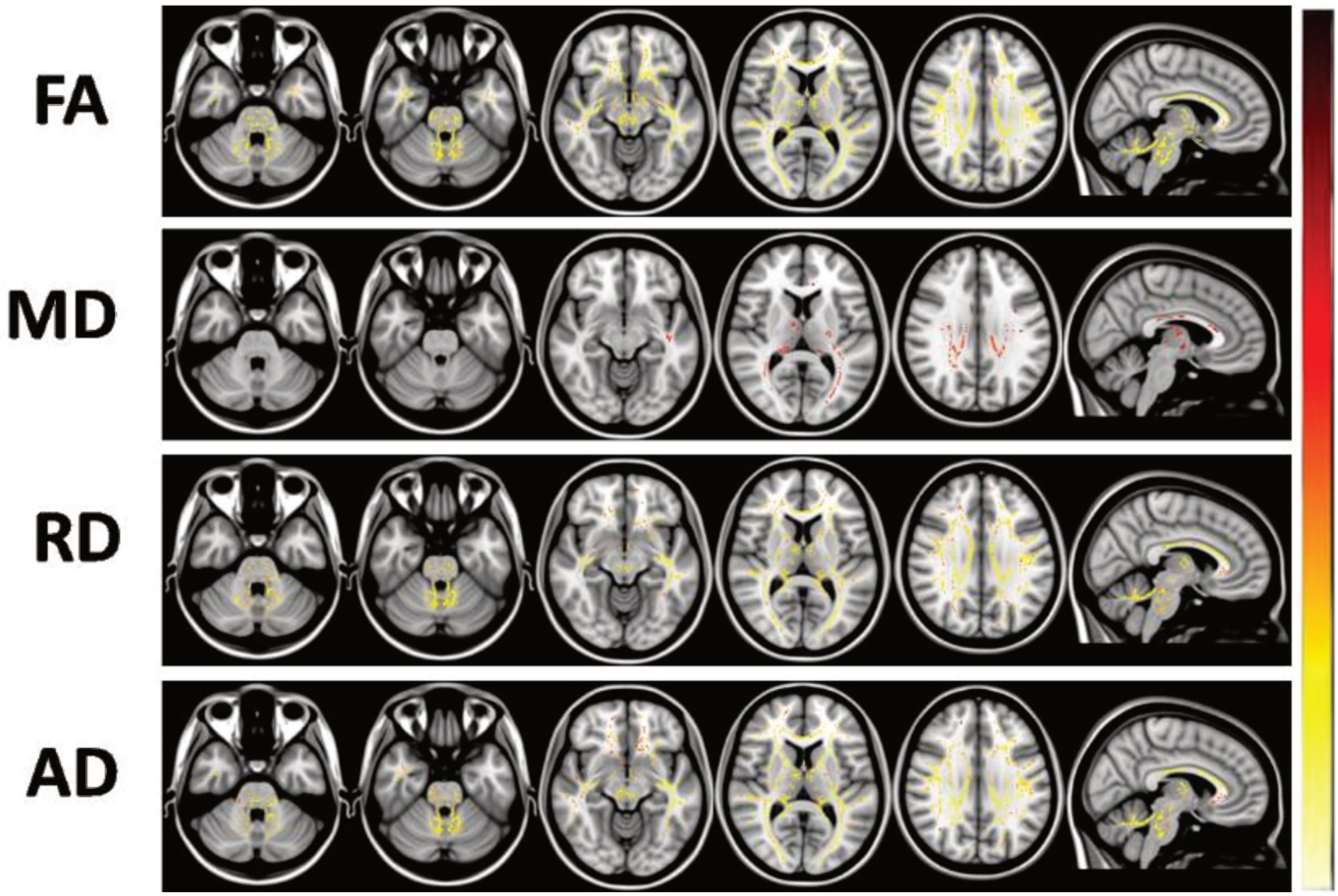

## Discussão

### *Sintomas não-motores*

A presença de sintomas neuropsiquiátricos e sua importância, recentemente, tem sido reconhecidas em diversas doenças neurodegenerativas. Distúrbios de sono, fadiga e distúrbios afetivos podem ter enorme impacto na qualidade de vida, tanto quanto a incapacidade motora. Na FRDA, entretanto, há poucos estudos que avaliam o impacto destes sintomas. Além disso, os dados disponíveis na literatura não são desenhados para avaliação específica destes sintomas e contam com número reduzido de pacientes (34, 35). Em nosso estudo,apenas um paciente com FRDA (3,7%) apresentou sintomas de sonolência diurna e de má qualidade de sono. Estes dados são contrários aos relatados por Corben et al. Em seu estudo, os autores encontraram sintomas de sonolência diurna em 25% dos pacientes e, em 21%, foi evidenciado síndrome da apnéia obstrutiva do sono (37). Esta diferença pode ser explicada pelo fato de o nosso grupo de pacientes apresentarmédia de idade e duração de doença menores em relação ao grupo analisado por Corben et al.

Nossos resultados, no entanto, mostraram que a fadiga apresentaimportante impacto nas atividades diárias em 29% dos pacientes com FRDA contra 5,1% dos controles, embora as médias dos escores não tenham sido significativamente diferentes. Analisando-se os componentes físico, cognitivo e social de forma separada, observou-se que o subescore físico (MFIS-F) é o maior responsável pelo sintoma e se correlaciona com a gravidade e duração da doença. Epstein et al observaram esta correlação com o escore total da MFIS, porém não analisou os sub-escores separadamente (35). Ao contrário do que se poderia supor, a presença de cardiopatia não foi um fator decisivo para a maior pontuação da MFIS-F.

Neste trabalho, o dado mais surpreendente é que o surgimento da fadiga é multifatorial. Além da gravidade e duração da doença, a MFIS correlacionou-se com escore da Escala de Sonolência Diurna (ESS) e do Inventário de Depressão de Beck (BDI), mostrando que os distúrbios de sono e depressivos influenciam na presença de fadiga nos pacientes com FRDA. O tratamento da fadiga, portanto, necessita ter abordagem ampla, atuando em múltiplos fatores. É preciso ainda pesquisar ativamente esse sintoma, pois os pacientes não apresentam esta queixa espontaneamente.

Na FRDA, White et al descreveram que a depressãoseria infrequente (29). Em nosso estudo, encontramos mais de 30% dos pacientes com critérios para depressão maior, similar à prevalência encontrada na Doença de Parkinson e na Ataxia Espinocerebelar tipo 3 (SCA3) e maior que a descrita em estudos populacionais (57, 58, 59). O estudo realizado por White et al, contudo, avaliaram um grupo pequeno de pacientes, sem diagnóstico confirmado por teste genético e excluiu indivíduos com força reduzida em mãos, fato que pode ter excluído pacientes com doença mais severa e de duração mais longa. O nosso estudo sugere, ainda, que a depressão é, provavelmente, não reconhecida nos pacientes com FRDA, pois apenas parte dos pacientes da coorte estava em tratamento farmacológico. Este fato mostra que é preciso pesquisar ativamente a presença de sintomas afetivos nos pacientes com FRDA, assim como a fadiga e distúrbios de sono.

Previamente, nas doenças neurodegenerativas, a depressão foi considerada, por muitos autores, como um processo reativo à limitação motora (57). Contudo, anormalidades estruturais e funcionais têm sido descritas, sugerindo que os sintomas depressivos possam ser secundários a estas alterações. Nosso estudo demonstrou que a depressão na FRDA está associada a anormalidades estruturais. Comparando-se pacientes com depressão (FRDA-DP)a indivíduos

sem depressão (FRDA-NDP), observamos que o grupo com depressão apresentou atrofia de SC em algumas áreas do lobo frontal, a saber: giros frontais mediais bilaterais, cingulado anterior bilateral, giro frontal superior direito, giro frontal médio direito e giro orbital direito. Além disso, a gravidade da doençaassociou-se com a área de atrofia do giro frontal superior direito.

Estas áreas de atrofia de SC encontradasno grupo FRDA-DP já foram observadas em estudos volumétricos de depressão maior, especialmente córtex cingulado anterior (CCA) (60, 61, 62, 63, 64, 65, 66, 67, 68, 69). Isto reforça o conceito de que a depressão maior seria consequência de uma disfunção de circuitos córtico-líbicos, de acordo com modelo proposto por Mayberg (61). Há oenvolvimento deuma rede neuronal extensa, compostapor um circuito dorsal (córtex pré-frontal dorsomedial e dorsolateral, cingulado anterior dorsal, córtex cingulado posterior), por um circuito ventral (cingulado anterior subgenual e amígdalas) e o CCA (61). Este últimotem papel significativo na regulação emocional, geração de estados negativos de humor e alterações somáticas (61, 70). As regiões orbitofrontais são relacionadasao reconhecimento de expressões faciais (71). Os giros frontais médio e superior, por sua vez, participam de aspectos cognitivos, como atenção relacionada à emoção, antecipação de emoções negativas, seleção de estímulos visuais e regulação do processo emocional (72, 73).

***Neuroimagem***

O desenvolvimento de biomarcadores ou marcadores de neuroimagem na FRDA é urgente, uma vez que pode ajudar no manejo de pacientes e no desenho de estudos clínicos. A partir do melhor conhecimento fisiopatológico, diversos parâmetros de neuroimagem têm sido

investigados, incluindo a volumetria do pedúnculo cerebelar superior e área de medula espinhal (41, 50).

Assim sendo, realizamos um estudo com diversas técnicas de neuroimagem a fim de caracterizar anormalidades estruturais em pacientes com FRDA e relacioná-los a parâmetros clínicos. Ainda nesse sentido, a realização de um braço longitudinal teve por objetivo determinar se alterações encontradas possam ser utilizadas como marcadores de evolução da ataxia.

***Relaxometria***

A partir da identificação do núcleo denteado do cerebelo como uma das estruturas-chaves na fisiopatologia da FRDA, diversos estudos de neuroimagem focaram na avaliação desta estrutura (23, 24, 43). Em particular, tem sido empregadas técnicas capazes de avaliar deposição de ferro local, visto que esse é um fenômeno característico da FRDA. Na relaxometria, o aumento do depósito de ferro no NDC leva a uma redução do tempo de relaxação T2 (T2), ou seja, aumenta o valor do R2, uma vez que R2=1/T2. O mesmo efeito ocorre no tempo de relaxação T2* e o R2* (R2*=1/T2*).

Em nosso estudo, confirmamos que há redução do T2 (ou um aumento do R2) nos núcleos denteados (NDC T2) em pacientes com FRDA, seletivamente, pois o mesmo não foi visto em outros núcleos subcorticais. Este dado está em acordo com estudos prévios (23, 43). Além disso, evidenciamos que NDC T2 apresenta redução significativa após um ano, o que não ocorre em controles saudáveis.

O susbtrato anatômico para estas anormalidades de imagem são a perda neuronal, a redução volumétrica do núcleo denteado e, principalmente, a redistribuição de ferro em seu interior (1, 9). Estudos patológicos já evidenciaram que não há aumento da quantidade total de

ferro no tecido. Na verdade, ocorre uma relocação do ferro, localizado previamente em neurônios, como ferritina em astrócitos e na micróglia. Koeppen sugeriu, então, que há aumento da concentração local de ferro no NDC secundário (9).

Resultados obtidos também indicam que NDC T2 é fortemente relacionado à idade dos pacientes, semelhante ao descrito previamente (43). Este fato sugere que o depósito de ferro é dependente da duração da deficiência de frataxina e, provavelmente, inicia-se antes das manifestações clínicas. Interessantemente, o tamanho da expansão dos tripletos de (GAA) no gene *FXN* foi diretamente associado com alteração do NDC T2. Assim sendo, esses dados sugerem que, além do efeito do tempo (idade), expansão de (GAA) acelera o depósito de ferro no NDC.

Dois estudos clínicos prévios investigaram os efeitos dos quelantes de ferrona FRDA e utilizaram a R2* no NDC como instrumento para avaliar se houve a redução de ferro nesta localização (23, 24). No primeiro estudo, os autores encontraram, no tempo 0, um pequeno aumento significativono R2* em pacientes, quando comparados a controles. Porém, não houve correlação com idade (23). O segundo estudo mostrou uma redução significativa do R2* nos pacientes com FRDA submetidos ao tratamento, demonstrando que o houve quelação do ferro no NDC. Entretanto, os autores não mencionaram se R2* correlacionou-se com a gravidade da ataxia ou idade dos pacientes (24).

Na nossa análise clínica, o NDC T2 apresentou correlação significativa comaincapacidade motora. NDC T2 mostrou uma correlação inversa com o escore total da FARS, assim comoo subescore FARS III (exame neurológico propriamente dito). Análise longitudinal também revelou que a taxa de redução do NDC T2 está associada à deterioração

clínica após um ano de seguimento. Este resultado é inédito e sugere fortemente que o NDC T2 pode ser um marcador de imagem para evolução da FRDA.

***Estudo multimodal de neuroimagem***

Na FRDA, o dano macroestrutural no SNC evidenciado em nosso estudo é mais extenso do que previamente relatado na literatura. Confirmamos a atrofia na SC e SB em núcleos denteados de cerebelo e no tecido adjacente, além de tronco cerebral e pedúnculo cerebelar superior (47, 48, 49, 50, 74). Contudo, observamos importante dano supratentorial: 1) redução de SC em ambos os giros pré-centrais; e 2) atrofia de SB em regiões periventriculares, como em corpo caloso.

Da mesma forma, evidenciamos dano microestrutural da SB mais proeminente do que relatado previamente e incluindoos tractos piramidais e o corpo caloso (49, 51, 74, 75). O pedúnculo cerebelar superior é também afetado, como já descrito previamente, e corroborando com a degeneração de tractos entre cerebelo e estruturas supratentoriais, descritos por Akhlaghi e Zalesky et al (51, 52, 56, 76). A análise de DTI mostrou aumento dos valores tanto de AD quanto de RD, indicando uma disfunção combinada de axonios e de oligodendrócitos. Seria, portanto, um fenomeno semelhante ao observado no sistema nervoso periférico dos pacientes com FRDA, em que há um padrão misto de lesão histológica, com disfunção deaxônios e células de Schwann (77). Estudos de patologia mostraram que há redução de células gigantes de Betz na camada V do córtex pré-motor e conseqüente redução de fibras mielinizadas, o que está em acordo com o dano encontrado nos tractos piramidais na análise de DTI e a redução de substância cinzenta em giros pré-centrais no estudo de VBM (77).

O núcleo denteado de cerebelo é um dos sítios de maior degeneração na FRDA (1). Nossos resultados corroboram com esta afirmação, uma vez que mostraram importante correlação entre parâmatros de gravidade da ataxia e a perda de SB e SC em cerebelo e suas conexões. A correlação entre a lesão microestrutural em corpo caloso e a incapacidade motora, entretanto, é inédita na FRDA. Corpo caloso, entretanto, é importante para a execução de provas complexas que envolvem controle bimanual e pode ser útil como marcador de neuroimagem na FRDA.

O estudo longitudinal mostrou que há atrofia progressiva de SC nas regiões frontais e temporais e hemisférios cerebelares, além de redução de SB progressiva em regiões límbicas e giro cingulado. A redução volumétrica em áreas motoras, como nos giros pré-centrais, pode estar relacionada à deterioração clínica nos pacientes com FRDA. Não houve, porém, redução progressiva nos núcleos denteados e pedúnculos cerebelares superiores. Este fato pode ter ocorrido devido a um "floor effect", ou seja, estas estruturas já apresentam atrofia tão acentuada, que se torna difícil documentar piora adicional numa população de adultos. Diante disso, estudos em crianças e adolescentes seriam uma boa alternativa para avaliar melhor este aspecto. Outra explicação possível teria a ver com a progressão lenta da atrofia, de modo que num intervalo curto de 2 anos não seria possível a comprovação de mudança. Neste sentido, estudos com seguimento maior dos pacientes seriam bastante válidos.

## Conclusão

1. Depressão na FRDA é frequente, ocorrendo em 36,3% dos pacientes estudados. A fadiga também é igualmente frequente, sendo identificada em 29,6% dos pacientes com FRDA. Ambas são pouco reconhecidas e tratadas nos pacientes com FRDA. Os distúrbios de sono ou sonolência diurna não são sintomas frequentes nesta população.
2. A depressão, nos pacientes com FRDA, está relacionada à lesão estrutural da região frontal, especialmente do giro cingulado anterior.
3. A relaxometria T2 nos NDC é anormal nos pacientes com FRDA, progressiva ao longo do tempo e correlaciona-se com a gravidade da doença. A relaxometria T2 nos NDC, assim sendo, pode ser utilizada como um marcador de imagem para evolução da FRDA.
4. Os pacientes com FRDA apresentam extensa atrofia de substância branca e cinzenta, afetando regiões infratentoriais (principalmente região de núcleos denteados de cerebelo) e supratentoriais (principalmente giros pré-centrais), e estas regiões correlacionam-se à gravidade da doença.
5. O dano microestrutural da SB é igualmente extenso, afetando vias eferentes do cerebelo, tractos piramidais e corpo caloso. A lesão em corpo caloso apresenta correlação com a incapacidade motora da doença.
6. Os pacientes com FRDA apresentam atrofia progressiva de substância branca e cinzenta, acometendo as regiões frontais e temporais e hemisférios cerebelares.
7. Não houve redução significativa nos volumes dosNDC e dos pedúculos cerebelares superiores nos pacientes com FRDA ao longo de 2 anos. Da mesma forma, os parâmetros da tractografia de tractos piramidais e corpo caloso não se modificaram de forma significativa neste período.

**Referências**

1. Koeppen AH. Friedreich's ataxia: pathology, pathogenesis and molecular genetics. J Neurol Sci 2011;303:1-12.

2. Alper G, Narayanan V. Friedreich's ataxia. Pediatr Neurol 2003;28:335-41.

3. Fogel BL, Perlman S. Clinical features and molecular genetics of autosomal recessive cerebellar ataxias. Lancet Neurol 2007;6:245-57.

4. Campuzano V, Montermini L, Moltò MD, Pianese L, Cossée M, Cavalcanti F, et al. Friedreich's ataxia: autosomal recessive disease caused by anintronic GAA triplet repeat expansion. Science 1996;271:1423-7.

5. Pandolfo M.Friedreich ataxia. Arch Neurol 2008;65:1296-303.

6. Schmucker S, Puccio H. Understanding the molecular mechanisms of Friedreich's ataxia to develop therapeutic approaches. Hum Mol Genet 2010;19:R103-10.

7. Morral JA, Davis AN, Qian J, Gelman BB, Koeppen AH. Pathology and pathogenesis of sensory neuropathy in Friedreich's ataxia. Acta Neuropathol 2010;120:97-108.

8. Koeppen AH, Kuntzsch EC, Bjork ST, Ramirez RL, Mazurkiewicz JE, Feustel PJ. Friedreich ataxia: metal dysmetabolism in dorsal root ganglia. Acta Neuropathol Commum 2013;1-26.

9. Koeppen AH, Michael SC, Knutson MD, Haile DJ, Qian J, Levi S, et al. The dentate nucleus in Friedreich's ataxia: the role of iron-responsive proteins. Acta Neuropathol. 2007;114:163-73.

10. Koeppen AH, Ramirez RL, Yu D, Collins SE, Qian J, Parsons PJ, et al. Friedreich's ataxia causes redistribution of iron, copper and zinc in the dentate nucleus. Cerebellum 2012;11:845-60.

11. Mateo I, Llorca J, Volpini V, Corral J, Berciano J, Combarros O. GAA expansion size and age at onset of Friedreich's ataxia. Neurology 2003;61:274-5.

12. La Pean A, Jeffries N, Grow C, Ravina B, Di Prospero NA. Predictors of progression in patients with Friedreich ataxia. Mov Disord 2008;23:2026-32.

13. Di Prospero NA, Baker A, Jeffries N, Fischbeck KH. Neurological effects of high-dose indebenone in patients with Friedreich's ataxia: a randomized, placebo-controlled trial. Lancet Neurol 2007;6:878-86.

14. Lynch DR, Perlman SL, Meier T. A phase 3, double-blind, placebo-controlled trial of idebenone in Friedreich ataxia. Arch Neurol 2010;67:941-7.

15. Lagedrost SJ, Sutton MS, Cohen MS, Satou GM, Kaufman BD, Perlman SL, et al. Idebenone in Friedreich ataxia cardiomyopathy-results from a 6-month phase III study (IONIA). Am Heart J 2011;161:639-45.

16. Meier T, Perman SL, Rummey C, Coppard NJ, Lynch DR. Assessment of neurological efficacy on idebenone in pediatric patients with Friedreich's ataxia: data from a 6-month controlled study followed by a 12-month open-label extension study. J Neurol 2012;259:284-91.

17. Sturm B, Stupphann D, Kaun C, Boesch S, Schranzhofer M, Wojta J, et al. Recombinant human erythropoietin: effects on frataxin expression in vitro. Eur J Clin Invest 2005;35:711-7.

18. Sturm B, Helminger M, Steinkellner H, Heidari MM, Goldenberg H, Scheiber-Mojdehkar B. Carbamylated erythropoietin increases frataxin independent from erythropoietin receptor. Eur J Clin Invest 2010;40:561-5.

19. Boesch S, Sturm B, Hering S, Scheiber-Mojdehkar B, Steinkellner H, Goldenberg H, et al. Neurological effects of recombinant human erythropoietin in Friedreich's ataxia: a clinical pilot trial. Mov Disord 2008;23:1940-4.

20. Subramony SH, May W, Lynch D, Gomez C, Fischbeck K, Hallet M, et al. Measuring Friedreich ataxia: interrater reliability of a neurologic rating scale. Neurology 2005;64:1261-2.

21. Nachbauer W, Hering S, Deifert M, Steinkellner H, Sturm B, Scheiber-Mojdehkar B, et al. Effects of erythropoietin on frataxin levels and mithocondrial function in Friedreich ataxia – a dose-responsive trial. Cerebellum 2011;10:763-9.

22. Mariotti C, Fancellu R, Caldarazzo S, Nanetti L, Di Bella D, Plumari M, et al. Erythropoietin in Friedreich ataxia: no effect on frataxim in a randomized controlled trial. Mov Disord 2012;27:446-9.

23. Boddaert N, Sang KHLQ, Rötig A, Leroy-Willlig A, Gallet S, Brunelle F, et al. Selective iron chelation in Friedreich ataxia: biologic and clinical implications. Blood. 2007;110:401-8.

24. Velasco-Sánchez D, Aracil A, Montero R, Mas A, Jiménez L, O'Callaghan M, et al. Combined therapy with Idebenone and Deferiprone in patients with Friedreich's Ataxia. Cerebellum. 2011;10:1-8.

25. Marriotti C, Nachbauer W, Panzeri M, Poewe W, Taroni F, Boesch S. Erythropoietin in Friedreich ataxia. J Neurochem 2013;126(Suppl1):80-7.

26. Friedman LS, Farmer JM, Perlman S, Wilmot G, Gomez CM, Bushara KO, et al. Measuring the rate of progression in Friedreich ataxia: implications for clinical trial design. Mov Disord 2010;25:426-32.

27. Saute JA, Donis KC, Serrano-Munuera C, Genis D, Ramirez LT, Mazzetti P, et al. Ataxia rating scales – psychometric profiles, natural history and their application in clinical trials. Cerebellum 2012;11:488-504.

28. Hart RP, Kwentus JA, Leshner RT, Frazier R. Information processing speed in Friedreich's ataxia. Ann Neurol 1985;17:612-4.

29. White M, Laconde R, Botez-Marquard T. Neuropsychologic and neuropsychiatric characteristics of patients with Friedreich's ataxia. Acta Neurol Scand 2000;102:222-6.

30. Wollmann T, Barroso J, Montón F, Nieto A. Neuropsychological test performance of patients with Friedreich's ataxia. J Clin Exp Neuropsychol 2002;24:677-86.

31. de Nóbrega E, Nieto A, Barroso J, Montón F. Differential impairment in semantic, phonemic and action fluency performance in Friedreich's ataxia: possible evidence of prefrontal dysfuction. J Int Neuropsychol Soc 2007;13:944-52.

32. Nieto A, Correia R, de Nóbrega E, Montón F, Hess S, Barroso J. Cognition in Friedreich ataxia. Cerebellum 2012;11:834-44.

33. Wilson CL, Fahey MC, Corben LA, Collins VR, Churchyard AJ, Lamont PJ, et al. Quality of the life in Friedreich ataxia: what clinical, social and demographic factors are important? Eur J Neurol 2007;14:1040-7.

34. Paulsen EK, Friedman LS, Myers LM, Lynch DR. Health-related quality of life in children with Friedreichataxia. Pediatr Neurol 2010;42:335-7.

35. Epstein E, Farmer JM, Tsou A, Perman S, Subramony SH, Gomez CM, et al. Health related quality of life measures in Friedreich ataxia. J Neurol Sci 2008;272:123-8.

36. Frauscher B, Hering S, Högel S, Gschliessed V, Ulmer H, Poewe W, et al. Restless legs syndrome in Friedreich ataxia: a polysomnographic study. Mov Disord 2011;26:302-6.

37. Corben LA, Ho M, Copland J, Tai G, Delatycki MB. Increased prevalence of sleep-disordered breathing in Friedreich ataxia. Neurology 2013;81:46-51.

38. Paty DW, Li DK. Interferon beta-1b is effective in relapsing-remitting multiple sclerosis. II. MRI analysis results of a multicenter, randomized, double-blind, placebo-controlled trial. UBC MS/MRI Study Group and the IFNB Multiple Sclerosis Study Group. Neurology 1993;43:662-7.

39. De Michele G, Di Salle F, Filla A, D'Alessio G. Ambrosio G, Viscardi L, et al. Magnetic resonance imaging in "typical" and "late onset" Friedreich's disease and early onset cerebelar ataxia with retained tendo reflexes. J Neurol Sci. 1995;16:303-8.

40. Klockgether T, Petersen D, Grodd W, Dichgans J. Early onset cerebelar ataxia with retained tendon reflexes. Clinical, eletrophysiological and MRI observations in comparisson with Friedreich's ataxia. Brain. 1991;114:1559-73.

41. Chevis C, Silva CB, D'Abreu A, Lopes-Cendes I, Cendes F, Bergo FPG, et al. Spinal cord atrophy correlates with disability in Friedriech's ataxia. Cerebellum. 2013;12:43-7.

42. Schenck JF. Magnetic resonance imaging of brain iron. J Neurol Sci. 2003;207:99-102.

43. Waldvogel D, Gelderen P, Hallet M. Increased iron in the dentate nucleus of patients with Friedreich's ataxia. Ann Neurol. 1999;46:123-5.

44. Martin WR. Quantitative estimation of regional brain iron with magnetic resonance imaging. Parkinsonism and Relat Disord. 2009;15(suppl3):S215-8.

45. Hasan KM, Walimuni IS, Kramer LA, Narayana PA. Human brain mapping using atlas-based T2 relaxometry. Magn Reson Med. 2011;67:731-9.

46. Hikita T, Abe K, Sakoda S, Tanaka H, Murase K, Fujita N. Determination of transverse relaxation rate for estimating iron deposits in central nervous system. Neurosci Res. 2005;51:67-71.

47. Della Nave R, Ginestroni A, Giannelli M, Tessa C, Salvatore E, Salvi F, et al. Brain structural damage in Friedreich's ataxia. J Neurol Neurosurg Psychiatry 2008;79:82-5.

48. França Jr MC, D'Abreu A, Yassuda CL, Bonadia LC, Silva MS, Nucci A, et all. A combined voxel-based morphometry and H-MRS study in patients with Friedreich's ataxia. J Neurol 2009;256:1114-20.

49. Della Nave R, Ginetrini A, Tessa C, Salvatore E, Bartolomei I, Salvi F, et al. Brain white matter tracts degeneration in Friedreich ataxia. Na in vivo MRI study using tract-based spatial statistics ans voxel-based morphometry. NeuroImage 2008;40:19-25.

50. Akhlaghi H, Corben L, Georgiou-Karistianis N, Bradshaw J, Storey E, Delatycki MB, et al. Superior cerebellar peduncle atrophy in Friedreich's ataxia correlates with disease symptoms. Cerebellum 2011; 10: 81-7.

51. Della Nave R, Ginestroni A, Diciotti S, Salvatore E, Soricelli A, Mascalchi M. Axial diffusivity in increased in the degenerating superior cerebellar peduncles of Friedreich's ataxia. Neuroradiology 2011; 53: 367-72.

52. Hohenberg CC, Schoke MF, Wigand MC, Nachbauer W, Guttmann CRG, Kubicki M, et al. Radial diffusivity in cerebellar peduncles correlates with clonical severity in Friedreich ataxia. Neurol Sci 2013; 34: 1459-62.

53. Akhlaghi H, Corben L, Georgiou-Karistianis N, Bradshaw J, Delatychi MB, Storey E, et al. A functional MRI study dysfuction in Friedreich's ataxia. Brain Res 2012;1471:138-54.

54. Ginestroni A, Diciotti S, Cecchi P, Pesaresi I, Tessa C, Gioanelli M, et al. Neurodegeneration in Friedreoch's ataxia is associated with a mixed activation pattern of the brain. A fMRI study. Hum Brain Mapp 2012;33:1780-91.

55. Georgiou-Karistianis N, Akhlaghi H, Corben LA, Delatycki MB, Storey E, Bradsshaw JL, et al. Brain Cogn 2012;79:200-8.

56. Zalesky A, Akhlaghi H, Corben LA, Bradshaw JL, Delatycki MB, Storey E, et al. Cerebello-cerebral connectivity déficits in Friedreich ataxia. Brain Struct Funct2014;219:969-81.

57. Cardoso EF, Maia FM, Fregni F, Myczkowski ML, Melo LM, Sato JR, et al. Depression in Parkinson's disease: converge from voxel-based morphometry and functional magnetic resonance in limbic thalamus. NeuroImage 2009;47:467-72.

58. Cecchin CR, Pires AP, Rieder CR, Monte TL, Silveira I, Carvallo T, et al. Depressive symptoms in Machado-Joseph disease (SCA3) patients and their relatives.Community Genet2007;10:19-26.

59. Flerck MP, Berlim MT, Lafer B, Sougey EB, Del Porto JA, Brasil MA, et al. Review of the guidelines of the Brazilian Medical Association for the treatment of depression. Rev Bras Psiquiatr 2009;31:S7-17.

60. Lee HY, Tae WS, Yoon HK, Lee BT, Paik JW, Son KR, et al. Demonstration of decreased gray matter concentration in the midbrain encompassing the dorsal raphe nucleus and the limbic subcortical regions in major depressive disorder: an optimized voxel-based morphometry study. J Affect Disord 2011;133:128-36.

61. Bora E, Fornito A, Pantelis C, Yücel M. Gray matter abnormalities in major depressive disorder: a meta-analysis of voxel based morphometry studies. J Affect Disord 2012;138:9-18.

62. Kostic VS, Filippi M. Neuroanatomical correlates of depression and apathy in Parkinson's disease: magnetic resonance imaging studies. J Neurol Sci 2011;310:61-3.

63. Zou K, Deng W, Li T, Zhang B, Jiang L, Huang C, et al. Changes of brain morphometry in first-episode, drug-naive, non-late-life adult patients with major depression: an optimized voxel-based morphometry study. Biol Psychiatry 2010;67:186-8.

64. Wagner G, Koch K, Schachtzabel C, Reichenbach JR, Sauer H, Schlöser Md RG. Enhanced rostral anterior cingulate cortex activation during cognitive control is related to orbitofrontal volume reduction in unipolar depression. J Psychiatry Neurosci 2008;33:199-208.

65. Vasic N, Walter H, Höse A, Wolf RC. Gray matter reduction associated with psychopathology and cognitive dysfunction in unipolar depression: a voxel-based morphometry study. J Affect Disord 2008;109:107-16.

66. Peng J, Liu J, Nie B, Li Y, Shan B, Wang G, et al. Cerebral and cerebellar gray matter reduction in first-episode patients with major depressive disorder: a voxel-based morphometry study. Eur J Radiol 2011;80:395-9.

67. Campbell S, Marriott M, Nahmias C, MacQueen GM. Lower hippocampal volume in patients suffering from depression: a meta-analysis. Am J Psychiatry 2004;161:598-607.

68. Hamilton J, Siemer M, Gotlib I. Amygdala volume in major depressive disorder: a meta-analysis of magnetic resonance images studies. Mol Psychiatry 2008;13:993-1000.

69. Koolschijn P, van Haren N, Lensvelt-Mulders G, Hulshoff Pol HE, Kahn RS. Brain volume abnormalities in major depressive disorder: a meta-analysis of magnetic resonance imaging studies. Hum Brain Mapp 2009;30:3719-35.

70. Ye T, Peng J, Nie B, Gao, J, Liu J, Li Y, et al. Altered functional connectivity of dosrsolateral prefrontal cortex in first-episode patients with major depressive disorder. Eur J Radiol 2012;81:4035-40.

71. Carballedo A, Scheuerecker J, Meisenzahl E, Bokde A, Möller HJ, Doyle M, et al. Functional connectivity of emotional processing in depression. J Affect Disord 2011;134:272-9.

72. Ochsner KN, Gross JJ. The cognitive control of emotion. Trends Cogn Sci 2005;9:242-9.

73. Leung KK, Lee TMC, Wong LS, Li LSW, Yip PSF, Khong L. Neural correlates of attention biases of people with major depressive disorder: a voxel-based morphormetry study. Psychol Med 2009;39:1097-106.

74. Pagani E, Ginestroni A, Della Nave R, Agosta F, Salvi F, De Michele G, et al. Assessment of brain white matter bundle atrophy in patients with Friedreich ataxia. Radiology 2010; 255: 882-7.

75. Rizzo G, Tonon C, Valentino ML, Manners D, Fortuna F, Gellera G, et al. Brain diffusion-weighted imagind in Friedreich's ataxia. Mov Disord 2011; 26: 705-12.

76. Akhlaghi H, Yu J, Corben L, Georgiou-Karistianis N, Brandshaw J, Storey E, et al. Cognitive deficits in Friedreich ataxia correlate with micro-structural changes in dentatorubral tract. Cerebbelum 2014; 13: 187-98.

77. Koeppen AH, Mazurkiewicz JE. Friedreich ataxia: neuropathology revised. J Neuropathol Exp Neurol 2013; 72: 78-90.

*Anexo 1*

UNICAMP

**FACULDADE DE CIÊNCIAS MÉDICAS**
**COMITÊ DE ÉTICA EM PESQUISA**

www.fcm.unicamp.br/fcm/pesquisa

CEP, 08/04/11
(Grupo III)

**PARECER CEP:** N° 131/2011 (Este n° deve ser citado nas correspondências referente a este projeto).
**CAAE**: 0090.0.146.000-11

**I - IDENTIFICAÇÃO:**

PROJETO: **"AVALIAÇÃO PROSPECTIVA DE NEUROIMAGEM NA ATAXIA DE FRIEDREICH".**
PESQUISADOR RESPONSÁVEL: Cynthia Bonilha da Silva
INSTITUIÇÃO: Hospital das Clínicas/UNICAMP
APRESENTAÇÃO AO CEP: 02/03/2011
**APRESENTAR RELATÓRIO EM: 08/04/12** (O formulário encontra-se no *site* acima).

**II – OBJETIVOS.**

Determinar o padrão e a extensão de anormalidades estruturais no sistema nervoso central nos pacientes com Ataxia de Friedreich (FRDA) e correlacionar com a evolução clínica.

**III – SUMÁRIO.**

O estudo visa Identificar alterações neurodegenerativas na substância branca e cinzenta, quantificar depósitos de ferro em núcleos denteados e correlacionar tais alterações com a disfunção clínica nos pacientes com FRDA, de forma prospectiva. Farão parte da amostra, pacientes com diagnóstico confirmado de FRDA e um grupo controle constituído por pessoas sadias. Os pacientes serão submetidos a: a) avaliação clínica-neurológica, com a utilização da escala Friedreich Ataxia Rating Scale - FARS; b) exame de ressonância magnética (RM) no mesmo dia da avaliação clínica. Ambos os procedimentos serão realizados em um momento inicial e após 12 meses. Para o grupo controle, serão considerados indivíduos com histórico negativo para ataxias e neuropatias hereditárias, ausência de sintomatologia neurológica e exame clínico-neurológico normal.

**IV - COMENTÁRIOS DOS RELATORES**

Após respostas às pendências, o projeto encontra-se adequadamente redigido e de acordo com a Resolução CNS/MS 196/96 e suas complementares, bem como o Termo de Consentimento Livre e Esclarecido.

**V - PARECER DO CEP**

O Comitê de Ética em Pesquisa da Faculdade de Ciências Médicas da UNICAMP, após acatar os pareceres dos membros-relatores previamente designados para o presente caso e atendendo todos os dispositivos das Resoluções 196/96 e complementares, resolve aprovar sem

Comitê de Ética em Pesquisa - UNICAMP
Rua: Tessália Vieira de Camargo, 126
Caixa Postal 6111
13083-887 Campinas – SP

FONE (019) 3521-8936
FAX (019) 3521-7187
cep@fcm.unicamp.br

restrições o Protocolo de Pesquisa, bem como ter aprovado o Termo do Consentimento Livre e Esclarecido, assim como todos os anexos incluídos na Pesquisa supracitada.

O conteúdo e as conclusões aqui apresentados são de responsabilidade exclusiva do CEP/FCM/UNICAMP e não representam a opinião da Universidade Estadual de Campinas nem a comprometem.

## VI - INFORMAÇÕES COMPLEMENTARES

O sujeito da pesquisa tem a liberdade de recusar-se a participar ou de retirar seu consentimento em qualquer fase da pesquisa, sem penalização alguma e sem prejuízo ao seu cuidado (Res. CNS 196/96 – Item IV.1.f) e deve receber uma cópia do Termo de Consentimento Livre e Esclarecido, na íntegra, por ele assinado (Item IV.2.d).

Pesquisador deve desenvolver a pesquisa conforme delineada no protocolo aprovado e descontinuar o estudo somente após análise das razões da descontinuidade pelo CEP que o aprovou (Res. CNS Item III.1.z), exceto quando perceber risco ou dano não previsto ao sujeito participante ou quando constatar a superioridade do regime oferecido a um dos grupos de pesquisa (Item V.3.).

O CEP deve ser informado de todos os efeitos adversos ou fatos relevantes que alterem o curso normal do estudo (Res. CNS Item V.4.). É papel do pesquisador assegurar medidas imediatas adequadas frente a evento adverso grave ocorrido (mesmo que tenha sido em outro centro) e enviar notificação ao CEP e à Agência Nacional de Vigilância Sanitária – ANVISA – junto com seu posicionamento.

Eventuais modificações ou emendas ao protocolo devem ser apresentadas ao CEP de forma clara e sucinta, identificando a parte do protocolo a ser modificada e suas justificativas. Em caso de projeto do Grupo I ou II apresentados anteriormente à ANVISA, o pesquisador ou patrocinador deve enviá-las também à mesma junto com o parecer aprovatório do CEP, para serem juntadas ao protocolo inicial (Res. 251/97, Item III.2.e)

Relatórios parciais e final devem ser apresentados ao CEP, de acordo com os prazos estabelecidos na Resolução CNS-MS 196/96.

## VII- DATA DA REUNIÃO

Homologado na III Reunião Ordinária do CEP/FCM, em 22 de março de 2011.

**Prof. Dr. Carlos Eduardo Steiner**
PRESIDENTE do COMITÊ DE ÉTICA EM PESQUISA
FCM / UNICAMP

*Anexo 2*

**TERMO DE CONSENTIMENTO LIVRE E ESCLARECIDO**

Título do projeto: **Avaliação Prospectiva de Neuroimagem na Ataxia de Friedreich**

Investigador principal: Dr. Marcondes França e Cynthia Bonilha da Silva

OBJETIVO DA PESQUISA:

Eu _____ entendo que fui convidado (a) a participar em um projeto de pesquisa envolvendo pacientes com ataxia de Friedreich. O objetivo geral do estudo é o de determinar a utilidade da imagem por Ressonância Magnética nesta doença, o que pode, eventualmente, melhorar o diagnóstico e levar a um melhor tratamento dessa doença. As informações médicas a meu respeito que forem obtidas para esse estudo, poderão ser compartilhadas com outros pesquisadores que trabalham com diversos tipos de doenças neurodegenerativas, podendo ser utilizadas para outros fins de pesquisa sobre ataxias.

A ressonância magnética é uma técnica capaz de produzir imagens de alta qualidade e nitidez anatômica, assim como informações sobre a bioquímica (funcionamento) dos tecidos. As imagens são obtidas por um campo magnético (como imã), e transmitidas a um computador, forma as imagens.

PROCEDIMENTO:

Eu entendo que, se concordar em participar desse estudo, os pesquisadores participantes farão perguntas a respeito dos meus antecedentes médicos e de minha família. Eu serei submetido a um exame físico neurológico para estabelecer meu estado clínico. Hospitalização não será necessária.

O procedimento de ressonância magnética é semelhante a uma tomografia. Eu fui informado que eu serei colocado em uma maca e serei movido lentamente para dentro do aparelho. Por um alto poderei me comunicar com as pessoas responsáveis pelo exame. Durante todo o tempo, o pessoal médico e paramédico poderão me ver e ouvir e o exame pode ser parado a qualquer momento se for preciso (por exemplo, se durante o exame eu me sentir mal ou desconfortável). O exame pode durar entre 30 a 45 minutos.

VANTAGENS:

Eu entendo que não terei nenhuma vantagem com a minha participação nesse estudo e que o meu diagnóstico e o meu tratamento provavelmente não serão modificados. Contudo, os resultados desse estudo podem oferecer vantagens para os indivíduos com ataxias, possibilitando melhor diagnóstico e tratamento mais adequado. Os resultados do meu exame de ressonância magnética ficarão à disposição dos médicos responsáveis pelo meu tratamento, e poderão ser úteis no futuro.

RISCO E DESCONFORTO:

O único desconforto relacionado a este exame é o ruído intermitente durante os primeiros 15 minutos, tipo marteladas. Depois disso o ruído será muito menor.

REQUERIMENTOS

É **muito importante** informar aos médicos(as) e técnicos(as) caso eu tenha um **marca-passo cardíaco, um clipe de cirurgia para aneurisma cerebral ou qualquer outro objeto metálico em meu corpo,** que tenha sido implantado durante uma cirurgia ou alojado em meu corpo durante um acidente, pois estes podem parar de funcionar ou causar acidentes devido ao forte campo magnético que funciona como um imã muito forte. Eu também devo remover todos os objetos metálicos que estiverem comigo (relógio, canetas, brincos, colares, anéis, etc), pois estes também podem movimentar ou aquecer dentro do aparelho.

SIGILO:

Eu entendo que todas as informações médicas decorrentes desse projeto de pesquisa farão parte do meu prontuário médico e serão submetidos aos regulamentos do HC- UNICAMP referentes ao sigilo da informação médica. Se os resultados ou informações fornecidas forem utilizados para fins de publicação científica, nenhum nome será utilizado.

FORNECIMENTO DE INFORMAÇÃO ADICIONAL:

Eu entendo que posso requisitar informações adicionais relativas ao estudo a qualquer momento. O Dr. Marcondes França e a Dra Cynthia Bonilha da Silva, tel: (19) 9838-8616 ou 3521-7754 ou e-mail: cynthia.bonilha@gmail.com , estará disponível para responder minhas questões e preocupações. Em caso de recurso, dúvidas ou reclamações contatar a secretaria da Comissão de Ética da Faculdade de Ciências Médicas-UNICAMP, tel. (019) 3521-7232.

RECUSA OU DESCONTINUAÇÃO DA PARTICIPAÇÃO:

Eu entendo que a minha participação é voluntária e que eu posso me recusar a participar ou retirar meu consentimento e interromper a minha participação no estudo a qualquer momento sem comprometer os cuidados médicos que recebo atualmente ou receberei no futuro no HC-UNICAMP.

TERMO DE CONSENTIMENTO:-

Eu confirmo que o(a) Dr(a)._____

me explicou o objetivo do estudo, os procedimentos aos quais serei submetido e os riscos, desconforto e possíveis vantagens advindas desse projeto de pesquisa. Eu li e compreendi esse formulário de consentimento e estou de pleno acordo em participar desse estudo.

_____

Nome do participante ou responsável

_____ _____

Assinatura do participante ou responsável data

RESPONSABILIDADE DO PESQUISADOR:

Eu expliquei a _____ o objetivo do estudo, os procedimentos requeridos e os possíveis riscos e vantagens que poderão advir do estudo, usando o melhor do meu conhecimento. Eu me comprometo a fornecer uma cópia desse formulário de consentimento ao participante ou responsável.

_____

Nome do pesquisador ou associado

_____ _____

Assinatura do pesquisador ou associado data

*Anexo 3*

**Técnicas de análise de imagem utilizadas neste estudo**

*Relaxometria T2*

Foram utilizadas imagens da sequência T2 multi-eco, adquirida em um plano perpendicular ao eixo longitudinal do hipocampo (TE = 30-60-90-120-150 ms, TR = 3300ms, voxels of 0.41 x 0.41 x 3.0 $mm^3$, FOV = 180 x 108, 36 fatias, 3mm de espessura). As imagens foram analisadas em um programa desenvolvido em nosso laboratório de neuroimagem, chamado Aftervoxel 3D Mediacl Image Visualization (http://www.liv.ic.unicamp.br/~bergo/aftervoxel) (Guimarães et al, 2013). Neste programa, as estruturas de interesse são segmentadas de forma manual, porém os valores da relaxometria são obtidos de modo automático. Os núcleos denteados do cerebelo, substância negra, putamen e substância branca do cerebelo foram marcados com ROIs circulares e a relaxometria T2 foi obtida de cada estrutura.

*Análise por Morfometria baseda em voxels – VBM*

Foram obtidas imagens volumétricas (3D) na sequência T1, adquiridas em um plano sagital, com espessura de 1 mm (flip angle=35°, TR=7.1 ms, TE=3.2 ms, matrix=240×240, field of view=24×24 cm).

Primeiramente, as imagens volumétricas são convertidas em um formato NIfTI. Os programas SPM 8 (Wellcome Department of Imaging Neuroscience, London, England, www.fil.ion.ucl.ac.uk) e VBM 8 (http://dbm.neuro.uni-jena.de/vbm8/), rodados dentro da plataforma MATLAB 8.0, são utilizados para realizar os passos automáticos de pré-

processamento, que incluem etapas de normalização espacial, segmentação, modulação e suavização ("smoothing"). A normalização espacial é a transformação de todas as imagens em um mesmo espaço estereotáxico e utiliza em conjunto o algorítmo DARTEL, o qual reduz de forma significativa imprecisões nesta etapa (Ashburner, 2007). Em seguida, são realizadas as etapas de segmentação, ou seja, a separação da substância branca, substância cinzenta e líquor, e de modulação, que é a correção de alterações nos volumes induzidas pela normalização espacial. Por fim, a suavização é realizada, ou seja, o uso de um filtro para deixar as bordas da segmentação mais definidas. As imagens processadas são comparadas usando análise estatística *voxel-wise* (Ashburner e Friston, 2000). No SPM, teste T e regressão múltipla foram utilizados para avaliar, respectivamente, diferenças nos volumes de substância branca e cinzenta entre pacientes e controles, e a correlação entre os volumes obtidos com parâmetros clínicos. Ambas as análises foram corrigidas para múltiplas comparações através de *false discovery rate* (FDR) e definido como significativo $p < 0,05$. O programa XJVIEW (http://www.alivelearn.net/xjview/) foi utilizado para analisar os resultados e obter a localização anatômica. Na análise longitudinal, as diferenças entre os grupos foram examinadas através do desenho fatorial flexível, levando em consideração o tempo (tempo 0 e *follow-up*) e o grupo (paciente e controle). Aqui, os resultados significativos foram definidos como $p < 0,001$ (não corrigido) (Gläscher and Gitelman, 2008; Jason et al, 2014).

*Análise das regiões de interesse – ROIs*

Neste estudo, foram utilizadas as imagens volumétricas 3D. As regiões de interesse (ROI) foram manualmente definidas nos núcleos denteados de cerebelo e nos pedúnculos cerebelares superiores em um *template* normalizado. Este *template* foi criado a partir das imagens dos

controles, ponderadas na sequência T1. Posteriormente, utiliza-se um método de deformação 3D em cada sujeito para aplicar uma operação de normalização inversa (*SPM8-Deformation fields algorithm*), para trazer os ROIs normalizados para o espaço específico de cada indivíduo. Finalmente, cada ROI deformado é sobreposto nas imagens de cada indivíduo e os valores quantitativos das médias de intensidade e dos volumes são estimados individualmente.

*Análise de espessura cortical – FreeSurfer*

As espessuras corticais e os volumes subcorticais foram determinados utilizando-se o programa FreeSurfer (versão 5.3), de acordo com com protocolo desenvolvido pot Fischl e Dale (Fisch e Dale, 2000). Primeiramente, as imagens são corrigidas para inohomogeneidade do campo magnético e convertidas para o atltas de Talairach e Tournoux (Talairach e Tournoux, 1988). Depois, os voxels são separados em substância branca, substância cinzenta e líquor. Utilizando rendilhados triangulares, são criadas duas superficies: a branca, que é definida como a interface entre substância branca e cinzenta, e a superfície pial. A espessura cortical é calculada a partir da distância mínima entre ambas as superfícies em cada vertex ao longo do manto cortical. Para todas as análises, usamos um filtro Gaussiano de 10mm para suavização. O volume intracraniano total (eTIV) (Buckner et al, 2004) e o volume de estruturas subcorticais foram calculados (Fischl et al, 2002). A espessura cortical foi comparada entre os grupos (pacientes x controles) através de uma regressão linear, tendo a idade, sexo e eTIV como regressores. As regiões corticais foram definidas de acordo com o atlas anatômico de Desikan (Desikan et al, 2006). Utilizamos correção para múltiplas comparações atráves do teste de Dunn-Sidak, considerando o nível de significância alfa = 0,001. Realizamos ainda a correlação entre as

regiões que foram significativamente diferentes entre pacientes e controles (espessuras corticais e os volumes subcorticais) com os parâmetros clínicos, considerando como significativo $p < 0,05$ (não corrigido).

*Análise das imagens por tensor de difusão (DTI) – Tract based spatial statistics (TBSS)*

As imagens por tensor de difusão (DTI) foram adquiridas em uma sequência ecoplanar não-collinear de 32 direções (flip angle=90°, voxel size=1×1×2 $mm^3$, TR=8500 ms, TE=61 ms, matrix=128×128, field of view=256×256 mm, 70 cortes com 3 mm de espessura, b value=1000). Obtivemos os mapas de anisotropia fracionada (FA), difusividade média (MD), difusividade radial (RD) e difusividade axial (AD), usando o *FMRIB diffusion toolbox,* que faz parte do programa FSL versão 4.1.4 (Smith et al, 2006). No pré-processamento, as imagens de FA são alinhadas para um espaço determinado (standard), usando registro não-linear. Em seguida, um *template* médio de FA é obtido, que possibilita a criação de um "esqueleto" médio da FA. Cada mapa de FA de cada indivíduo, então, é projetado netes esqueleto. O mesmo procedimento é realizado para obter os mapas estatísticos de MD, RD e AD. Aplicamos a seguir um teste t para avaliar diferenças estatísticas entre os grupos relativas a cada parâmetro. O *Threshold-Free Cluster Enhancement (TFCE)* foi utilizado para correção dos mapas estatísticos para múltiplas comparações ($p < 0,05$). O atlas de substância branca de Johns Hopkins foi utilizado para identificar os tractos específicos.

*Análise das imagens por tensor de difusão (DTI) – tractografia*

Baseados nos resultados do TBSS, optamos por estudar separadamente os tractos piramidais e o corpo caloso de cada indivíduo através da tractografia. O tensor calculado para todas as imagens foi realizado utilizando-se o programa ExploreDTI (A. Leemans, University Medical Center, Utrecht, Holanda). As regiões de interesse (ROIs) são definidas manualmente em um *template* normalizado, que foi criado a partir das imagens de DTI de 10 controles. Em seguida, utiliza-se uma matriz de deformação 3D para cada indivíduo a fim de aplicar uma operação de normalização inversa *(SPM8-deformation fields algorithm)*, e usando as variações entre o espaço nativo e de referência para trazer os ROIs normalizados ao espaço de cada indivíduo. Finalmente, o ROI ajustado é usado como meio para rastrear as fibras de cada tracto (parâmetros: FA minima para iniciar e manter rastreamento = 0,25; ângulo máximo do trato 20°; tamanho mínimo = 10mm). O tracto resultante foi visualmente checado e a média da FA, AD, RD foi calculada em cada hemisfério. O teste de Mann-Whitney foi utilizado para comparar os valores de pacientes e controles; e o coeficiente de correlação de Spearman para avaliar correlação entre os valores obtidos e os parâmetros clínicos. Na análise longitudinal, o teste de Wilcoxon foi usado para comparar cada grupo ao longo do tempo separardamente ($p < 0,05$).

*Referências*

1. Guimarães RP, D'Abreu A, Yasuda CL, et al. A multimodal evaluation of microstructural White matter damage in spinocerebbelar ataxia type 3. Mov Disord. 2013;28:1125-32.

2. Ashburner JA. A fast diffeomorphic image registration algorithm. Neuroimage 2007; 38: 95-113.

3. Ashburner J, Friston KJ. Voxel-based morphometry – the methods. Neuroimage 2000; 11: 805-21.

4. Gläscher J, Gitelman D. Contrast weights in flexible factorial design with multiple groups of subjects. https://www.jiscmail.ac.uk/cgibin/webadmin?A2=ind0803&L=SPM&P=R1 6629, 2008.

5. Jason S, Menekka KS, Winston GP, Bartlett P, McEvoy AW, Symms MR, et al. Working memory network platicity after anterior temporal lobe resection: a longitudinal functional magnetic resonance imaging study. Brain 2014; 137: 1439-53.

6. Fischl B, Dale AM. Measuring the thickness of the human cerebral cortex from magnetic resonance images. Proc Natl Acad Sci USA 2000; 97: 11050-5.

7. Talairach J, Tournoux P. Co-planar Stereotaxic Atlas of the Human Brain, Thieme, NY. 1988.

8. Buckner RL, Head D, Parker J, Fotenos AF, Marcus D, Morris JC, et al. A unified approach for morphometric and functional data analysis in young, old, and demented adults using automated atlas-based head size normalization: reliability and validation against manual measurement of total intracranial volume. Neuroimage. 2004; 23: 724-38.

9. Fischl B, Salat DH, Busa E, Albert M, Dieterich M, Haselgrove C, et al. Whole brain segmentation: automated labeling of neuroanatomical structures in the human brain. Neuron. 2002; 33: 341-55.

10. Desikan RS, Segonne F, Fischl B, Quinn BT, Dickerson BC, Blacker D, et al. An automated labeling system for subdividing the human cerebral cortex on MRI scans into gyral based regions of interest. Neuroimage. 2006; 31: 968-80.

11. Smith SM, Jenkinson M, Johansen-Berg H, Rueckert D, Nichols TE, Mackay CE, et al. Tract-based spatial statistics: voxelwise analysis of multi-subject diffusion data.Neuroimage 2006; 31: 1487-505.

*Anexo 4*

## Escala de sonolência de EPWORTH (ESS-BR)

Nome: _____

Data: _____ Idade (anos) _____

Qual a probabilidade de você cochilar ou dormir, e não apenas se sentir cansado, nas seguintes situações?

Considere o modo de vida que você tem levado recentemente. Mesmo que você não tenha feito algumas destascoisas recentemente, tente imaginar como elas o afetariam. Escolha o número mais apropriado para respondercada questão.

0 = nunca cochilaria

1 = pequena probabilidade de cochilar

2 = probabilidade média de cochilar

3 = grande probabilidade de cochilar

Sentado e lendo 0 1 2 3

Assistindo TV 0 1 2 3

Sentado, quieto, em um lugar público

(por exemplo, em um teatro, reunião ou palestra) 0 1 2 3

Andando de carro por uma hora sem parar, como passageiro 0 1 2 3

Sentado quieto após o almoço sem bebida de álcool 0 1 2 3

Em um carro parado no trânsito por alguns minutos 0 1 2 3

*Anexo 5*

## Índice de Qualidade de Sono de Pittsburgh – PSQI-BR

Nome:_____ Idade:_____
Data:_____

Instruções:

As seguintes perguntas são relativas aos seus hábitos de sono durante o último mês somente. Suas respostas devem indicar a

lembrança mais exata da maioria dos dias e noites do último mês. Por favor, responda a todas as perguntas.

1. Durante o último mês, quando você geralmente foi para a cama à noite?

Hora usual de deitar _____

2. Durante o último mês, quanto tempo (em minutos) você geralmente levou para dormir à noite?
Número de minutos _____

3. Durante o último mês, quando você geralmente levantou de manhã?

Hora usual de levantar _____

4. Durante o último mês, quantas horas de sono você teve por noite? (Este pode ser diferente do número de horas que você ficou na

cama). Horas de sono por noite _____

Para cada uma das questões restantes, marque a melhor (uma) resposta. Por favor, responda a todas as questões.

5. Durante o último mês, com que freqüência você teve dificuldade de dormir porque você...

(a) Não conseguiu adormecer em até 30 minutos

Nenhuma no último mês _____ Menos de 1 vez/ semana _____

1 ou 2 vezes/ semana _____ 3 ou mais vezes/ semana _____

(b) Acordou no meio da noite ou de manhã cedo

Nenhuma no último mês _____ Menos de 1 vez/ semana _____

1 ou 2 vezes/ semana _____ 3 ou mais vezes/ semana _____

(c) Precisou levantar para ir ao banheiro

Nenhuma no último mês _____ Menos de 1 vez/ semana _____

1 ou 2 vezes/ semana _____ 3 ou mais vezes/ semana _____

(d) Não conseguiu respirar confortavelmente

Nenhuma no último mês _____ Menos de 1 vez/ semana _____

1 ou 2 vezes/ semana _____ 3 ou mais vezes/ semana _____

(e) Tossiu ou roncou forte

Nenhuma no último mês _____ Menos de 1 vez/ semana _____

1 ou 2 vezes/ semana _____ 3 ou mais vezes/ semana _____

(f) Sentiu muito frio

Nenhuma no último mês _____ Menos de 1 vez/ semana _____

1 ou 2 vezes/ semana _____ 3 ou mais vezes/ semana _____

(g) Sentiu muito calor

Nenhuma no último mês _____ Menos de 1 vez/ semana _____

1 ou 2 vezes/ semana _____ 3 ou mais vezes/ semana _____

(h) Teve sonhos ruins

Nenhuma no último mês _____ Menos de 1 vez/ semana _____

1 ou 2 vezes/ semana _____ 3 ou mais vezes/ semana _____

(i) Teve dor

Nenhuma no último mês _____ Menos de 1 vez/ semana _____

1 ou 2 vezes/ semana _____ 3 ou mais vezes/ semana _____

(j) Outra(s) razão(ões), por favor descreva _____

Com que freqüência, durante o último mês, você teve dificuldade para dormir devido a essa razão?

Nenhuma no último mês _____ Menos de 1 vez/ semana _____

1 ou 2 vezes/ semana _____ 3 ou mais vezes/ semana _____

6. Durante o último mês, como você classificaria a qualidade do seu sono de uma maneira geral?

Muito boa _____ Boa _____ Ruim ____ Muito ruim _____

7. Durante o último mês, com que freqüência você tomou medicamento (prescrito ou ‘‘por conta própria’’) para lhe ajudar a dormir?

Nenhuma no último mês _____ Menos de 1 vez/ semana _____

1 ou 2 vezes/ semana _____ 3 ou mais vezes/ semana _____

8. No último mês, com que freqüência você teve dificuldade de ficar acordado enquanto dirigia, comia ou participava de uma atividade

social (festa, reunião de amigos, trabalho, estudo)?

Nenhuma no último mês _____ Menos de 1 vez/ semana _____

1 ou 2 vezes/ semana _____ 3 ou mais vezes/ semana _____

9. Durante o último mês, quão problemático foi para você manter o entusiasmo (ânimo) para fazer as coisas (suas atividades habituais)?

Nenhuma dificuldade _____ Um problema leve _____ Um problema razoável _____

Um grande problema _____

10. Você tem um(a) parceiro [esposo(a)] ou colega de quarto? ____

Parceiro ou colega, mas em outro quarto ____

Parceiro no mesmo quarto, mas não na mesma cama ____

Parceiro na mesma cama ____

Se você tem um parceiro ou colega de quarto, pergunte a ele/ela com que freqüência, no último mês, você teve …

(a) Ronco forte

Nenhuma no último mês _____ Menos de 1 vez/ semana _____

1 ou 2 vezes/ semana _____ 3 ou mais vezes/ semana _____

(b) Longas paradas na respiração enquanto dormia

Nenhuma no último mês _____ Menos de 1 vez/ semana _____

1 ou 2 vezes/ semana _____ 3 ou mais vezes/ semana _____

(c) Contrações ou puxões nas pernas enquanto você dormia

Nenhuma no último mês _____ Menos de 1 vez/ semana _____

1 ou 2 vezes/ semana _____ 3 ou mais vezes/ semana _____

(d) Episódios de desorientação ou confusão durante o sono

Nenhuma no último mês _____ Menos de 1 vez/ semana _____

1 ou 2 vezes/ semana _____ 3 ou mais vezes/ semana _____

(e) Outras alterações (inquietações) enquanto você dorme; por favor, descreva
_____

Nenhuma no último mês _____ Menos de 1 vez/ semana _____

1 ou 2 vezes/ semana _____ 3 ou mais vezes/ semana ____

Componente 1: Qualidade Subjetiva do Sono _____

Componente 2: Latência do Sono _____

Componente 3: Duração do Sono _____

Componente 4: Eficiência Habitual do Sono_____

Componente 5: Distúrbios do Sono_____

Componente 6: Uso de Medicação para Sono _____

Componente 7: Disfunção Diurna _____

*Anexo 6*

**Inventário de Depressão de Beck (BDI)**

**Nome: _____ Idade:_____**
**Data: _____**

Este questionário consiste em 21 grupos de afirmações. Depois de ler cuidadosamente cada grupo, faça um círculo em torno do número (0, 1, 2 ou 3) próximo à afirmação, em cada grupo, que descreve melhor a maneira que você tem se sentido na última semana, incluindo hoje. Se várias afirmações em um grupo parecerem se aplicar igualmente bem, faça um círculo em cada uma. Tome cuidado de ler todas as afirmações, em cada grupo, antes de fazer a sua escolha.

**1.** 0 Não me sinto triste.
1 Eu me sinto triste.
2 Estou sempre triste e não consigo sair disto.
3 Estou tão triste ou infeliz que não consigo suportar.

**2.** 0 Não estou especialmente desanimado quanto ao futuro.
1 Eu me sinto desanimado quanto ao futuro.
2 Acho que nada tenho a esperar.
3 Acho o futuro sem esperança e tenho a impressão de que as coisas não podem melhorar.

**3.** 0 Não me sinto um fracasso.
1 Acho que fracassei mais do que uma pessoa comum.
2 Quando olho para trás, na minha vida, tudo que posso ver é um monte de fracassos.
3 Acho que, como pessoa, sou um completo fracasso.

**4.** 0 Tenho tanto prazer em tudo como antes.
1 Não sinto mais prazer nas coisas como antes.
2 Não encontro um prazer real em mais nada.
3 Estou insatisfeito ou aborrecido com tudo.

**5.** 0 Não me sinto especialmente culpado.
1 Eu me sinto culpado grande parte do tempo.
2 Eu me sinto culpado na maior parte do tempo.
3 Eu me sinto sempre culpado.

**6.** 0 Não acho que esteja sendo punido.
1 Acho que posso ser punido.
2 Creio que serei punido.
3 Acho que estou sendo punido.

**7.** 0 Não me sinto decepcionado comigo mesmo.
1 Estou decepcionado comigo mesmo.
2 Estou enjoado de mim.

3 Eu me odeio.

**8.** 0 Não me sinto, de qualquer modo, pior do que os outros.
1 Sou crítico em relação a mim por minhas fraquezas ou erros.
2 Eu me culpo sempre por minhas falhas.
3 Eu me culpo por tudo de mau que acontece.

**9.** 0 Não tenho quaisquer idéias de me matar.
1 Tenho idéias de me matar, mas não as executaria.
2 Gostaria de me matar.
3 Eu me mataria se tivesse oportunidade.

**10.** 0 Não choro mais do que o habitual.
1 Choro mais agora do que costumava.
2 Agora, choro o tempo todo.
3 Costumava ser capaz de chorar, mas agora não consigo, mesmo que queira.

**11.** 0 Não sou mais irritado agora do que já fui.
1 Fico aborrecido ou irritado mais facilmente do que costumava.
2 Atualmente me sinto irritado o tempo todo.
3 Não me irrito mais com as coisas que costumava me irritar.

**12.** 0 Não perdi o interesse pelas outras pessoas.
1 Estou menos interessado pelas outras pessoas do que costumava estar.
2 Perdi a maior parte do meu interesse pelas outras pessoas.
3 Perdi todo o meu interesse pelas outras pessoas.

**13.** 0 Tomo decisões tão bem quanto antes.
1 Adio as tomadas de decisões mais do que costumava.
2 Tenho mais dificuldade em tomar decisões do que antes.
3 Não consigo mais tomar decisões.

**14.** 0 Não acho que minha aparência esteja pior do que costumava ser.
1 Estou preocupado por estar parecendo velho ou sem atrativos.
2 Acho que há mudanças permanentes na minha aparência que me fazem parecer sem atrativos.
3 Acredito que pareço feio.

**15.** 0 Posso trabalhar tão bem quanto antes.
1 Preciso de um esforço extra para fazer alguma coisa.
2 Tenho que me esforçar muito para fazer alguma coisa.
3 Não consigo mais fazer trabalho algum.

**16.** 0 Consigo dormir tão bem como o habitual.
1 Não durmo tão bem auqnto costumava.

2 Acordo uma a duas horas mais cedo que habitualmente e tenho dificuldade em voltar a dormir.
3 Acordo várias horas mais cedo do que costumava e não consigo voltar a dormir.

**17.** 0 Não fico mais cansado do que o habitual.
1 Fico cansado com mais facilidade do que costumava.
2 Sinto-me cansado ao fazer qualquer coisa.
3 Estou cansado demais para fazer qualquer coisa.

**18.** 0 Meu apetite não está pior do que o habitual.
1 Meu apetite não é tão bom quanto costumava ser.
2 Meu apetite está muito pior agora.
3 Não tenho mais nenhum apetite.

**19.** 0 Não tenho perdido muito peso, se é que perdi algum recentemente.
1 Perdi mais de dois quilos e meio.
2 Perdi mais de cinco quilos.
3 Perdi mais de sete quilos.
Estou tentando perder peso de propósito, comendo menos: ( ) sim ( ) não.

**20.** 0 Não estou mais preocupado com a minha saúde do que o habitual.
1 Estou preocupado com problemas físicos, tais como dores, indisposição do estômago ou prisão de ventre.
2 Estou muito preocupado com meus problemas físicos e é difícil pensar em outra coisa.
3 Estou tão preocupado com meus problemas físicos que não consigo pensar em qualquer coisa.

**21.** 0 Não notei qualquer mudança recente no meu interesse por sexo.
1 Estou menos interessado por sexo do que costumava estar.
2 Estou menos interessado em sexo atualmente.
3 Perdi completamente o interesse por sexo.

TOTAL: _____

*Anexo 7*

**Escala modificada do impacto da fadiga (MFIS)**

Fadiga é uma sensação de cansaço físico e falta de energia que muitas pessoas sentem de tempos em tempos, porém indivíduos com algumas doenças, como a Esclerose Múltipla, experimentam sensações mais intensas de fadiga, com mais freqüência e com maior impacto que as demais.

Há seguir há uma lista com diversos itens que descrevem os efeitos da fadiga. Por favor, leia cada um deles cuidadosamente, e então circule um número que melhor indicar como a fadiga afetou você durante s quatro últimas semanas (se precisar de ajuda para marcar suas respostas, fale para o entrevistador o número da melhor resposta). Por favor, responda todas as questões. Se você não tem certeza sobre qual resposta selecionar, escolha a resposta que está mais próxima da sua realidade. Se necessário peça ao entrevistador para explicar algumas palavras ou frases que você não entendeu.

Por causa da minha fadiga nas quatro últimas semanas:

0 = nunca 1 = raramente 2 = poucas vezes 3 = muitas vezes 4 = sempre

| | |
|---|---|
| 1. Eu estou menos alerta. | |
| 2. Tenho dificuldade em manter minha atenção por muito tempo. | |
| 3. Tenho dificuldade para pensar com clareza. | |
| 4. Estou desajeitado e incoordenado. | |
| 5. Tenho tido esquecimentos. | |
| 6. Tenho que me adequar nas minhas atividades físicas. | |
| 7. Estou menos motivado para fazer qualquer atividade que solicite esforço físico. | |
| 8. Estou menos motivado para participar de atividades sociais. | |
| 9. Tenho sentido limitações para realizar tarefas longe de casa. | |
| 10. Tenho problemas em manter atividades físicas por longos períodos. | |
| 11. Eu tenho dificuldade em tomar decisões. | |
| 12. Estou menos motivado para realizar qualquer atividade que envolva raciocínio. | |
| 13. Meus músculos estão fracos. | |
| 14. Tenho desconforto físico. | |
| 15. Eu tenho dificuldade em terminar tarefas que envolvam pensamento. | |
| 16. Eu tenho dificuldades para organizar meus pensamentos quando realizo atividades em casa ou trabalho. | |
| 17. Eu sou menos capaz de completar tarefas que envolvam esforço físico. | |
| 18. Meus pensamentos estão mais lentos. | |
| 19. Tenho problemas de concentração. | |
| 20. Tenho limitado minhas atividades físicas. | |
| 21. Eu preciso descansar mais frequentemente ou por períodos mais longos. | |

*Anexo 8*

**Friedreich's Ataxia Rating Score**

## I. FUNCTIONAL STAGING FOR ATAXIA

Increment by 0.5 may be used if the status is about the middle between two stages.

**STAGE** ☐☐

**STAGE 0:** Normal.

**STAGE 1.0:** Minimal signs detected by physician during screening. Can run or jump without loss of balance. No disability.

**STAGE 2.0:** Symptoms present, recognized by patient, but still mild. Cannot run or jump without losing balance. The patient is physically capable of leading an independent life, but daily activities may be somewhat restricted. Minimal disability.

**STAGE 3.0:** Symptoms are overt and significant. Requires regular or periodic holding onto wall/furniture or use of a cane for stability and walking. Mild disability. (Note: many patients postpone obtaining a cane by avoiding open spaces and walking with the aid of walls/ people etc. These patients are grades as stage 3.0)

**STAGE 4.0:** Walking requires a walker, Canadian crutches or two canes. Or other aids such as walking dogs. Can perform several activities of daily living. Moderate disability.

**STAGE 5.0:** Confined but can navigate a wheelchair. Can perform some activities of daily living that do not require standing or walking. Severe disability.

**STAGE 6.0:** Confined to wheelchair or bed with total dependency for all activities of daily living. Total disability.

**I. ACTIVITIES OF DAILY LIVING** (increments of 0.5 may be used if strongly felt that a task falls between 2 scores)

**1. Speech** ☐

0 - Normal

1 - Mildly affected. No difficulty being understood.

2 - Moderately affected. Sometimes asked to repeat statements.

3 - Severely affected. Frequently asked to repeat statements.

4 - Unintelligible most of the time.

**2. Swallowing** ☐

0 - Normal.

1 - Rare choking (< once a month).

2 - Frequent choking (< once a week, > once a month).

3 - Requires modified food or chokes multiple times a week. Or patient avoids certain foods.

4 - Requires NG tube or gastrostomy feedings.

**3. Cutting Food and Handling Utensils** ☐

0 - Normal.

1 - Somewhat slow and clumsy, but no help needed.

2 - Clumsy and slow, but can cut most foods with some help needed. Or needs assistance when in a hurry.

3 - Food must be cut by someone, but can still feed self slowly.

4 - Needs to be fed.

**4. Dressing** ☐

0 - Normal.

1 - Somewhat slow, but no help needed.

2 - Occasional assistance with buttoning, getting arms in sleeves, etc. or has to modify activity in some way (e.g. Having to sit to get dressed; use velcro for shoes, stop wearing ties, etc.).

3 - Considerable help required, but can do some things alone.

4 - Helpless.

**5. Personal Hygiene** ☐

0 - Normal.

1 - Somewhat slow, but no help needed.

2 - Very slow hygienic care or has need for devices such as special grab bars, tub bench, shower chair, etc.

3 - Requires personal help with washing, brushing teeth, combing hair or using toilet.

4 - Fully dependent

**6. Falling (assistive device = score 3)** ☐

0 - Normal.

1 - Rare falling (< once a month).

2 - Occasional falls (once a week to once a month).

3 - Falls multiple times a week or requires device to prevent falls.

4 - Unable to stand or walk.

**7. Walking (assistive device = score 3)** ☐

0 - Normal.

1 - Mild difficulty, perception of imbalance.

2 - Moderate difficulty, but requires little or no assistance.

3 - Severe disturbance of walking, requires assistance or walking aids.

4 - Cannot walk at all even with assistance (wheelchair bound).

**8. Quality of Sitting Position**

0 - Normal.

1 - Slight imbalance of the trunk, but needs no back support.

2 - Unable to sit without back support.

3 - Can sit only with extensive support (Geriatric chair, posy, etc.).

4 - Unable to sit.

**9. Bladder Function (if using drugs for bladder, automatic score of 3)**

0 - Normal.

1 - Mild urinary hesitance, urgency or retention (< once a month).

2 - Moderate hesitance, urgency, rare retention/incontinence (> once a month, but < once a week).

3 - Frequent urinary incontinence (> once a week).

4 - Loss of bladder function requiring intermittent catheterization/indwelling catheter

**TOTAL ACTIVITIES OF DAILY LIVING SCORE:**

**III.NEUROLOGICAL EXAMINATION** (rate each item on the basis of the patient status during examination. To the extent possible, sequential patient examinations should be carried out at the same time of the day. If the patient is taking any medication, the examination should be carried out prior to dosing, or at a fixed time following the dosing based on the maximum expected therapeutic response. Increments of 0.5 may be used if examiner feels an item falls between 2 defined severities)

**A. BULBAR**

**1. Facial Atrophy, Fasciculation, Action Myoclonus, and Weakness:**

0 - None

1 - Fasciculations or action myoclonus, but no atrophy.

2 - Atrophy present but not profound or complete.

3 - Profound atrophy and weakness.

2. **Tongue Atrophy, Fasciculation, Action Myoclonus and Weakness:** ☐
   0 - None.

   1 - Fasciculations or action myoclonus, but no atrophy.

   2 - Atrophy present but not profound or complete.

   3 - Profound atrophy and weakness.

3. **Cough:** (Patient asked to cough forcefully 3 times) ☐

   0 - Normal.

   1 - Depressed.

   2 - Totally or nearly absent.

4. **Spontaneous Speech** (ask the patient to read or repeat the sentences "The President lives in the White House" or "The traffic is heavy today":

   0 - Normal. ☐

   1 - Mild (all or most words understandable).

   2 - Moderate (most words not understandable).

   3 - Severe (no or almost no useful speech).

**TOTAL BULBAR SCORE:** ☐

## B. UPPER LIMB COORDINATION

1. **Finger to Finger Test** (The index fingers are placed in front of each other with flexion at the elbow about 25 cm. from the sternum. Observe for 10 seconds. Score amplitude of oscillations):

Right Left

0 - Normal.

1 - Mild oscillations of finger (< 2 cm.). ☐ ☐

2 - Moderate oscillations of finger (2-6 cm.).

3 - Severe oscillations of finger (> 6 cm.).

**2. Nose-Finger Test** (**Assess kinetic** or intention **tremor** during and towards the end of movement: examiner holds index finger at 90% reach of patient; test at least 3 nose-finger-nose trials; movement slow > 3 sec.):

Right Left

0 - None ☐ ☐

1 - Mild (< 2 cm. amplitude).

2 - Moderate (2-4 cm. amplitude or persisting through movement).

3 - Severe (> 6 cm. & persisting through movement).

4 - Too poorly coordinated to perform task.

**3.Dysmetria** (Fast Nose-Finger) **Test:(Assess dysmetria**: The patient touches tip of examiner's finger 8 times as rapidly as possible while the examiner moves his finger and stops st different locations at about 90% reach of the patient. Assess dysmetria – i.e. inaccuracy of reaching the target- at examiner's finger):

Right Left

0 - None.

1 - Mild (misses 2 or fewer times). ☐ ☐

2 - Moderate (misses 3-5 times).

3 - Severe (misses 6-8 times.).

4 - Too poorly coordinated to perform task.

**4. Rapid Alternating Movements of Hands** (Forearm pronation/supination 15 cm. above thigh; 10 full cycles as fast as possible; assess rate, rhythm, accuracy; practice 10 cycles before rating, if time > 7 sec. add 1 to score. Use stopwatch):

Right Left

0 - Normal.

1 - Mild (slightly irregular or slowed). ☐ ☐

2 - Moderate (irregular and slowed).

3 – Too poorly coordinated to perform task.

**5. Finger Taps** (index fingertip-to-thumb crease; 15 reps as fast as possible; practice 15 reps once before rating; if time > 6 sec., add 1 to rating. Use stopwatch):

Right Left

0 - Normal.

1 - Mild (misses 1-3 times). ☐ ☐

2 - Moderate (misses 4-9 times).

3 - Severe (misses 10-15 times).

4 - Cannot perform the task.

**TOTAL UPPER LIMB COORDINATION SCORE** ☐

## C. LOWER LIMB COORDINATION

**1. Heel Along Shin Slide** (under visual control, slide heel on the contralateral tibia from the patella to the ankle up and down, 3 cycles at moderate speed, 2 sec./cycle, one at a time. May be seated with contralateral leg extended or supine but perform same way each time. Circle which: supine seated):

0 - Normal (stay on shin).

1 - Mild (abnormally slow, tremulous but contact maintained).

2 - Moderate (goes off shin a total of 3 or fewer times during 3 cycles). ☐ ☐

3 - Severe (goes off shin 4 or more times during 3 cycles).

4 - Too poorly coordinated to attempt the task.

2. **Heel-to-Shin Tap** (patient taps heel on midpoint of contralateral shin 8 times on each side from about 6-10", one at a time. May be seated with contralateral leg extended or supine but perform the same way each time. Circle which: supine seated):

0 - Normal (stays on target). Right Left

1 - Mild (misses shin 2 or < times). ☐ ☐

2 - Moderate (misses shin 3-5 times).

3 - Severe (misses shin > 4 times).

4 - Too poorly coordinated to perform task.

**TOTAL LOWER LIMB COORDINATION SCORE** ☐

## D. PERIPHERAL NERVOUS SYSTEM

1. **Muscle Atrophy** (score most severe atrophy in either upper or lower limb):

Right Left

0 - None.

1 - Present - mild/moderate ☐ ☐

2 - Severe/total wasting

2. **Muscle Weakness** (Test deltoids, interossei, iliopsoas and tibialis anterior. Score most severe weakness in either upper or lower limb):

Right Left

0 - Normal (5/5). ☐ ☐

1 - Mild (movement against resistance but not full power 4/5).

2 - Moderate (movement against gravity but not with added resistance 3/5)

3 - Severe (movement of joint but not against gravity 2/5).

4 - Near paralysis (muscular activity without movement 1/5).

5 - Total paralysis (0/5).

**3. Vibratory Sense** (Educate patient regarding the sensation. Tested with 128 cps tuning fork set to near full vibration; eyes closed; test over index finger and great toe. Abnormal < 15 seconds for toes and <25 seconds for hands):

| | Right | Left |
|---|---|---|
| Time felt for toes: | _____ | _____ |
| Time felt for fingers: | _____ | _____ |

| | Right | Left |
|---|---|---|
| 0 - Normal. | | |
| 1 - Impaired at toes. | ☐ | ☐ |
| 2 - Impaired at toes or fingers. | | |

**4. Position Sense** (test using minimal random movement of distal interphalangeal joints of index finger and big toe)

| | Right | Left |
|---|---|---|
| 0 - Normal. | | |
| 1 - Impaired at toes/or fingers. | ☐ | ☐ |
| 2 - Impaired at toes and fingers. | | |

**5. DTR** (0-absent; 1 -hyporeflexia; 2 -normal; 3 -hyperreflexia; 4 -pathologic hyperreflexia)

Right:

BJ_____ BrJ_____ KJ_____ AJ_____

Left:

BJ_____ BrJ_____ KJ_____ AJ____

| | Right | Left |
|---|---|---|
| 0 - No areflexia. | | |
| 1 - Areflexia in either upper or lower limbs. | ☐ | ☐ |
| 2 - Generalized areflexia. | | |

**TOTAL PERIPHERAL NERVOUS SYSTEM SCORE** ☐

**E. UPRIGHT STABILITY** (For sitting posture patient can sit in a chair or examination table. For standing and walking assessment instruct patient to wear best walking shoes and record below if barefoot, footwear or AFOs used. Stance assessment begins with feet 20 cm apart. Place marker tapes in the exam room 20 cm apart and the insides of the feet are lined up against these. Subsequent stance tests get more difficult. For feet together the entire inside of the feet should be close together as much as possible. For tandem stance, the dominant foot is in the back and the heel of the other foot is lined with the toes of the dominant foot but not in front of the toes (because this makes it even more difficult). For one foot stance, the patient is asked to stand on dominant foot and the other leg is elevated by bringing it forward with knee extended; this gives some advantage to the patient. If a patient can stand in a particular position for 1 mintues or longer in trial 1, the trials 2 and 3 are abandoned. Otherwise each of 3 trials is timed and then averaged. Grading scores are then given as noted. Tandem walk and gait are performed in a hallway. Preferably no carpet but at least serial examinations should be on the same surface. For gait place markers 25 feet apart. Patient walks the distance turns around and comes back and the activitiy is

timed. Note if the gait was achieved with or without device and serial examinations should be done with the same device as in the first examination.

Stance and gait tests may be done barefoot if patient does have appropriate footwear, however, it should be done the same way for serial measurement.)

Circle which: Barefoot Footwear

Also, indicate if AFOs are used: Yes No

1. **Sitting Posture** (Patient seated in chair with thighs together, arms folded, back unsupported; observe for 30 sec.):

   0 - Normal. ☐

   1 - Mild oscillations of head/trunk without touching chair back or side.

   2 - Moderate oscillations of head/trunk; needs contact with chair back or side for stability.

   3 - Severe oscillations of head/trunk; needs contact with chair back or side for stability.

   4 - Support on all 4 sides for stability.

2. **Stance feet apart– Inside of feet 20 cm apart marked on floor. Use stopwatch; 3 attempts; time in seconds):**

   Trial 1 ☐ Trial 2 ☐ Trial 3 ☐ AVG ☐

   0 - 1 minute or longer.

   1 - <1 minute, >45 sec.

   2 - <45 sec., >30 sec.

   3 - <30 sec., >15 sec.

   4 - <15 sec. or needs hands held by assistant/device.

3. **Stance - Feet Together (use stopwatch; 3 attempts; time in seconds):**

   Trial 1 ☐ Trial 2 ☐ Trial 3 ☐ AVG ☐

   0 - 1 minute or longer.

   1 - <1 minute, >45 sec.

2 - <45 sec., >30 sec.

3 - <30 sec., >15 sec.

4 - <15 sec.

**4. Tandem Stance** (use stopwatch; 3 attempts, dominant foot in front; time in seconds)

Trial 1 ☐ Trial 2 ☐ Trial 3 ☐ AVG ☐

0 - 1 minute or longer.

1 - <1 minute, >45 sec.

2 - <45 sec., >30 sec.

3 - <30 sec., >15 sec.

4 - <15 sec.

**5. Stance on Dominant Foot** (use stopwatch; 3 attempts; time in seconds):

Trial 1 ☐ Trial 2 ☐ Trial 3 ☐ AVG ☐

0 - 1 minute or longer.

1 - <1 minute, >45 sec.

2 - <45 sec., >30 sec.

3 - <30 sec., >15 sec.

4 - <15 sec.

**6. Tandem Walk** (tandem walk 10 steps in straight line; performed in hallway with no furniture within reach of 1 m / 3 ft. and no loose carpet):

0 - Normal (able to tandem walk >8 sequential steps). ☐

1 - Able to tandem walk in < perfect manner/can tandem walk >4 sequential steps, but <8.

2 - Can tandem walk, but fewer than 4 steps before losing balance.

3 - Too poorly coordinated to attempt task.

7. **Gait** (use stopwatch; walk 8 m/25 ft. at **normal pace**, turn around using single step pivot and return to start; performed in hallway with no furniture within reach of 1 m/3 ft. and no loose carpet):

   Device, if any:_____ ☐

   Time in seconds:_____

   0 - Normal.

   1 - Mild ataxia/veering/difficulty in turning; no cane/other support needed to be safe.

   2 - Walks with definite ataxia; may need intermittent support/or examiner needs to walk with patient for safety sake.

   3 - Moderate ataxia/veering/difficulty in turning; walking requires cane/holding onto examiner with one hand to be safe.

   4 - Severe ataxia/veering; walker or both hands of examiner needed.

   5 - Cannot walk even with assistance (wheelchair)

**TOTAL UPRIGHT STABILITY SCORE** ☐

**TOTAL NEUROLOGIC EXAMINATION SCORE** ☐

**TOTAL SCORE** ☐

## *Anexo 9*

## *Artigos - Copyright*

**ELSEVIER LICENSE**
**TERMS AND CONDITIONS**

May 29, 2014

This is a License Agreement between Cynthia Bonilha da Silva ("You") and Elsevier ("Elsevier") provided by Copyright Clearance Center ("CCC"). The license consists of your order details, the terms and conditions provided by Elsevier, and the payment terms and conditions.

**All payments must be made in full to CCC. For payment instructions, please see information listed at the bottom of this form.**

| | |
|---|---|
| Supplier | Elsevier Limited<br>The Boulevard,Langford Lane<br>Kidlington,Oxford,OX5 1GB,UK |
| Registered Company Number | 1982084 |
| Customer name | Cynthia Bonilha da Silva |
| Customer address | Rua Barão de Atibaia 499 ap 32 |
| | Campinas, Sao Paulo 13023-010 |
| License number | 3398460505623 |
| License date | May 29, 2014 |
| Licensed content publisher | Elsevier |
| Licensed content publication | Parkinsonism & Related Disorders |
| Licensed content title | Fatigue is frequent and multifactorial in Friedreich's ataxia |
| Licensed content author | Cynthia B. da Silva,Camila F. Chevis,Anelyssa D'Abreu,Iscia Lopes-Cendes,Marcondes C. França |
| Licensed content date | August 2013 |
| Licensed content volume number | 19 |
| Licensed content issue number | 8 |
| Number of pages | 2 |
| Start Page | 766 |
| End Page | 767 |
| Type of Use | reuse in a thesis/dissertation |
| Intended publisher of new work | other |
| Portion | full article |
| Format | both print and electronic |
| Are you the author of this Elsevier article? | Yes |
| Will you be translating? | No |
| Title of your thesis/dissertation | Estudo longitudinal clínico e de imagem na Ataxia de Friedreich |
| Expected completion date | Sep 2014 |
| Estimated size (number of pages) | 150 |
| Elsevier VAT number | GB 494 6272 12 |

| | |
|---|---|
| Permissions price | 0.00 USD |
| VAT/Local Sales Tax | 0.00 USD / 0.00 GBP |
| Total | 0.00 USD |
| Terms and Conditions | |

**JOHN WILEY AND SONS LICENSE TERMS AND CONDITIONS**

May 29, 2014

This is a License Agreement between Cynthia Bonilha da Silva ("You") and John Wiley and Sons ("John Wiley and Sons") provided by Copyright Clearance Center ("CCC"). The license consists of your order details, the terms and conditions provided by John Wiley and Sons, and the payment terms and conditions.

**All payments must be made in full to CCC. For payment instructions, please see information listed at the bottom of this form.**

| | |
|---|---|
| License Number | 3398451414356 |
| License date | May 29, 2014 |
| Licensed content publisher | John Wiley and Sons |
| Licensed content publication | European Journal of Neurology |
| Licensed content title | Dentate nuclei T2 relaxometry is a reliable neuroimaging marker in Friedreich's ataxia |
| Licensed copyright line | © 2014 The Author(s) European Journal of Neurology © 2014 EFNS |
| Licensed content author | C. Bonilha da Silva,F. P. G. Bergo,A. D'Abreu,F. Cendes,I. Lopes-Cendes,M. C. França |
| Licensed content date | Apr 30, 2014 |
| Start page | n/a |
| End page | n/a |
| Type of use | Dissertation/Thesis |
| Requestor type | Author of this Wiley article |
| Format | Print and electronic |
| Portion | Full article |
| Will you be translating? | No |
| Title of your thesis / dissertation | Estudo longitudinal clínico e de imagem na Ataxia de Friedreich |
| Expected completion date | Sep 2014 |
| Expected size (number of pages) | 150 |
| Total | 0.00 USD |
| Terms and Conditions | |

Springer the language of science

**Title:** Neuroanatomical Correlates of Depression in Friedreich's Ataxia: a Voxel-Based Morphometry Study
**Author:** Cynthia B. da Silva
**Publication:** The Cerebellum
**Publisher:** Springer
**Date:** Jan 1, 2012




## Order Completed

Thank you very much for your order.

This is a License Agreement between Cynthia Bonilha da Silva ("You") and Springer ("Springer") The license consists of your order details, the terms and conditions provided by Springer, and the payment terms and conditions.

| | |
|---|---|
| License number | Reference confirmation email for license number |
| License date | Jun 19, 2014 |
| Licensed content publisher | Springer |
| Licensed content publication | The Cerebellum |
| Licensed content title | Neuroanatomical Correlates of Depression in Friedreich's Ataxia: a Voxel-Based Morphometry Study |
| Licensed content author | Cynthia B. da Silva |
| Licensed content date | Jan 1, 2012 |
| Volume number | 12 |
| Issue number | 3 |
| Type of Use | Thesis / Dissertation |
| Title of your thesis / dissertation | Estudo longitudinal clínico e de imagem na Ataxia de Friedreich |
| Expected completion date | None |
| Estimated size(pages) | 100 |
| Billing Type | Invoice |
| Billing address | Rua Barão de Atibaia 499 ap 32 |
| | Campinas, Sao Paulo 13023-010 |
| | Brazil |
| Total | 0.00 USD |